T-PM-Min1 THERMODYNAMIC TREATMENT OF PHASE TRANSITIONS IN SIMPLE LIPID MIXTURES. Keith W. Miller.* Depts. of Pharmacol. and Anesthesia, Harvard Med. Sch. and Massachusetts Gen. Hosp. Boston, Ma. 02114

The effect of a second component on the phase transition behaviour of a single phospholipid should be predictable by thermodynamic principles. In dilute solutions of a second component ideal behaviour is expected. A simple case is the addition of fatty alcohols or acids to a phospholipid with fully saturated acyl chains. Such solutes are found to either raise or lower the phase transition temperature. Which behaviour will occur with a given solute can be predicted by a simple thermodynamic model originally derived for bulk solutions. Solutes which raise the phase transition are predicted to partition preferentially into the low temperature phase. Elevation of the phase transition thus results from stabilization of the low temperature phase and is largely unrelated to solute induced changes in fluidity in the high temperature phase. The application of these principles to solutions of fatty alcohols in lecithins will be described and the molecular basis for gel stabilization discussed. These studies provide both a thermodynamic basis for considering more complex systems and a rationale for the design of phase selective spectroscopic probes.

T-PM-Min2 LATERAL PHASE SEPARATIONS IN BINARY MIXTURES OF PHOSPHATIDYLCHOLINE AND CHOLESTEROL. Diether J. Recktenwald and Harden M. McConnell, Stanford University, Stanford, CA 94305.

A number of recent studies of binary mixtures of cholesterol and phosphatidylcholine have led to the conclusion that this bilayer membrane system has a remarkable structure in the composition-temperature range $X_{chol} \leq 20$ mol%, $T < T_m$, where T_m is the chain melting transition temperature. In this temperature-composition region the bilayers consist of alternating, parallel bands of "solid" phosphatidylcholine and "fluid", where the "fluid" contains 20 mol% cholesterol. For a summary description of this model and relevant experiments, see Owicki and McConnell.[1] This interpretation of the structure of the bilayer membrane $X_{chol} \leq 20$ mol%, $T < T_m$ has now been further supported by paramagnetic resonance experiments using two spin labels, TEMPO and a phospholipid head group spin label. The resonance spectra can be accounted for quantitatively in terms of the compositions predicted by the alternating solid phase-fluid phase banding model. For example, the partitioning of TEMPO into the bilayer membrane is strictly a decreasing linear function of cholesterol concentration below 20 mol% cholesterol, and this partitioning shows a sharp break in slope at 20 mol%. Most of the present spin label data are in accord with the phase diagrams of phosphatidylcholine-cholesterol proposed by Shimshick and McConnell[2] and particularly the existence of lateral phase separations involving two fluid phases. The data also provide strong evidence against the percolation model for lateral diffusion in these mixtures proposed by Snyder and Freiere.[3]

1. J.C. Owicki and H.M. McConnell, Biophys. J. 30, 383-397 (1980).
2. E.J. Shimshick and H.M. McConnell, Biochem. Biophys. Res. Comm. 53, 446-451 (1973).
3. B. Snyder and E. Freire, Proc. Natl. Acad. Sci. USA 77, 4055-4059 (1980).

[We acknowledge support from NSF Grant no. PCM 77-23586 and DFG Fellowship no. Re 493/1.]

T-PM-Min3 DOMAIN STRUCTURE AND PHYSICAL PROPERTIES OF LIPID MEMBRANES. Ernesto Freire, Dept. of Biochemistry, University of Virginia, Charlottesville, Virginia 22908.

We have investigated the lateral distribution of molecules in two-component membrane systems using calorimetric and spectroscopic techniques in conjunction with Monte Carlo calculations designed to simulate physical processes with the computer. The combination of these techniques allows transformation of energetic and physicochemical data into the parameters describing the lateral organization of the bilayer. These studies have resulted in the development of a rigorous description of the lateral distribution of membrane components in terms of the number of contacts between molecular species, the size distribution and geometry of compositional domains, the radial distribution and the pair connectedness function. These studies have revealed the existance of very sharp percolation processess characterized by the rapid passage of the system from a state in which specific compositional domains are isolated and dispersed within the bilayer, to a state in which these domains become connected one with each other forming an intricate network that extends over the entire bilayer surface. These changes in the lateral connectivity of the compositional domains can be induced by changes in composition, temperature and by changes in the magnitude of the intermolecular potentials. For binary mixtures of phosphatidylcholines percolation occurs at ≈50 mole % whereas for cholesterol-lipid mixtures the cholesterol rich lipid domains become connected at ≈20 mole % cholesterol. Quantitative correlations between organizational and functional parameters indicate that these changes in the lateral organization of the bilayer might play an important role in the regulation of transport processes across and along the plane of the bilayer. (Supported by USPHS, NIH grants GM-27244 and GM-26894).

T-PM-Min4 MAPPING THE GEOMETRY OF DOMAINS BY ELECTRON MICROSCOPY AND DIFFRACTION. S. W. Hui and T. P. Stewart, Roswell Park Memorial Institute, Buffalo, New York 14263.

Several microscopic techniques were applied to visualized lipid domains in membranes. Utilizing the differences in electron diffraction patterns, we have distinguished laterally phase separated domains by electron optical filtration of low dose electron images of single bilayers of mixed phospholipids and cholesterol. The domains were seen as a patchwork in the plane of the bilayer, with widths varying between 0.05 to 0.5 μm. The percentage of gel phase area measured from diffraction contrast micrographs at various temperatures agree in general with those depicted by phase diagrams. The shape and size of the domains resemble those distinguishable in freeze fractured multilamellar vesicles. Temperature-related changes in domain size and in phase boundary per unit area depend on the miscibility of the mixture. Lipid domains in erythrocyte membrane were also visualized from the forced redistribution of proteinaceous intramembrane particles upon lipid phase separation. The geometry of these domains changes with temperature and cholesterol contents of the membrane. Linear structural defects (including domain boundaries) in bilayers are revealed by a water vapor decoration method in freeze fracture. In lipid mixture containing highly unsaturated phosphatidylethanolamine, point defects in the form of cusps (lipidic intramembrane particles) are also visible by freeze fracture. The geometry of these point and linear defects has definite effects on membrane properties. Supported by ACS grant BC-248 and NIH Grant GM-28120.

T-PM-Min5 LIPID DOMAINS IN MEMBRANES. A.M. Kleinfeld, W.J. Pjura, R.L. Hoover, R.D. Klausner and M.J. Karnovsky. Biophysical Lab. and Dept. of Pathology, Harvard Medical School, Boston, MA 02115 and NIH, Bethesda, MD 20014.

We recently presented evidence (Klausner *et al*, 1980, J. Biol. Chem. 255, 1286) derived from free fatty acid (ffa) perturbation and from fluorescent lifetime heterogeneity of diphenylhexatriene (DPH), for the existence of lipid domains in mouse lymphocyte membranes. We now have extended our study to plasma membranes from WTS lymphoma, baby hamster kidney, bovine aortic endothelial cells and platelets. The results are qualitatively similar to those obtained for the lymphocyte: fluorescence polarization of membrane bound DPH is decreased (between 5 and 15%) by incorporation of cis unsaturated ffa but is unchanged by saturated ffa, and to varying degrees fluorescence decay of DPH is heterogeneous in these membranes. However, in red cell membranes, both cis unsaturated and saturated ffa decrease DPH polarization. Furthermore, in contrast to other membranes, fluorescence decay of DPH in red cell membranes is homogeneous. Based upon these criteria, lipid organization of red cell membranes is homogeneous. To investigate the role of cholesterol in the formation of domain structure we have measured fluorescence decay of DPH in liposomes composed of phosphatidylcholine and up to 40 mol % cholesterol. In all systems the decay appears to be homogeneous. At temperatures above phase transition (Tm), the lifetime increased, and below Tm the lifetime decreased, as cholesterol increased from 0 to 20 mole %. Above 20 mole %, either above or below Tm, the lifetime remained constant. These results, in agreement with other studies (Rubenstein *et al* (1979) PNAS 76, 15; Snyder and Freier (1980) PNAS 77, 4055), suggest a reorganization of lipid topology at 20 mole % cholesterol. (Supported by NIH grants GM 26350, and AI10677, HL29191 and JFRA-15 from the Amer. Cancer Soc.).

T-PM-Min6 SELECTIVITY OF FLUORESCENT LIPID ANALOGUES FOR LIPID DOMAINS, David E. Wolf* and Richard Klausner+, *Dept. of Biology, Johns Hopkins University, Baltimore, MD 21218 and +LTB NIH, Bethesda, MD 20205.

We have examined the phase partition preferences of the even chain length (n = 10 to 18) diacyl-3,3'-indocarbocyanine Iodides ($C_n$diI) incorporated in disaturated lecithin (PC) vesicles. Two parameters were used to determine this phase preference: (i) the direction of shift of the phase transition temperature (T_m) induced by the dyes, and (ii) the self-quenching of fluorescence due to aggregation in the gel phase of those dyes which preferentially partition into the fluid. Dyes that lower T_m preferentially partition into the fluid phase; those that raise T_m preferentially partition into the gel. By these criteria in dimristoyl PC, C_{10}diI and C_{12}diI preferentially partition into the fluid phase, C_{14}diI and C_{16}diI show no preferential partition, C_{18}diI preferentially partitions into the gel, C_{20}diI and C_{22}diI preferentially partition into the fluid. In dipalmitoyl PC the pattern of preference is identical with that observed in dimyristoyl PC only shifted to longer chain length diI's by two carbons. Diffusion measurements by fluorescence photobleaching recovery (FPR) or these dyes in gel phase multilayers showed them all to be immobile $D<10^{-10}$ cm^2/s, while in fluid phase multilayers they all had diffusion coefficients of $D\sim10^{-8}$ cm^2/s independent of chain length. In mixed phase multilayers, however, each $C_n$diI showed mobile fractions which reflected its phase partition preference. The $C_n$diI's can thus be used to probe the domain organization of membranes. FPR measurements with these probes on cell membranes suggesting the existence of domains will be discussed.

This work was supported in part by NIH Grants CA-06399 and AI-14584.

T-PM-Min7 LATERAL DIFFUSION OF A LIPID ANALOG IN THE SURFACE MEMBRANE OF CELLS AND IN MULTIBILAYERS FORMED FROM PLASMA MEMBRANE LIPIDS. K. Jacobson[1], Y. Hou[2], Z. Derzko[1], J. Wojcieszyn[1] and D. Organisciak[3], [1]Lab. for Cell Biology, Department of Anatomy, Univ. of North Carolina, Chapel Hill, NC 27514; [2]Roswell Park Memorial Institute, Buffalo, NY 14263 and [3]School of Medicine, Wright State Univ., Dayton, OH 45401.

The diffusion, as measured by fluorescence recovery after photobleaching, of a fluorescent lipid analog, dihexadecylindocarbocyanine [diI-C_{16}(3)], was compared in several systems: the cell surface membrane of living human fibroblasts, the bottom surface membrane remaining after the top surface, nucleus and cytoplasm were removed, multibilayers reconstituted from the total cell lipids, and multibilayers reconstituted from plasma membrane (PM) lipids. Diffusion coefficients (D) for diI-C_{16}(3) inserted into the living cell's surface membrane or bottom surface ghosts were similar--ranging from about 3.5 x $10^{-9}cm^2$/sec at 5° to about 2 x $10^{-8}cm^2$/sec at 37° with a change in slope at about 25°. For diI-C_{16}(3) incorporated into extracted PM lipid multibilayers, D ranged from about 5 x $10^{-9}cm^2$/sec at 5° to over 6 x $10^{-8}cm^2$/sec at 37° with a discontinuity at 10° and slope change at 25°. Above 25°, the temperature dependence of D was similar in all systems with activation energies (E_a) in the range of 5-7 kcal/mole. Below 25°, E_a ranged from 9-11 kcal/mole for the intact cells and bottom surface ghosts to 17 kcal/mole for the PM lipid multibilayer. Although at 5°, diffusion in the PM was nearly matched by that in the PM lipid multibilayer, at 37°, diI-C_{16}(3) diffusion was four times faster in the multibilayer composed of PM lipids than in the PM itself. The membrane proteins in the PM could produce the observed reduction in diI-C_{16}(3) mobility by generally increasing membrane viscosity, channeling diffusion, or binding the probe at protein-lipid interfaces.

T-PM-Min8 LATERAL ORGANIZATION OF MEMBRANE PROTEINS N. D. Gershon[+], L. Jarett[*@], R. M. Smith[*@], and J. B. Schweizer[*@], [+]PSL, DCRT, NIH, Bethesda, MD 20205 and [@]Dept. of Pathology and Laboratory Medicine, University of Pennsylvania, Philadelphia, PA 19104

Two ways in which proteins are aggregated in membranes are distinguished. One type of aggregation is the result of a restriction in the location of some proteins to certain regions on the cell membrane, i.e. areas associated with microvilli or caps. A second type of protein aggregation is the clustering of individual molecules into groups, or small domains, in the plane of the membrane. Methods to quantitatively analyze these situations as seen on electron micrographs are discussed. One method is to calculate the average density of neighbors around a molecule (e.g. Gershon et al, Exp. Cell Res. 122, 115 (1979)). In the second approach, the distribution of groups of proteins present on the membranes, according to size, is calculated (Gershon et al, J. Membr. Biol., in press). Such groups were found in insulin binding sites on rat adipocytes (Jarett and Smith, J. Clin. Invest. 63, 571 (1979)) but not on rat liver plasma membranes (Jarett et al, Science, in press). Cytochalasin B (CB) was found to partially disrupt these groups on adipocytes. Quantitative analysis of these cases showed that insulin binding sites on rat adipocytes were nonrandomly distributed and that, in the presence and absence of CB, the distance between near neighbors in a group did not appear to exceed 400Å. Further biochemical studies and possible significance of receptor aggregation in physiological action, in these and other systems, will be reviewed.

T-PM-Min9 LATERAL DIFFUSION OF INTRAMEMBRANE PARTICLES: LOCAL RATES OF DIFFUSION ARE DEPENDENT ON LOCAL INTRAMEMBRANE PARTICLE CONCENTRATIONS. Arthur E. Sowers and Charles R. Hackenbrock, Laboratories for Cell Biology, Dept. of Anatomy, School of Medicine, University of North Carolina, Chapel Hill, N.C. 27514

We have previously shown that an electrophoretic force causes intramembrane particles (IMP) in spherical-shaped mitochondrial inner membranes to move laterally in the plane of the membrane and accumulate into an IMP-rich island and leave the remainder of the membrane free of IMP (Fed. Proc. 39,1655[1980]). Release from the electrophoretic force permitted the IMP to freely diffuse laterally and return to a random distribution. To measure the lateral diffusion coefficient, D, for IMP, membranes were frozen at a known time after release from the electrophoretic force but before the IMP distribution reaches equilibrium. The IMP concentrations were measured and plotted for different locations along a meridian extending from the center of the IMP-rich island to the center of the IMP-free area on each membrane. The IMP concentration profile along the meridian was compared with computer-generated concentration profiles based on Huang's mathematical model for particles diffusing on a spherical membrane (J. Theor. Biol.40,11;Fig.2). From the average slope of the entire concentration profile on each of 16 membranes, the value for D was calculated to be $2.4x10^{-10}$ cm^2/sec. However, in individual segments of the profile in which the IMP concentrations were higher or lower than at equilibrium, the slopes were steeper or shallower, respectively, than predicted by theory. Correcting for this effect, analysis indicates that in segments along the meridian where the local concentrations of IMP were 8% above and 4% below equilibrium the lateral diffusion coefficients were $1.2x10^{-11}$ cm^2/sec and $5.5x10^{-10}$ cm^2/sec, respectively. Supported by NSF grant PCM 7910968 to CRH and a NRSA to AES.

T-PM-Min10 PHOTOBLEACHING RECOVERY STUDIES OF ANTIGEN-SPECIFIC MOUSE LYMPHOCYTE STIMULATION BY DNP-CONJUGATED POLYMERIZED FLAGELLIN. J.S. Peacock and B.G. Barisas, St. Louis University School of Medicine, St. Louis, MO 63104

We have used fluorescence photobleaching recovery (FPR) to study diffusion of antigen-receptor complexes during stimulation of DNP-specific mouse lymphocytes with the T-independent antigens DNP-polymerized flagellin (DNP-pol). Depending on epitope density and dose, these materials can behave either as immunogens or tolerogens. Lymphocyte DNP receptors binding $DNP_{0.5}$ flagellin monomer show $D = 2.2 \times 10^{-10}$ cm^2 sec^{-1} and ca 60% fluorescence recovery after bleaching. For DNP-pol binding to DNP-specific lymphocytes, the observed diffusion constants decrease monotonically with increased antigen dose and epitope density. Under optimally immunogenic conditions of $DNP_{2.3}$-pol at 1µg/ml, $D = 1.5 \times 10^{-11}$ cm^2 sec^{-1} implying that ~14 receptors have been crosslinked. Under tolerogenic conditions lower diffusion constants approaching 0.8×10^{-11} cm^2 sec^{-1} are observed implying somewhat larger receptor aggregates. The fraction of aggregates mobile on the time scale of the experiment remains constant at 50-60% in all immunogenic situations but falls abruptly to 25-33% in precisely those situations where the antigen/dose combination is tolerogenic. This might support hypotheses that there exist critical epitope densities above which antigens and receptors form rigidly crosslinked aggregates which are tolerogenic. Receptor aggregate diffusion is unaffected by colchicine or cytochalasin B and by the presence or absence of T cells in culture. This research supported in part by NSF grant PCM 78-13708 and by NIH RCDA AI 00291.

T-PM-A1 ROLE OF HISTONE VARIANTS IN NUCLEOSOMAL STRUCTURE. C. G. SAHASRABUDDHE. Department of Molecular Biochemistry, The University of Texas System Cancer Center M. D. Anderson Hospital and Tumor Institute, Houston, Texas 77030.

Several laboratories have reported recently the existence of nucleosomal subclasses. Most of these studies were based on the differences in electrophoretic mobilities of the nucleosomes. Unfortunately these differences in electrophoretic mobilities can be directly correlated to the length of DNA in the nucleosomes and presence or absence of histone H1, HMG 14/17 etc. One wonders if the appearance of such heterogeneity, therefore, is not due to kinetics of digestion, since in long term digestion of chromatin only nucleosomal cores are obtained. We have taken an approach to address the question of nucleosomal heterogeneity in which stripped nucleosomes are used. The stripped nucleosomes are prepared by extracting nucleosomes with 0.45 M NaCl. The use of differential affinity of nucleosomes for hydroxylapatite is made in order to fractionate stripped nucleosomes. Our results show that 10% of the stripped nucleosomes from human placenta form a structurally and compositionally different subclass. The presence of usual ladder of nucleosomal DNA repeat in this fraction shows that the fractionation is not achieved on the basis of DNA length. It is shown that there is a particular histone variant present in this subclass which is absent from the rest of the nucleosomes. Circular dichroic studies reveal that the α-helical content in the histone core of this subclass of nucleosomes is higher than the bulk. The possibility of existence of more nucleosomal subclasses is discussed.

T-PM-A2 THE RELEASE OF PHOSPHOPEPTIDES FROM HIGHLY PURIFIED CALF THYMUS DNA DURING ITS CLEAVAGE INTO SUBUNITS
R. S. Welsh and K. Vyska, Institute of Medicine, Nuclear Research Center Jülich, 517 Jülich, West Germany

The DNA (N-DNA), prepared from calf thymus nuclei under conditions eliminating the exposure of chromatin to cytoplasmic conponents, exhibits some properties not observed for DNA prepared by standard methods from the whole calf thymus tissue (S-DNA). N-DNA, having a sedimentation coefficient of 24.7S (the amount of firmly bound protein being 0.7% w/w), can be cleaved (in contrast to S-DNA) as a result of treatment with chelating agents, into stable subunits having a mean molecular weight (mw) of about 500,000 daltons. This cleavage was shown to be an ordered process, which involved no enzymatic degradation. It was accompanied by the release of phosphopeptides. The analysis of these phosphopeptides revealed the presence of two main fractions (from Sephadex G-10). One contained phosphoserine and glycine (mw of about 1400 daltons), and the other contained phosphoserine, glycine, alanine, glutamic and aspartic acids (mw of about 900 daltons). The amount of released phosphopeptides could be correlated to the extent of cleavage. At the completion of the cleavage procedure, the subunits still contain about 1/2 of the proteinaceous material as compared to that observed initially in N-DNA. This material cannot be removed by any of the treatments known to disrupt bonds of non-covalent type.

T-PM-A3 STRUCTURE STABILITY OF FILAMENTOUS BACTERIOPHAGES. G.J. Thomas, Jr. and L.A. Day, Dept. of Chem., Southeastern Massachusetts University, N. Dartmouth, MA 02747, and The Public Health Research Institute, New York, N.Y. 10016.

Laser-Raman and circular dichroism spectra of a number of filamentous bacteriophages, fd, Pf1, Xf, Pf3 and others, show that the coat proteins in each are predominantly α-helical. At concentrations approaching 100 mg/ml used in Raman studies, we have found that the subunits of Pf3 and Xf viruses can be converted to predominantly β-structures by raising the temperature. Such changes are not observed for fd and Pf1. The $\alpha \rightarrow \beta$ transitions in Pf3 and Xf are partially reversible, the transition temperatures depending on phage concentration and solution ionic strength. At concentrations of 0.1 mg/ml or less used in CD studies only small changes in conformation are observed as functions of temperature. Thus under certain conditions the structure of a virion can depend on total virus concentration. The Raman and CD spectra provide little direct information about the DNA structures in the native viruses, although features expected for classical A-type and B-type structures are not observed. The $\alpha \rightarrow \beta$ transitions are accompanied by changes in molecular environments of the DNAs as well as of aromatic side groups of the proteins.

Supported by U.S.P.H.S. grants AI 09049 and AI 11855.

T-PM-A4 KINETICS OF HEAD-TAIL JOINING IN BACTERIOPHAGE T4D: EFFECTS OF TEMPERATURE, pH, AND IONIC STRENGTH. J. A. Benbasat and V. A. Bloomfield, Dept. of Biochemistry, St. Paul, MN 55108

We have determined the effects of temperature, pH, and ionic strength on the kinetics of attachment of purified T4D heads and tails, with the aim of understanding some of the mechanistic details of this viral assembly reaction. To produce heads for the reaction, we used an osmotic shock resistant mutant deficient in tails and tail fibers ($10^-/18^-/19^-/34^-/36^-/37^-$); for tails, a $13^-/23^-$ mutant. To follow the reaction, we used quasielastic light scattering (QLS), in effect measuring the decrease in average translational diffusion coefficient of the heads as tails are attached. The head and tail concentrations were in the range 6×10^{10} and 1.2×10^{11} particles/ml respectively, corresponding to about 1 or 2×10^{-10} M. This extreme dilution, which is possible because of the high scattering power of the head, slows down the very rapid bimolecular reaction to $t_{1/2} \simeq 400$ sec. We were able to measure the QLS autocorrelation function once every 50 sec. Over a temperature range from 10°C to 37°C, the second order rate constant k increased from 0.79×10^7 M^{-1} sec^{-1} to 1.46×10^7 M^{-1} sec^{-1}. An Arrhenius plot of ln k vs 1/T was linear, yielding $E_a = 4.06$ kcal/mol as expected for a diffusion-controlled reaction; and $\Delta S^{\ddagger} = -12.6$ cal/mol-deg, corresponding to a steric factor of 1/567. This is consistent with our previous estimate based on the deviation from von Smoluchowski's diffusion-controlled reaction theory. The pH dependence of k was measured between pH 5.4 and pH 8.3. It reached a maximum of 2×10^7 M^{-1} sec^{-1} at pH 5.8. The fall-off in more acid conditions was due to destabilization of the heads. Over the range 5.8 to 8.3, the pH dependence was fit well by the ionization of a single group with pKa = 6.8. The rate constant decreased with increasing ionic strength, suggesting that the reaction brings together groups of opposite charge.

T-PM-A5 LOCATION OF HIGH MOBILITY GROUP (HMG) PROTEINS IN POLYTENE CHROMOSOMES OF DROSOPHILA MELANOGASTER. John C. Wooley, Jongsang Park, Melissa McCoy and Su-yun Chung, Biochemical Sciences Department, Princeton University, Princeton, New Jersey 08544.

HMG 14 and 17 appear to modulate nucleosome structure in regions of active chromatin. To study the role of HMGs, we have prepared antisera specific for HMG 14 and 17 (isolated from calf thymus). Using immunofluorescence, we find that the antisera binds strongly to active and potential active transcriptional (puff) sites on Drosophila melanogaster polytene chromosomes. The antisera also binds at a lower level along entire chromosomes. Although active chromatin sites are thought to be enriched, HMG 14 and 17 are probably more uniformly distributed in chromatin than suggested by the relative distribution pattern we observe. Thus, the polypeptides recognized by the anti-HMG sera might be more accessible in regions of active chromatin and/or are in an altered configuration exposing a different antigenic determinant. We are using the anti-sera to determine the Drosophila polypeptides homologous to HMG 14 and 17 of mammals. We have already identified a number of Drosophila polypeptides which appear to be HMGs based on standard criteria. These putative HMGs include 5 unique low molecular weight polypeptides in addition to D1 (65 K), previously characterized by Alfageme et al. (Chromosoma 78, 1, 1980). We term these P4 (19K), P5 (18.3K), P6 (16K), P7 (14.5K) and P8 (13.5K). Antisera to P6 show a distribution pattern very different from HMG antisera. That is, antisera to P6 react at a limited number of non-puff sites, which differ from those observed for D1 by Alfageme et al. (loc. cit.). We are now characterizing the chromosomal location of P4, P5, P7 and P8 using the immunofluorescent technique.
Research supported by NIH GM26332 and ACS CD-15.

T-PM-A6 DOMAINS OF SUPERCOILING IN CHROMOSOMES OF LIVING PROKARYOTIC AND EUCARYOTIC CELLS, Richard R. Sinden. (Intr. by T.T. Puck), University of Colorado Health Sciences Center, Department of Biochemistry/Biophysics/Genetics, Denver, CO 80262.

We have recently shown that torsional tension in the winding of the DNA double-helix can be detected in vitro and in living E. coli cells from measurements of the rate of 4,5',8-trimethylpsoralen photobinding to DNA (Sinden, Carlson and Pettijohn, Cell 21, 773-783, 1980). The rate of me$_3$psoralen photobinding to DNA is directly proportional to the negative superhelical density of the DNA. This provides a sensitive and reproducible assay for unrestrained superhelical tension in the chromosomal DNA of living cells. As nicks are introduced into the E. coli chromosomal DNA by γ-irradiation the rate of DNA-me$_3$psoralen photobinding decreases, suggesting that negative superhelical tension is relaxed. The extent of relaxation is determined by the number of nicks introduced into the DNA. Approximately 160 nicks were required to relax >95% of the tension. Chromosomes in cells in which tension was relaxed after inhibiting the intracellular DNA gyrase, photobind me$_3$psoralen at a rate independent of nicks introduced by γ-irradiation. The results are consistent with a model in which chromosomes in growing E. coli cells (mgt = 30 min) are segregated into 43 ± 10 domains of supercoiling per genome equivalent of DNA or 120 ± 30 domains per nucleoid. Analogous studies of chromosomes of cultured Drosophila and hamster cells are in progress. Supercoiled domains appear to be quite stable in cells even under conditions where a fraction of the domains are relaxed. Nascent RNA molecules do not appear to be required for the stabilization of domains of supercoiling. The number of domains per chromosome varied in cells grown at different rates in different media suggesting that the interactions defining domains of supercoiling in vivo may be dynamic.

T-PM-A7 NEUTRON SCATTERING STUDIES OF NATIVE AND TRYPSIN CLEAVED HISTONE COMPLEXES. R. D. Carlson and T. H. Kelley, Biology Department, Brookhaven National Laboratory, Upton, New York 11973.

Several specific histone complexes can be isolated from chromatin: an octamer containing 2 each of the core histones H2A, H2B, H3 and H4, a tetramer with 2 each of H3 and H4 and an H2A-H2B dimer. Studying their conformations in solution provides important information about the complexes themselves as well as their possible organization within the histone core of the nucleosome. Solution neutron scattering methods have been used to determine the radii of gyration and dry volumes of native histone complexes isolated by salt extraction at pH 7 from chicken RBC chromatin bound to hydroxyapatite columns and to provide additional information about their shapes. By then using trypsin to cleave the highly charged N-terminal tails that extend from the complexes, it has been possible in a similar manner to focus on the structure of the globular portions.

(Supported by the U.S.D.O.E.)

T-PM-A8 ORGANIZATION OF MAMMALIAN CHROMATIN AND THE RADIOSENSITIVITY OF THE NUCLEAR PERIPHERY. Arthur Cole, The University of Texas System Cancer Center, Houston, Texas 77030

Our recent studies suggest that mammalian chromosomes contain eight extended circular nucleohistone fibrils which are laterally grouped to form a sixteen stranded structure. Each of the fibrils is attached at periodic intervals to a backbone structure. The fibrils loop outward from the backbone between the attachment bands to form two classes of radiating loops; short and long. In dehistonized material the short loops extend to a well defined border about 0.5μm from the backbone while the long loops extend various distances up to about 4μm. In interphase cells the backbones appear to be organized on the inner nuclear membrane and consequently both the chromosomal backbones and the histonized short loops would be constrained to a shell of about 0.2μm thickness at the nuclear periphery. Our previous radiation studies using partly penetrating particle irradiations of cell monolayers suggest that major radiosensitive targets are constrained to a region of 0.2μm or less thickness at the nuclear periphery. Chromosomal backbone and short loop chromatin may constitute such targets. The total areas projected by these chromosomal components are compatible with optimum alpha particle action cross-sections measured for a variety of biological responses including DNA damage, chromosomal damage, division delay, and lethality. Chromosomal structures will be illustrated by stereo electron microscopic projections. (Supported in part by DOE contract DE-AS05-76EV02832).

T-PM-A9 STRUCTURE OF THE 5S RNA-L18 RIBONUCLEOPROTEIN COMPLEX FROM *ESCHERICHIA COLI* UTILIZING A REVERSIBLE, BIFUNCTIONAL CROSS-LINKING REAGENT. Linda A. Brewer. Department of Biological Sciences, Stanford University, Stanford, CA 94305.

5S RNA plays a key role in the structure and function of the ribosome. If omitted from reconstituted subunits, the 50S particles exhibit both reduced ribosomal protein complement and protein synthetic activity. The ribosomal protein which binds 5S RNA most strongly, L18, is also necessary for its stable reconstitution. Both molecules are well-characterized, thus the 5S RNA-L18 complex has been recognized as a convenient model system for studying the mechanism of specific nucleic acid-protein interactions. Further, since the 5S RNA sequences protected from nuclease digestion or chemical modification, by L18 binding, are known, it is a fertile system for the comparison of these data with those from cross-linking studies. In these experiments, complexes of ^{32}P-labelled 5S RNA (A form) and ribosomal protein L18 were formed *in vitro* by incubating the RNA with sufficient excess protein such that saturation binding occurred. Ribonucleoprotein complexes were then covalently cross-linked with the bifunctional reagent, ethylene glycol- bis-3-(2- ketobutyraldehyde) ether. In order to identify the specific sequences of 5S RNA covalently joined to L18 in the complex, the RNA was first exhaustively digested with T_1 ribonuclease. T_1 oligonucleotides cross-linked to L18 were separated from unbound sequences by Sephadex G50 chromatography, under denaturing conditions. 16% of the ^{32}P (labelling the RNA fragments) was recovered in the L18 peak. These 5S RNA oligonucleotides were released from the protein by taking advantage of the fact that glyoxal-related compounds are unstable in mild base, particularly in the absence of borate. Standard RNA sequencing methods then served to identify the sites in 5S RNA that had been joined to L18 in the complex. (Supported by AAUW and UC).

T-PM-A10 PHYSICAL PARAMETERS OF ESCHERICHIA COLI TRANSLATIONAL INITIATION FACTOR 3 BINDING TO POLY(A). Eric Wickstrom, Lois J. Wickstrom, and R. Weslie Tyson, Department of Chemistry, University of Denver, Denver, Colorado 80208 (Intr. by John R. Cann)

Study of the protein-nucleic acid interactions of IF3 may be of help in elucidating its role in binding mRNA initiation regions to 30S ribosomal subunits. The circular dichroism of poly(A) in 10 mM Na_2HPO_4, pH 7.5, 0.1 mM EDTA, 1 mM DTT, 5% glycerol is 21 M^{-1} cm^{-1} at 0°, 14 M^{-1} cm^{-1} at 25°, and 7 M^{-1} cm^{-1} at 60°. At either 6° or 25°, IF3 titrates the circular dichroism of poly(A) to an endpoint of 7 M^{-1} cm^{-1}, with a stoichiometry of 14 ± 1 nucleotides/IF3. Poly(A) saturated with IF3 at 25° may be back-titrated to the original 14 M^{-1} cm^{-1} by addition of NaCl to 160 mM. The circular dichroism titration data at 25° have been used to calculate binding densities and free protein concentrations for Scatchard plots. The Scatchard plot data have been fitted to the McGhee and von Hippel equation for ligands binding cooperatively to overlapping sites on a lattice, using LINCVX, a nonlinear least squares multiparameter curve fitting program (Scientific Programmers, Bethlehem, PA). Assuming a site size, n, of 14 nucleotides, the intrinsic binding constant, K, is (7±3) x 10^5 M^{-1}, and the cooperativity constant, ω, is 18±7. The product, $K\omega$, is thus 1.3 x 10^7 M^{-1}, close to that observed for IF3 binding to 30S ribosomal subunits. Estimates of $K\omega$ at various ionic strengths, from the NaCl back-titration data, allowed a Record plot estimate of m', the number of ionic interactions between IF3 and a single binding site, which is approximately 6. This work was supported by NIH grants GM 23248, 24128, and 27462.

T-PM-A11 CLEAVAGE CATALYZED AT APURINIC SITES IN DUPLEX DNA BY AN EXTRACELLULAR NUCLEASE FROM ALTEROMONAS ESPEJIANA. C.-F. Wei, R. J. Legerski, D. L. Robberson and H. B. Gray, Jr., Department of Biophysical Sciences, University of Houston, Houston, TX 77004 and Department of Molecular Biology, M. D. Anderson Hospital and Tumor Institute, Houston, TX 77030.

A highly purified sample of an extracellular nuclease from Alteromonas espejiana can cleave covalently modified duplex DNA under conditions for which nonmodified DNA is affected very little (Legerski et al. (1977) J. Biol. Chem. 252, 8740). Nonsupercoiled covalently closed circular PM2 DNA (PM2 DNA I°) was reacted with methylmethanesulfonate and the nuclease-catalyzed cleavage of the remaining closed circular DNA was examined. The results indicated that apurinic sites were being generated during incubation in the reaction buffer, presumably due to the loss of methylated purine bases, and that cleavage by the highly purified nuclease of the above studies was taking place at these apurinic sites. Experiments to demonstrate cleavage at apurinic sites produced directly by heating DNA I° at acid pH were inconclusive; however, these samples contained not more than two sites per molecule. Samples of the nuclease partially purified using a different initial purification step (affinity chromatography) have been observed to have different kinetic properties than does the enzyme of the above studies. When Alteromonas nuclease partially purified using affinity chromatography was incubated with PM2 DNA I° containing apurinic sites introduced by heating at acid pH, definite evidence for cleavage at apurinic sites was obtained. The rate and extent of cleavage of the modified DNA I° was dependent upon the average number of apurinic sites per molecule and cleavage was readily detectable in a sample containing an average of 2.1 sites per molecule. The results suggest that the Alteromonas nuclease can exist in a form which cleaves duplex DNA efficiently at apurinic sites. (Supported by NIH Grants GM-21839 and CA-11761)

T-PM-A12 RELATIONSHIP OF DNA DAMAGE TO MAMMARY GLAND CARCINOGENESIS, **S.M. D'Ambrosio, D. Mhaskar, J. Raber and M. Chang, Depts. of Pharmacology and Radiology, The Ohio State University, Columbus, Ohio 43210**

N-Ethylnitrosourea (ENU) is a potent chemical carcinogen to the rat mammary gland. Like many direct acting alkylators, ENU produces a variety of types of damage in cellular DNA. The majority of damage induced consist of ethylphosphotriester (approx. 60%) followed by N7 (11%) and O^6 (7.5%) ethylguanine. Alkyphosphotriesters in the DNA are alkaline labile and the resulting DNA damage detectable as single-strand breaks following sedimentation in alkaline sucrose gradients. Using this method and a recently developed sensitive method for detecting nanogram quantities of non-radiolabeled mammary DNA, we determined: a) the initial levels of ethylphosphotriesters induced; and b) the fate of such damage in 30 and 50 day old female Sprague-Dawley rats. Our data showed that: a) the initial level of damage induced was higher in the mammary gland of the 50 than in the 30 day old rat; b) damage persisted in the 30 day old rat; and c) damaged decreased over the 7 day period in the 50 day old rat. However, after correcting for the high level of mammary gland proliferation in the 50 day old rat, we find that damage also persisted at this age. These data relate the induction and persistance of DNA damage (phosphotriesters) to mamary gland carcinogenesis as a function of gland development. **Supported by NCI Contract #84226.**

T-PM-B1 DIRECT RECORDING OF INDIVIDUAL FLUORESCENCE SPECTRA FROM A FLUOROPHORE MIXTURE BY PHASE-SENSITIVE DETECTION OF FLUORESCENCE, by Joseph R. Lakowicz and Henryk Cherek, University of Maryland School of Medicine, Department of Biological Chemistry, 660 West Redwood Street, Baltimore, Maryland 21201.

Phase fluorometers are generally regarded to be lifetime instruments, an emphasis which has slowed other potential applications. Using mixtures of two fluorophores we demonstrated that phase sensitive detection of the emission allows the emission spectra of each component to be recorded individually. The simple mixtures used in our studies were TNS and PRODAN, dibenzo (c,g,) carbazole and dibenzo (a,h) anthracene, and indole and 2.3- dimethylindole.

Consider a sample containing two fluorophores, each with a different lifetime. When excited with sinuosoidally modulated light the emission is also sinuosoidal. However, this signal is composed of two sine waves, each with a characteristic phase angle relative to the exciting light. We examined these complex signals using a phase sensitive detector. Emission spectra were recorded at various phase angles relative to the exciting light. The intensities of the individual components varied differently, depending on their characteristic phase angles. Perhaps most importantly, the emission of any single component could be suppressed by choosing the detector phase to be out of phase with this component. The emission spectra we obtained overlapped precisely that of the remaining component. Our initial experiment was performed using fluorophore mixtures. However, this novel method should be of value in analysis of heterogeneous protein fluorescence, excimer and exciplex formation, and dipolar relaxation processes in proteins and membranes. Such experiments are in progress.

T-PM-B2 SECONDARY ION MASS SPECTROMETRY OF MOLLUSCAN CENTRAL NEURONS. F. Jung, P. Williams, J. E. Baker, and J. A. Connor. Dept. of Physiology and Biophysics and Material Research Lab., University of Illinois, Urbana, Illinois 61801.

In our studies of intracellular calcium regulation in molluscan neurons, ion microscopy (SIMS) appears to offer distinctive advantages over conventional techniques in the measurement of sub-micromolar ion concentration. High sensitivity, high mass resolution, and the capability of providing 2- or 3-dimensional profiles of ion concentrations are some of the advantages. We have obtained mass spectra and 2-dimensional images of intracellular Na^+, K^+ (or NaO^-), and Ca^{2+} distributions in the pleural and pedal ganglion cells of Archidoris monteryensis, a marine gastropod mollusc. In one technique, conventional chemical fixation and embedding was used. In a second technique, freeze-substitution (Van Zyle et al. (1976) Micron 7: 213-224) was used in order to minimize leaching of diffusible ions. These freeze-substituted samples were embedded and polymerized in resin without ethanol dehydration. Sections 5 μ thick were floated onto small drops of water (chemically fixed samples) or a thin film of polyethylene glycol or hexylene glycol (freeze-substituted samples) on gold-sputtered coverslips. By moderate heating, the excess liquids were evaporated and the sections flattened onto the coverslips. The dried sections were again gold-sputtered. The results demonstrated that relatively sharp ion images of neurons can be obtained. In addition, distinctive differences in ion concentrations can be seen between the nucleoplasmic and cytoplasmic zones. Further work is required to calibrate the mass spectra in order to interpret the concentrations in absolute terms. (Supported by HEW GM 7283 to F. J. and HEW-PHS-NS 15186 to J.A.C.)

T-PM-B3 POINT-PROJECTION IMAGING OF MACROMOLECULE CONTOURS;* J. A. Panitz,# Sandia National Laboratories,† Albuquerque, New Mexico, 87185.

Since the early 1950's, attempts have been made to image biomolecules with field-electron and field-ion techniques. We are currently developing a point-projection, field-desorption microscopy which appears to be capable of imaging the morphological contour of macromolecules deposited on tungsten substrates at magnification approaching 10^6. Since no lenses are used, and the imaging process is immune to external vibration, image sharpness and contrast is extremely high. Recent images obtained for a 100Å diameter globular protein, ferritin, have demonstrated ≈30 angstrom spatial resolution. The images are reproducible from day-to-day and unaffected by repeated substrate exposed to laboratory ambient, suggesting the imaging process is non-destructive. By photographing molecular contours at successively higher desorption fields, quasi-three-dimensional images of clusters of ferritin molecules have been obtained.

*This work was supported by the U.S. Department of Energy under Contract DE-AC04-76-DP00789.
†A U.S. Department of Energy facility.
#In collaboration with I. Giaever, The General Electric Research and Development Center, Schenectady, New York, 12301.

T-PM-B4 A NEW METHOD FOR MEASURING DENSE PIGMENTS. L.E. Lipetz, Div. Sensory Biophysics, The Ohio State University, 1314 Kinnear Road, Columbus, Ohio 43212.

A new method of indirectly measuring the absorption spectrum and peak optical density, Dp, of a highly dense pigment sample is to: (1) measure the absorption spectrum of a sample whose pigment optical pathlength has been reduced, (2) measure the short-wavelength cutoff, λc, of an intact sample, (3) calculate Dp from these measurements, either analytically by the equations given below, or graphically by computer. In theory the results of this method are independent of the presence of stray light in the measuring instrument. λc is defined as the wavelength intercepted at the value of minimum transmittance, M, by the line tangent to the transmittance curve at Tmid, where Tmid = 0.5(M + 1).

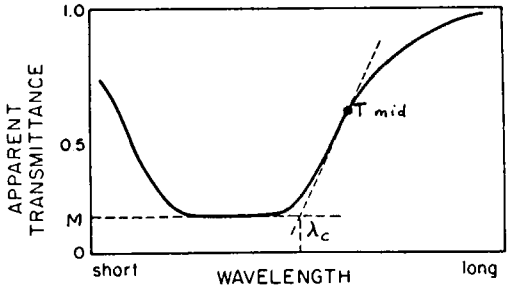

If in the spectral region used to find λc, log D (density) = $a\lambda + b$, where a and b are constants, then λc can be calculated analytically from: $\lambda c = (1/a)(-b - \log Dp + \log(-\log 0.5 - \log(\text{antilog}(-Dp) + 1)) + ((\log e)^2 (\text{antilog}(-Dp) - 1)/(\text{antilog}(-Dp) + 1)(\log 0.5 + \log(\text{antilog}(-Dp) + 1))$. As Dp increases, this equation approaches: $\log Dp = -a\lambda c - b + 0.10516$. For spectra not meeting these criteria, the definition of λc can be used to compute graphically the values of λc for various assumed values of Dp, using the spectrum of (1) above. This gives Dp for any measured λc. Applications will be illustrated.

T-PM-B5 CELL-SUBSTRATE CONTACTS ILLUMINATED BY TOTAL INTERNAL REFLECTION FLUORESCENCE. Daniel Axelrod, Biophysics Research Division and Dept. of Physics, University of Michigan, Ann Arbor, Michigan 48109.

A technique for exciting fluorescence exclusively from regions of contact between cultured cells and the substrate is presented. The technique is an application of total internal reflection (TIRF) to cellular microscopy and is an extension to fluorescence of the total internal reflection microscope illumination system introduced by E.J. Ambrose (1961) to detect light scattered at cell-substrate contacts. The evanescent wave of a totally internally reflecting laser beam excites only those fluorescent molecules in the cell membrane or submembrane within 1000 Å or less of the substrate surface. Fluorescent light is gathered through the conventional epifluorescence system of the microscope. Demonstrations of this technique are presented for two cell types growing on glass substrates. On rat primary myotubes labeled by fluorescent α-bungarotoxin, TIRF brightly visualizes the dense acetylcholine receptor patches which are known to localize at cell-substrate contact regions, but not the more diffusely distributed acetylcholine receptors elsewhere on the myotubes. On human skin fibroblasts labeled by a fluorescent lipid probe, the cell-substrate contact regions are seen to run in bands often parallel to the straight edges of the cells. Increasing the depth of the evanescent wave (by decreasing the angle of incidence of the totally internally reflecting laser beam) excites a larger portion of the cell surface near the substrate. TIRF illumination is easily interchangeable with epifluorescence and phase contrast. The technique appears to have promising applications, including dramatic reduction of autofluorescence from debris and thick cells, visualization of the membrane and underlying cytoplasmic structures at cell-substrate contacts, mapping of membrane topography, and visualization of reversibly bound fluorescent ligands at membrane receptors. (Sup. by PHS NS 14565).

T-PM-B6 SORTING OF AGING IMR90 FIBROBLAST CULTURES USING FORWARD ANGLE LIGHT SCATTER AND AUTOFLUORESCENCE. R.O. Kelley, B.D. Perdue and L.F. Marek, Department of Anatomy, University of New Mexico, School of Medicine, Albuquerque, NM 87131.

Considerable structural and metabolic heterogeneity develops in late passage cultures of diploid fibroblasts (IMR90), factors which complicate studies of cell populations as uniform systems for experimental analyses of aging (Hayflick, Exp. Cell Res. 37: 614, 1965). To segregate subpopulations in late passage cultures, we have used a fluorescence activated cell sorter to separate cells on the basis of light scatter and autofluorescence from an argon ion laser operating at a wavelength of 488nm. Early passage cultures (up to population doubling level, PDL, 40) have a single population of cells which exhibit a narrow graphic distribution for light scatter and autofluorescence. Electron microscopy reveals that cells from this population are uniform in shape, volume and ultrastructure. In contrast, late passage cultures (greater than PDL 53) exhibit at least two subpopulations which can be separated on the basis of differential light scatter and autofluorescence. The subgroup with lowest levels of light scatter and autofluorescence is similar in size, shape and ultrastructure to early passage cells. The other subpopulation exhibits increased forward angle light scatter; increased autofluorescence; multipolar cell shapes; and heterogeneity of nuclear organization; and, in addition, fails to incorporate ^{3}H-thymidine for up to 48h following plating after sorting. We conclude that cells with properties of increased light scatter and autofluorescence have traversed into the phase III period of senescence. In addition, caution is urged when examining features of aging using heterogeneous, late passage cell populations. (Supported by AG00191 from NIH).

T-PM-B7 CHARACTERIZATION OF ARSENAZO I AS AN INDICATOR FOR THE SIMULTANEOUS DETERMINATION OF pH AND pMg. Paul De Weer, Linda A. Freeman, and Ronald W. Ratzlaff. Department of Physiology and Biophysics, Washington University School of Medicine, St. Louis, MO 63110.

The metallochromic indicator dye 3[(2 arsonophenyl)azo]-4,5 dihydroxy-2,7 naphtalene disulfonic acid (Arsenazo I, Neothorin, Uranone) was obtained commercially, freed of impurities by molecular sieving chromatography, and studied spectrophotometrically. The dye has a wide absorption peak (ϵ = ~ 2.5 x 10^4/M.cm) around 500 nm, which broadens with rising pH. Upon complexation with divalent metals (affinity: Mg > Ca > Sr > Ba), the absorption maximum shifts towards ~ 540 nm. At ~560 nm, where the differential molar absorptivity of the Mg complex is maximal (~ 2 x 10^4/M.cm), the molar absorptivity of the free dye is only ~ 3 x 10^3/M.cm. The dye forms 1:1 complexes with Mg over a wide concentration range and, at physiologic pH, loses 1-2 protons in the process. The relevant pKa's (~7.5 and ~10.5, varying with ionic strength) can be titrated spectrophotometrically. A simple equation accurately describes the dye's behavior in the physiologic ranges of pH and pMg. K_m (Mg) is ionic strength- and pH-dependent, and is in the millimolar range for physiologic pH values. Only three dye forms are present in appreciable concentrations: monoprotonated, diprotonated, and metal-bound. Pure spectra for these species were generated and least-squares fitted to empirical equations. Mixed spectra from solutions of unknown pH and pMg were resolved into their components, and the corresponding pH and pMg computed. Isobestic points, and wavelengths for maximal sensitivity to either pH or pMg changes could be determined from first principles. The dye may find application in the simultaneous determination of intracellular pH and pMg. Supported by NIH grant NS 11223.

T-PM-B8 APPLICATIONS OF THE CARBON SURFACE ELECTRODE FOR VOLTAGE CLAMPING, pH, AND MEMBRANE POTENTIAL STUDIES. A. Strickholm, Physiology Section, Medical Sciences Program, Indiana University, Bloomington, IN. 47405

A major technical problem in voltage clamping small diameter axons with the axial wire technique is that small diameter wires are required for the current electrode. If platinum wire is used, they are extremely fragile and difficult to maintain straight for the long wire lengths required. Secondly, the roughness of metallic surfaces readily destroys membrane integrity if contact is made with the axon surface. These technical problems have made difficult axial wire voltage clamping of small axons, and have thus limited progress in comparative electrophysiology. A solution to these problems appears possible by utilizing carbon surface or carbon fiber electrodes. These electrodes can be made by coating platinum wire with precursor material and pyrolizing in an inert atmosphere at 500 to 1000 ^{0}C. Alternatively, carbon fibers (ca, 7 to 15 um dia.) can be used which are available from commercial manufacturers. A unique feature discovered with these electrodes is that intracellular surface contact in axons produces minimal or no damage. The carbon fibers are extremely strong, they can be flexed 180^0, and recover with no kinking or permanent bends, features which are impossible to duplicate with platinum. The specific resistivity of the fibers ranges down to 10 ohm cm and the current passing ability compares with the platinum surface if the carbon surface is oxidized. Upon oxidizing the carbon surface, dissociable groups are produced which are pH sensitive and thus serve as a pH electrode. The oxidized carbon electrode can thus measure potential changes if axoplasm pH is stable or buffered. Experimental results with these electrodes will be described. (Supported by a Grant-in-Aid from the Northeast Indiana Chapter and the Indiana Affiliate of the American Heart Association).

T-PM-B9 SURFACE TENSION AT LOW LUNG VOLUMES: DEPENDENCE ON TIME AND ALVEOLAR SIZE. Samuel Schürch and Donald J.L. McIver. Departments of Biophysics, Medicine and Pharmacology, University of Western Ontario, London, Ontario, Canada. N6A 5C1.

We have measured surface tension in individual alveoli by observing the spreading properties of fluorocarbon test fluid droplets placed by micropipette on the alveolar surfaces. The test fluids were calibrated on monolayers of dipalmitoyl phosphatidyl choline and purified lung surfactant spread at the air-saline interface of a captive bubble. The air bubble was floated by buoyancy against a ceiling of 0.5% agar. The bubble surface tension could be altered by inflating and deflating the bubble in a similar way to changing the monolayer surface tension in a Langmuir surface tray. The value of the surface tension was determined by shape analysis for a sessile drop. Test fluid droplets were placed by micropipette onto the upper, flat bubble surface and the diameters of these droplets were measured by means of a microscope. In excised cat lungs held at 40% total lung capacity (FRC) and 37°C the surface tension remained below 1 mN.m^{-1} for about 10 min, and then increased slowly in a linear fashion to 9 mN.m^{-1} in 70 min. The low minimum surface tension of less than 1 mN.m^{-1} at 37°C and the extraordinary stability of surface tension with time at FRC are in good agreement with the film behaviour calculated from pressure-volume plots of intact lungs. During stepwise deflation from 70% total lung capacity to FRC the surface tension changed from approximately 10 mN.m^{-1} to less than 1 mN.m^{-1}. At each step during deflation we compared surface tension in alveoli of differing size and location. We measured equal surface tensions in very large alveoli, about 500 µm in diameter at the edge of a lung lobe and in alveoli of average size (100-200 µm) in diameter. At any given lung volume we were unable to detect a relationship between alveolar size and alveolar surface tension. (Supported by the M.R.C.)

T-PM-B10 IMAGE ANALYSIS OF FLUID FLOW AND PARTICLE MOTION IN THE VASCULAR SYSTEM. M.H. Sherebrin, Department of Biophysics, University of Western Ontario, London, Canada. N6A 5C1.

The analysis of motion using a video input to a digital computer has many applications in the study of blood flow. Tyml and Sherebrin (1) have developed a system using this method to measure red cell velocities in capillaries. The algorithm used was based on a pattern shifting and matching routine which was 100 times faster than the cross-correlation function tried initially. The two functions were compared with a computational model using moving and changing patterns. It was important to allow dispersion of the pattern with time because red cells and plasma gaps do not move uniformly through the capillary but often exhibit relative motion. The correlation function was compared to the absolute difference function used in the matching routine to determine the accuracy of the results and as a measure of the dispersion of the pattern with time. The latter also may be useful as an index of mixing during gas exchange in the capillary. (Computer equipment was purchased through MRC grants MA3336, MA5598 and DRB grant 8960-02.)

(1) Tyml, K. and M.H. Sherebrin. Microvasc. Res. 20: 1-8 (1980).

T-PM-B11 EVALUATION OF RIGHT HEART-PULMONARY UNIT (RHPU) BY USE OF Xe-133 IN SALINE. Shiv K. Gupta, Nilo E. Herrera, Richard P. Spencer, Thomas W. Crucitti. Dept. Nuclear Medicine, Univ. Connecticut Health Center, Farmington, CT 06032 and Danbury Hospital, Danbury, CT.

Output of the right side of the heart, barring shunts, is entirely to the lungs. The RHPU can be potentially investigated, noninvasively in the intact individual, by means of radiotracers which traverse this pathway. A tracer which remains within the vascular tree (such as radiolabeled red cells) can be used to estimate both right heart and left heart ejection fractions as well as intrapulmonary transit. However, such radiolabels stay in the system and thus interfere with rapid repeat examinations; in addition, the labeled red cells do not provide information on pulmonary gas exchange. We thus investigated the intravenous administration of a bolus of Xe-133 gas in saline, to estimate the right heart ejection fraction (as well as the established use in following gas exchange). In 3 healthy volunteers, the right ventricular ejection fraction (RVEF) was followed with a Baird 77 multicrystal scintillation camera. The RVEF was first determined by use of a bolus of 15 mCi of Xe-133 in saline. After the gas had cleared, the RVEF was also determined (again on first pass) by means of the soluble radiotracter Tc-99m-pertechnetate. Agreement between the values determined by the 2 methods was good (44 vs 49, 56 vs 57, and 46 vs 46% for RVEF). Thus the gas in saline could be used to measure RVEF on its first pass. Subjects were also attached to a rebreathing apparatus. As the Xe-133 cleared from the circulation, the patients rebreathed the gas, allowing estimates to be made of its intrapulmonary distribution. Intravenous Xe-133 in saline may allow a low radiation dose, and readily repeated, evaluation of RVEF as well as pulmonary function in suspected right heart disorders due to pulmonary disease. (Suppored by USPHS CA 17802 from the National Cancer Institute).

T-PM-B12 HIGH RESOLUTION ^{31}P NUCLEAR MAGNETIC RESONANCE SPECTROSCOPY OF DISEASED MUSCLE. T. Glonek*, M. Bárány and D.D. Doyle*, Chicago College of Osteopathic Medicine, Chicago, IL 60615 and University of Illinois Medical Center, Chicago, IL 60612

At 180-200 MHz and with a 20 mm probe filled with intact muscle, high resolution ^{31}P spectra may be obtained in only a few minutes. The concentration of phosphate metabolites in the muscle may be quantitated from the integrals of the peaks calculated by the computer of the spectrometer, the total phosphate content of the muscle determined after ashing, and the ATP content of the muscle determined by any analytical method. When the total phosphate and ATP content of a muscle is known, the concentration of phosphate metabolites may be calculated from the peak integrals directly. With this procedure we have found, in normal and hereditary dystrophic chicken pectoralis muscles, respectively, the following quantities of phosphate metabolites (μmole per gram muscle): 2.5 and 2.4 sugar phosphates, 6.0 and 7.1 P_i, 24.9 and 22.4 PCr, 7.1 and 4.2 ATP, 0.9 and 0.7 NAD. The dystrophic muscle also contained 1.0 μmole SEP/g. The breakdown of PCr followed first order kinetics, under anaerobic conditions, with rate constants of 0.011 and 0.024 min^{-1}, for normal and dystrophic muscle, respectively. At 200 MHz and with a 12 mm probe, using a 0.5 ml microcell assembly, we analyzed perchloric acid extracts from diseased human muscles. The glycerol 3-phosphorylcholine content of these muscles showed the greatest variation of the phosphates present, 0.05 to 4.6 μmole/g. Several muscles contained unusually high fructose-1,6-diphosphate concentrations, over 20 μmoles per gram muscle. (Supported by MDA).

T-PM-C1 ROD OUTER SEGMENT PERIPHERAL ENZYMES EXCHANGE BINDING SITES. David F. O'Brien, and Patricia N. Tyminski, Eastman Kodak Company, Research Laboratories, Rochester, NY 14650.

Light exposure of rhodopsin in rod outer segment (ROS) membranes results in activation of several GTPase and cyclic nucleotide phosphodiesterase (PDE) molecules. These peripheral membrane enzymes may be extracted from dark-adapted bovine ROS by hypotonic washes. Recombination of these enzymes with well-washed ROS or rhodopsin-phospholipid membrane vesicles in isotonic media restores the light-induced GTPase and PDE activities to levels similar to that observed in the unwashed ROS. The activity is independent of the lipid composition of the vesicles, which indicates the enzyme binding sites are associated with some of the rhodopsin molecules in the membranes. The light-induced enzyme activity remains with the pellet rather than the supernatant if the light-exposed membranes are rapidly sedimented; therefore, the activated enzymes are bound to the membranes. Light-exposure of enzyme-free membrane vesicles followed by mixing in the dark with unwashed ROS yields activation of some of the enzymes originally present on the unwashed and unexposed ROS. Subsequent light exposure of the mixture fully activates the remaining enzymes. These results indicate the peripheral enzymes exchange binding sites between membrane vesicles, and suggest the possibility that light-activation of the enzymes in rods is accomplished by movement of the enzymes to the bleached rhodopsin.

T-PM-C2 IDENTIFICATION OF THE CYCLIC GMP PHOSPHODIESTERASE INHIBITOR OF BOVINE RETINAL ROD OUTER SEGMENTS. James B. Hurley and Lubert Stryer, Dept. of Structural Biology, Sherman Fairchild Center, Stanford University School of Medicine, Stanford, CA 94305.

The phosphodiesterase (PDE) specific for cyclic GMP was extracted from bleached rod outer segments and purified by hexylagarose chromatography followed by HPLC gel filtration. The purified PDE appeared as three bands (88, 84, and 13 kdal) on SDS polyacrylamide gels. Purified PDE was activated by passing it through a trypsin-agarose column. The rate of activation of PDE corresponded to the rate of disappearance of the 13 kdal polypeptide. Heat treatment of purified PDE (3 min at 100 °C) at pH 2.5 or 12 precipitated the 88 and 84 kdal polypeptides, leaving the 13 kdal polypeptide in solution. Addition of this supernatant decreased the V_{max} of the trypsin-activated PDE (tPDE) by more than 99%. Trypsin degraded the inhibitory activity of this preparation. A 0.4 nanomolar solution of tPDE was 50% inhibited by addition of an equimolar amount of the 13 kdal polypeptide. We conclude that the PDE is inhibited by its 13 kdal subunit. The GNP complex of transducin (Fung, Hurley, and Stryer, PNAS, in press) activates the PDE to the same maximal level as does treatment with trypsin. This finding suggests that inhibition of the PDE by its 13 kdal subunit is relieved in vivo when GTP-transducin interacts with PDE. Supported by a grant from the National Eye Institute. JBH is a Helen Hay Whitney Fellow.

T-PM-C3 ROD LIGHT-INDUCED GTP BINDING AND PDE ACTIVATION HAVE THE SAME SENSITIVITY, KINETICS AND ATP REGULATION. P.A. Liebman, Dept. Anat. and E.N. Pugh, Jr., Dept. Psychol., Univ. of Pennsylvania, Philadelphia, PA 19104

Like the hormonally activated RBC cyclase system[1] light activated RDM bind and subsequently hydrolyse GTP, leaving membrane-bound GDP as product[2] Both RBC cyclase and RDM phosphodiesterase require GTP or its analogs to be bound for activation. If GTP binding and PDE activation are causally linked in the activation of a multienzyme pool by a single laterally diffusing R*, as proposed in the Liebman-Pugh hypothesis;[3,4] both the light-sensitivity and the kinetics of GTP binding should match those of PDE activation. We have measured the light sensitivities and kinetics of α-^{32}P binding of GTP and of PDE activation with non-hydrolysable GTP-γ-S or GNPP(NH)P in several species;[5] and find them identical within our sensitivity and time resolution. Furthermore, when ATP is present we find a severe reduction in number of α-^{32}P's bound and in the PDE activity caused by a single R*, consistent with the hypothesis that the R* state can be quenched via phosphorylation[4] in a fraction of a second. Thus, as previously outlined, RDM contain a two stage molecular amplifier. In the first stage, a single bleached rhodopsin, R*, diffuses laterally to form brief encounter complexes with a series of GTP-binding activator proteins, Γ, to which it (R*) catalyses firm binding of GTP, forming Γ*·GTP's. The Γ*·GTP's each convert a dormant cGMP phosphodiesterase, D, to the active form, Γ·GTP·D*, which can hydrolyse cGMP in a second stage amplification. Deactivation occurs in two steps; by hydrolysis of GTP to form Γ·D.GDP and by rhodopsin-kinase-mediated, ATP phosphorylation of R*. Supported by EY00012, EY01583 and EY00102.

[1]Cassel and Selinger, PNAS 75:4155, 1978.
[2]Fung and Stryer, PNSA 77:2500, 1980.
[3]Liebman and Pugh, Vis. Res. 19:375, 1979.
[4]Liebman and Pugh, Nature 287:734, 1980.
[5]Pugh and Liebman, Fed. Proc. 39:1815, 1980.

T-PM-C4 A PHOTON CORRELATION SPECTROSCOPY/INTEGRATED OPTICS STUDY OF PHOTORECEPTOR MEMBRANE. J. C. Selser, IBM Research Laboratory, San Jose, California 95193, K. J. Rothschild, Departments of Physics and of Physiology, Boston University, Boston, Massachussetts 02215, J. D. Swalen, IBM Research Laboratory, San Jose, California 95193 and F. Rondelez, Solid State Physics, College de France, 75231 Paris Cedex 05, France.

A new light scattering method of studying membrane dynamics is reported. In this method, the techniques of photon correlation spectroscopy and guided wave optics are combined and as a result, the dynamics of membrane systems can be investigated noninvasively and without the use of labels. In particular, the dynamics of thin films consisting of a multilamellar array of photoreceptor membrane were studied using the new method. The autocorrelation spectra of samples studied were single exponential in form exhibiting a typical relaxation time of 3/4 second. If these spectra result from spontaneous concentration fluctuations of the membrane protein, rhodopsin, the corresponding rhodopsin lateral diffusion coefficient is 3×10^{-11} cm^2/sec, a value consistent with protein lateral diffusion measurements in other multibilayer films. It is important to note that this new method probes dynamics on a scale of the order of the wavelength of the exciting laser light - a scale which is useful since it is intermediate between that probed locally by labels used in measuring membrane reorientational motion and the $\sim$1 micron scale employed in photobleaching measurements of membrane protein lateral diffusion.

T-PM-C5 UTILIZATION OF EXOGENOUS RETINOIDS BY BULLFROG PHOTORECEPTORS. Jay I. Perlman and David R. Pepperberg. Dept. of Biol. Sci., Purdue Univ., W. Lafayette, IN 47907

Isolation of the vertebrate retina from the back of the eye typically blocks the regeneration of (substantial amounts of) visual pigment in the rod photoreceptors, presumably by interrupting the supply of (an as yet unidentified) retinoid to the rods. We have examined which of several naturally occurring retinoids can promote the formation of rhodopsin and the related component of dark adaptation in bleached rod photoreceptors of the isolated bullfrog retina. In separate spectrophotometric and electrophysiological experiments, we measured transretinal absorbance and aspartate-isolated photoreceptor potentials (rapid PIII responses) before and after the treatment of bleached retinas with sonicated suspensions containing retinoid and (carrier) phosphatidyl choline.

Treatments with either 11-*cis* retinal or 11-*cis* retinol promote large recoveries in the responsiveness of the photoreceptors (decreases in threshold of 0.7-1.1 log units from the stable value attained after ~90% bleaching). These two retinoids also induce the formation of rhodopsin in the photoreceptors. The time required for 50% regeneration of the bleached pigment ($t_{\frac{1}{2}}$) ranges between 20-50 minutes with molar excesses of 11-*cis* retinal of $\geq$ 10 moles per mole opsin. Regeneration with 11-*cis* retinol is slower; $t_{\frac{1}{2}}$ is 200-300 minutes for similar molar excesses of the 11-*cis* retinol. Regeneration with 11-*cis* retinol is specifically inhibited by 10 mM HEPES; this finding argues against the possibility that the effects attributed to 11-*cis* retinol reflect the action of (contaminating) 11-*cis* retinal in the applied suspensions. The all-*trans* isomers of retinyl palmitate, retinol, and retinal lack sensitizing activity, and do not induce the formation of rhodopsin; treatments with these retinoids do not abolish the activity of (subsequently applied) 11-*cis* retinal. (supported by NIH Grant EY-02103.)

T-PM-C6 ARSENAZO III-Ca^{2+}: EQUILIBRIUM BINDING AT DIFFERENT pH EVALUATED WITH Ca-ION SENSITIVE ELECTRODE AND ABSORBANCE MEASUREMENTS. B. Rydqvist* and H. Mack Brown. (SPON: J.W. Woodbury). Dept. of Physiol.; Coll. of Med.; Univ. of Utah; Salt Lake City, Utah, 84108.

Arsenazo III (AIII) has been widely used as an indicator for free intracellular Ca^{2+} in biological systems. Two main problems persist in the application of the dye 1) the stoichiometry of the binding between Ca^{2+} and AIII and 2) the dependence on pH of absorbance changes and the dissociation constant (K_D) of the reaction. AIII solutions were assayed with a Ca-ion sensitive electrode (Ca-ISE). Absorbance changes were measured in a Cary 11 spectrophotometer and a dual wavelength spectrophotometer.

Job plots from equimolar mixtures of AIII and $CaCl_2$ showed that the stoichiometry for the reactions between AIII and Ca^{2+} is 1:1 for a number of experimental conditions. Scatchard plots from $CaCl_2$ titrations were also consistent with 1:1 binding. pH titration of AIII solutions showed that absorbance changes deviate considerably from changes in Ca-AIII determined with Ca-ISE beyond pH 5 and 8. This indicates pH dependence of the extinction coefficient. Between pH 6-8, the absorbance changes follow Ca-AIII formation. Absorbance changes of AIII solutions at low Ca^{2+} concentration showed considerable differences of pH dependent absorbance changes at 650 nm and 620 nm both in the Cary 11 and the dual wavelength spectrophotometer.

The dissociation constant (K_D) for the binding between Ca^{2+} and AIII was calculated in both pH titrated and $CaCl_2$ titrated solutions and in equimolar mixtures of AIII and $CaCl_2$. The mean value for the different methods was 12 μM at pH 7.25. The K_D value was heavily dependent on pH in the physiological range (i.e. around pH 7). (NIH Grant #EY 00762 and Swed. Med. Res. Counc. Grant #K79-14R-5539).

T-PM-C7 RAPID-SCANNING PHOTOMETRIC EXAMINATION OF INTRACELLULAR ARSENAZO III IN *LIMULUS* VENTRAL PHOTORECEPTORS. H. H. Harary and J. E. Brown, Dept. Physiology and Biophysics, SUNY, Stony Brook, N.Y. 11794

We have examined two questions implicit in the interpretation of light-induced changes of arsenazo III (A III) absorbance in *Limulus* ventral photoreceptors: (1) How does the spectrum of intracellular A III compare with the A III-Ca^{++} signature spectrum in a cuvette? (2) Does the intracellular Ca^{++} concentration (Ca_i) change uniformly throughout the photoreceptor? To address the first question we have constructed a novel rapid scanning microspectrophotometer which recorded A III absorption spectra from 450-750 nm every 16 msec during the light response of a ventral photoreceptor. These absorption spectra indicate that for early times during the photoreceptor's response to the onset of prolonged illumination (128 to 650 msec) the absorbance peaks at 660 and 610 nm rise together indicating an increase in Ca_i. During later times (640 msec to 3.2 sec) the peak at 660 nm falls more slowly than that at 610 nm. We examined the question of spatial uniformity of changes in Ca_i by scanning the absorbance change of A III across many points along the length of single cells at 660 nm. The absorbance profile scanned along the length of the cell indicated that Ca_i was highly localized usually in one region of the cell at times immediately following the beginning of illumination and at later times Ca_i began to diffuse throughout the cell. Therefore, photometric measurements of A III spectra that average over the whole cell produce a distorted view of the intracellular Ca^{++} kinetics. Because the shape of the Ca^{++}-A III spectrum depends on the relative concentration of Ca^{++} to dye, the non-uniformity of the light-induced increase of Ca_i might account for the differences between the average intracellular Ca-A III spectra measured at early and late times. Alternatively, these differences may be due to the binding of H^+ or Mg^{++} to the intracellular dye. Supported by NIH EY-01915.

T-PM-C8 THE EFFECT OF EXTERNAL CALCIUM ON THE LIGHT-INDUCED INCREASE OF INTRACELLULAR Ca^{2+} IN *LIMULUS* VENTRAL PHOTORECEPTORS. J.D. Owen*. Department of Physiology, College of Medicine, University of Utah, Salt Lake City, Utah, 84108.

Intracellular ionized calcium concentration, Ca_i, was measured in dark-adapted and light-adapted cells under three different conditions using calcium selective microelectrodes with tip diameters of less than one micrometer containing the calcium salt of the exchanger, di-(p-(1,1,3,3-tetramethylbutyl)phenyl)phosphoric acid (t-HDOPP): 1) in normal *Limulus* seawater containing 10 mM $CaCl_2$, 2) isosmolar $CaCl_2$ seawater and 3) 1% $CaCl_2$ (sucrose substituted) seawater. In the control situation, Ca_i was about 3×10^{-7}M in dark-adapted cells and Ca_i increased to 7×10^{-7}M upon exposure to bright white light. In isosmolar calcium chloride, there was no increase in Ca_i with light, but in 1% $CaCl_2$ the increase in Ca_i was larger than in the control. In 1% $CaCl_2$, the Ca_i increased to approximately 2×10^{-6}, or almost three times larger than in the control.
(Supported by NIH Grant #EY 02403 from the National Eye Institute)

T-PM-C9 CHANGES IN INTRACELLULAR H^+ AND Ca^{2+} IN *BALANUS* PHOTORECEPTOR ASSESSED WITH ION-SENSITIVE ELECTRODES AND INDICATOR DYES. H. Mack Brown* and B. Rydqvist. Department of Physiology, University of Utah, Salt Lake City, Utah, 84108.

The role and interrelationship of changes in intracellular free Ca^{2+} and H^+ in *Balanus* photoreceptor are being investigated with ion sensitive electrodes (ISE) in conjunction with microspectrophotometry of cells injected with indicator dyes Phenol Red (PR) and Arsenazo III (AIII). The intent is to validate absorbance changes of the dyes by comparing them with the more easily quantified but slower responding ISE.

The pH_i changes calculated from absorbance changes of PR injected cells deviate from pH_i changes obtained with pH-ISE. This was the case for light induced pH changes as well as cells rendered acidic with CO_2 salines. Such cells show only a fraction of the pH change indicated by pH-ISE; the fraction varied with PR concentration.

pH_i and Ca_i changes were investigated in cells injected with AIII and $10K_D$ Ca_f/EGTA. Theoretically predictable changes in Ca_f should be obtained by acidifying the cells to a known pH. Acidifying the cytolsol by 0.5 pH unit (pH-ISE) produced a membrane hyperpolarization and abolished the receptor potential; Ca-ISE indicated a transient increase in pCa_i to 5.2. AIII absorbance changes at 650 nm, corrected for the influence of pH, indicated a pCa_i of about 5.3, in good agreement with the Ca-ISE. The time course of Ca_i recovery monitored by AIII and Ca-ISE was more rapid than pH_i monitored by AIII and pH-ISE. Recovery of the resting potential followed a time course similar to recovery of Ca_i whereas the receptor potential recovered with a slower time course more similar to pH_i recovery.
(NIH #EY 00762)

T-PM-C10 DOES A CHANGE IN CYTOSOLIC pH MEDIATE LIGHT-ADAPTATION IN LIMULUS VENTRAL PHOTORECEPTORS? J. E. Brown, Dept. of Physiology and Biophysics, SUNY, Stony Brook, N.Y. 11794 (Intr. by Tazewell Wilson)

A rise of cytosolic calcium ion concentration (Ca_i) has been proposed to be a messenger for light-adaptation in Limulus ventral photoreceptors. Consistent with that proposal, light induces a rise of Ca_i as determined both by aequorin and arsenazo III. Recently it has been suggested that the light-induced rise of Ca_i causes a rise of cytosolic H^+ concentration and that these H^+ are a messenger for light-adaptation. To test this suggestion, the potassium salt of the H^+ buffer MOPS (morpholino propane sulfonic acid) at pH 7.2 was pressure-injected inside cells previously injected with aequorin. The injection volume was determined by inclusion of $^{35}SO_4$ in the injected solutions; the intracellular concentration of the injected MOPS was calculated to be greater than 150 mM. The stimulus-induced increases in aequorin luminescence were unchanged by these large increases of cytosolic H^+ buffering capacity. Also, Ca^{++} was iontophoretically injected into photoreceptors during stimulation by repetitive flashes causing decreases in the responsiveness of the photoreceptors. These Ca^{++}-induced decreases in responsiveness were unchanged after injection of MOPS at pH 7.2 to greater than 150 mM inside the cells. Moreover, in cells injected to greater than 150 mM MOPS, there was no noticeable change in the waveform (initial transient declining to a plateau) of the voltage-clamp currents elicited by prolonged, bright stimuli. Therefore, it is unlikely that either (1) the Ca^{++}-induced decrease of responsiveness, (2) the light-induced increase of Ca_i or (3) light-adaptation is mediated by a light-induced change of cytosolic H^+ concentration in Limulus ventral photoreceptors.

Supported by NIH EY-01914 and EY-01915.

T-PM-C11 EXCITATION OF LIMULUS PHOTORECEPTORS IN THE DARK: A NEW PHARMACOLOGY OF VISUAL TRANSDUCTION.

D.W. Corson*, A. Fein and C. Shaw*, Marine Biological Laboratory, Woods Hole, Ma 02543

Discrete waves of depolarization are the unit response to photon absorptions in Limulus ventral photoreceptors. Discrete waves can now be elicited in the absence of light by injection of either fluoride, vanadate or GTP-γ-S (guanosine-5'-O-(3-thiotriphosphate)). Discrete waves elicited by these compounds have similiar waveforms to light-induced discrete waves. Both light-induced and pharmacologically-induced discrete waves undergo light adaptation following exposure to a bright adapting flash. In the presence of the pharmacological agents, responses to test flashes are prolonged. We tentatively conclude that all these pharmacological agents induce a process similiar or perhaps identical to visual excitation of the photoreceptor.

Pharmacological agents were injected in the photoreceptors by 1 nA hyperpolarizing currents from electrodes containing 100 mM solutions of the agents. Fluoride-containing electrodes were slightly acidified with HF to facilitate ejection of F^-. Injections of ATP (adenosine triphosphate), ATP-γ-S and GTP were without comparable effects indicating specificity for guanyl nucleotides over adenyl nucleotides and for the hydrolysis resistant form (GTP-γ-S) over GTP. The effects of fluoride and vanadate are reversible; those of GTP-γ-S are not.

Fluoride, vanadate and GTP-γ-S are all members of the class of compounds known to activate hormone regulated enzyme systems through action on a GTP-binding regulatory protein. From their similiar action on Limulus photoreceptors, we think it is very likely that a GTP-binding regulatory site is involved in the production of discrete waves.

Supported by grants from the NIH and the Rowland Foundation.

T-PM-C12 GTP AND GTP ANALOGUES MIMIC SOME ASPECTS OF THE LIGHT RESPONSE IN LIMULUS VENTRAL PHOTORECEPTORS. S. R. Bolsover and J. E. Brown, Dept. of Physiology and Biophysics, SUNY, Stony Brook, N.Y. 11794

We have pressure-injected the "non-hydrolysable" GTP analogues GMP-PNP, GMP-PCP and GTP-γ-S into Limulus ventral photoreceptors. Each of these compounds produces a marked increase in the frequency of "quantum bumps" that are recorded from the cell in darkness. After injection of GMP-PNP, illumination of the cell followed by a period of dark-adaptation was required before the increase in the frequency of quantum bumps in the dark was observed. An injection of GMP-PNP that markedly increased the frequency of quantum bumps in the dark did not change the sensitivity of the cell to light. GMP-PNP and GMP-PCP may be metabolized inside the cell to GMP of cGMP, plus PNP and PCP. Injection of GMP, cGMP or PCP were without effect, however PNP injections caused a profound fall in sensitivity (≤5 log units). The sensitivity recovered when extracellular calcium was reduced. Thus, none of these presumptive metabolic products mimic the effects of the GTP analogues. Injection of GTP had no long-term effect on ventral photoreceptor cells. However, preliminary results suggest that immediately after injection of GTP in the dark, the cell smoothly depolarized by up to 30 mV for ≈30 seconds. Under voltage clamp, GTP injections produce an inward current reversing at +45 to +55 mV, which is significantly more positive than the reversal potential of the light-induced current. Injections of GTP or its analogues thus produce membrane currents similar, but not identical, to the currents induced by light.

Supported by NIH grants EY-01914 and EY-01915.

T-PM-D1 CATION SELECTIVITY OF SQUID AXON MEMBRANE SODIUM CHANNELS IS VOLTAGE DEPENDENT. Ikunobu Muramatsu, Issei Seyema and Toshio Narahashi. Dept. of Pharmacol., Northwestern Univ. Med. Sch., Chicago, IL 60611.

Cation permeabilities of open Na channels in a value relative to Na permeability were determined in squid giant axons using four independent methods. In method I, permeability ratio (P_X/P_{Na}) was calculated from the reversal potentials for peak currents measured in K-free solutions outside and the standard solution inside. This method does not take into account the possible effects of the membrane potential on P_X/P_{Na}. In method II, the reversal potentials were measured as a function of external Na or test cation concentration in the absence of K, and P_X/P_{Na} was calculated at the potential where the Na and test cation solutions gave the same reversal potential. In method III, the reversal potentials were measured when a test cation was present only externally at various concentrations and Na was present only internally at a fixed concentration. In method IV, the reversal potentials were measured when a test cation was present only externally at a fixed concentration and Na was present only internally at various concentrations. Methods II, III and IV permitted measurements of P_X/P_{Na} at various membrane potentials. Method I gave P_X/P_{Na}: hydroxylamine (0.44), formamidine (0.27), guanidine (0.21), ammonium (0.21), methylguanidine (0.054), choline (0.034), cesium (0.028) and methylamine (0.025). The ratios P_X/P_{Na} for hydroxylamine, formamidine, guanidine, ammonium and methylguanidine as measured by method II were highly voltage dependent, increasing with hyperpolarization. The ratio for guanidine as measured by methods III and IV also increased with hyperpolarization from 0.25 at +40 mV to 1.0 at -40 mV. It was concluded that the mechanism whereby the cation selectivity is controlled is located at a site in the Na channel within the membrane field. Supported by NIH grant NS 14144.

T-PM-D2 UNIDIRECTIONAL FLUX-VOLTAGE RELATION IN THE SODIUM CHANNEL OF THE SQUID GIANT AXON. David Busath, Dept. of Physiology & Biophysics, U.T.M.B., Galveston, TX 77550, and Ted Begenisich, Dept. of Physiology, Strong Memorial Hospital, Rochester, NY 14642.

Unidirectional fluxes of Na and K through the sodium channel of voltage-clamped, perfused squid giant axons were measured using the tracer technique. Repetitive, short voltage step-depolarizations were applied and the increase in flux over the resting level was measured first without and then with TTX present. TTX blocked the extra flux of both ions. The extra flux measured this way depends both on the permeability of the channel and upon the gating process. To obtain unidirectional flux associated with channel permeability independent of the gating process, the extra flux per pulse was divided by the ratio of the integral of current during the pulse to "instantaneous current". The latter is the current measured immediately after a step to the test voltage from a depolarizing prepulse designed to open some fraction of the sodium channels. The unidirectional influx and efflux as well as the flux ratio were calculated from measurements at several voltages using 400 mM Na externally and either 50 mM Na, 150 mM Cs or 350 mM K internally. The results were compared to a three-barrier two-site model for ion permeation.

Supported by N.I.H. Fellowship 5 F32 NS-06084-02 and N.I.H. Grant NS-14138.

T-PM-D3 A MODEL FOR THE BLOCK OF SODIUM CHANNELS IN NERVE BY THE SIDE CHAIN OF ARGININE. Mei-Ven C. Lo and Peter Shrager. Dept. of Physiology, Univ. of Rochester, Rochester, N.Y. 14642.

When perfused internally in crayfish axons, n-propylguanidine (nPG), the side chain of arginine, speeds inactivation and reduces peak values of Na currents. Block of peak current is too great to be due solely to faster inactivation. Both block and changes in kinetics are voltage dependent and are more marked at stronger depolarizations. These effects are also larger when the Na concentration gradient is reversed from the normal. As the nPG concentration is raised, the block of peak currents increases, but the time constant of inactivation approaches an asymptote. We have attempted to describe all of these phenomena in a model involving a single site within the Na channel. Reaction of nPG with its receptor involves two steps: nPG + $R_1 \rightleftharpoons R_2 \rightleftharpoons R_3$. Both R_2 and R_3 represent blocked states. Normal inactivation proceeds independently of the drug. nPG shows no use-dependence and we allow interaction with both resting and open channels. The model predicts the time course of Na currents in nPG: both peak currents and decay kinetics are fitted satisfactorily. All four rate constants are simple exponential functions of membrane potential. The model further predicts the steep decrease in peak currents with [nPG] and the asymptotic behavior of decay τ. Fitting results at varying temperatures and potentials suggests that the first reaction step involves diffusion of nPG to a site at the inner mouth of the Na channel and close association with it. The second step may include a molecular transition of the complex towards a more interior position. Fits of the rate constants suggest that Na^+ ions near the selectivity filter may alter k_{32} and account for the dependence of nPG action on the Na concentration gradient. Supported by NIH grants 5-R01-NS10500 and 1-K04-NS00133.

T-PM-D4 BLOCKING ACTION OF POLY-L-ARGININE ON SQUID AXON MEMBRANE CURRENTS. C. H. Wu, Dept. of Pharmacology, Northwestern University Medical School, Chicago, Illinois 60611.

Recent studies have demonstrated that drugs may block ionic channels by binding to the gating moiety of channel molecule and keeping the channel in non-conducting states. Alternatively, the drug may enter and occlude the channel, thereby impeding the ion flow. For most of the blocking agents that have been studied, it is often difficult to distinguish between these two possible mechanisms because of their relatively modest sizes. The object of this study is to select a bulky drug incapable of entering the channel that the second possibility becomes remote. I have used the synthetic polypeptide, poly-L-arginine with a degree of polymerization about 300 and a molecular weight of 60,000 daltons for this study. The polypeptide preferentially blocks sodium channels when applied internally to the squid axon. The blocking action was dose-dependent: I_{Na} was reduced by 30% at 10^{-7} M and by 95% at 10^{-5} M. Potassium channels were blocked to a much less extent. Frequency-dependent block was not observed with the stimulation rate up to 4 cycles/sec. In addition, there was no observable time-dependent reduction in the currents. In contrast, solutions of arginine monomers at a concentration of 3 mM, equivalent to 10^{-5} M of the polymer concentration with respect to the guanidine groups, did not block either I_{Na} or I_K. Hyperpolarization pulses to -140 mV did not appear to reverse the blockage, suggesting that the block was not due to a simple shift in surface potential. Recovery upon washing with drug-free media was very slow with or without the addition of bovine serum albumin to the solution. Pronase treatment during washing seemed to enhance the recovery. These results suggest that the polymer interacts with the gating moiety of ionic channel at the inner surface and prevents its transition to the open conformation. Supported by NIH grant NS 14144.

T-PM-D5 BARBITURATE ANION BINDING SITE AT NODE OF RANVIER SODIUM CHANNELS. Joan J. Kendig, Department of Anesthesia, Stanford University School of Medicine, Stanford, CA. 94305.

The nature of the barbiturate binding site in axonal membrane was investigated in the voltage-clamped node of Ranvier of amphibian sciatic nerves. Intracellular pH was manipulated by diffusion of organic buffers (MES, HEPES, or CHES, 20-100 mM) to the nodal region from the cut internodes. Phenobarbital (1-2mM) block of sodium currents was time and voltage dependant. Time and voltage dependence was enhanced by increasing intracellular pH, thus increasing the ratio of charged to neutral drug in the axoplasm, whereas changing extracellular pH had little effect. Phenobarbital block was not frequency dependent, as strictly defined. A strongly acid barbiturate derivative, 5-phenyl barbituric acid, was tested for activity. This agent, pK 3.15, is essentially completely charged at neutral pH. On extracellular application, block by 5-phenyl barbituric acid (5mM) was of very slow onset; recovery on washout was also very slow. Increasing extracellular pH also delayed the onset of block by phenobarbital. Intracellular application of 5-phenyl barbituric acid by diffusion from the cut ends was effective in blocking sodium channels. These results suggest a binding site for the barbiturate anion closer to the axoplasm than the local anesthetic binding site in the sodium channel, and possibly on the intracellular side of a proton barrier in the membrane. Supported by NIH Grants GM22113, NS13108, and by ONR Contract N00014-75-C-1021.

T-PM-D6 LIDOCAINE BINDING TO RESTING AND INACTIVATED CARDIAC SODIUM CHANNELS Bruce P. Bean, Charles J. Cohen, and Richard W. Tsien, Department of Physiology, Yale University School of Medicine, 333 Cedar Street, New Haven, CT 06510

Lidocaine block of sodium currents was studied in short rabbit Purkinje fiber preparations using a two-microelectrode voltage clamp. Lidocaine block was strongly frequency-dependent. When evoked by widely separated depolarizing pulses from a negative holding potential, I_{Na} fell by ~5% with 20 uM lidocaine; the inhibition increased to 40% during a train of 0.5 s pulses at 1 Hz. In double pulse experiments with lidocaine present, reactivation of sodium channels following a long depolarizing pulse took place in two phases, one with the same time course as normal reactivation (τ<.2 s) and a second, slower component (τ~1.5 s). The slowly reactivating fraction increased with lidocaine concentration. Interpreting the slowly reactivating component as representing drug-bound, inactivated channels, the apparent K_D for lidocaine binding to inactivated channels was estimated as 15 uM. The apparent K_D for binding to resting channels was ~300 uM. The curve describing steady-state sodium channel availability vs. V_m was shifted in the hyperpolarizing direction by lidocaine, the amount of shift increasing with drug concentration in a manner consistent with these K_D values. Subthreshold pulses were sufficient to produce the slowly reactivating state; the half time of formation decreased from ~1 s at 20 uM lidocaine to ~0.1 s at 400 uM lidocaine (pH 7.0, 17 °C). These experiments suggest a picture of lidocaine binding to mammalian cardiac sodium channels which is very similar to that developed for frog skeletal muscle by Schwarz, Palade, and Hille (Biophys. J. 20: 343). It is possible that the greater apparent sensitivity of heart muscle to lidocaine simply reflects the fact that channels spend a larger fraction of time inactivated because of the action potential plateau.

T-PM-D7 RELATIVE POTENCIES OF SEVERAL DERIVATIVES OF SAXITOXIN: ELECTROPHYSIOLOGICAL AND TOXIN BINDING STUDIES. G. R. Strichartz, SUNY at Stony Brook, N.Y. 11794.

Saxitoxin (STX) specifically blocks sodium channels at a common receptor on excitable membranes. The potencies of several derivatives of saxitoxin have been determined by their ability to displace bound radiolabelled ^{3}H-saxitoxin from a membrane homogenate of rabbit brain and by their ability to block action potentials in frog myelinated nerve. At pH 7.1, the relative potencies (listed in brackets) from binding experiments are: STX [1.0], 11-hydroxysaxitoxin sulfate (GTX-II or GTX-III) [0.4], 1-hydroxysaxitoxin (neo-STX) [2.5], 12α-hydroxysaxitoxin [0.07-0.08], 12β-hydroxysaxitoxin [0.001]. Thus, additions at C-11 have small effects on potency, while stereo-selective reduction at C-12 results in potency ratios of 70-80. Also, the back-exchange rate of ^{3}H from ^{3}H-STX labelled at C-11 is the same for receptor-bound STX as the rate in solution (pH 7.2), showing that the C-11 moiety is probably not in contact with the receptor. Unlike the other derivatives, the potency of neo-STX increases with decreasing pH; on frog sciatic nerve neo-STX is about equipotent with STX at pH 7.6, but 6-8 times as potent as STX at pH 6.8. Since the 1-hydroxy group on neo-STX has an acidic pK_a of 6.75, the pH-dependent potency of neo-STX is due to both an increasingly positive charge on the molecule (Hille et al., 1975) and a functional role for the N-1 hydroxy group. These results suggest that the major bonds between STX and receptor are hydrogen bonds and electro-static interactions and that covalent bonds are probably not formed.

(Ref. Hille, Ritchie and Strichartz (1975). J. Physiol. 250:34:-35P. Supported by USPHS Grant NS 12828.

T-PM-D8 TRUE INACTIVATION DELAYS IN MYXICOLA. L. Goldman and J.L. Kenyon, Dept. of Physiology, School of Medicine, Univ. of Maryland, Baltimore, MD. 21201, and Cardiopulmonary Division, Univ. of Texas Health Science Center, Dallas, TX. 75235.

Gillespie and Meves (J. Physiol. 299:289,1980) simulated Na inactivation delay experiments (conditioning pulse-gap-test pulse) with Hodgkin-Huxley kinetics and series resistance, R_s. Simulated inactivation curves show an initial exponential decline corresponding to the H-H τ_c value, followed by a steeper decline, and finally return to the initial H-H exponential. The steeper decline is seen for conditioning pulses long enough to strongly activate, but not inactivate g_{Na}. Na tail currents, flowing across R_s, produce additional inactivation during the gap. They suggest this as a basis for previous findings of inactivation delays. We report that such R_s effects cannot account for delays in Na inactivation development in Myxicola either as described by Goldman and Schauf (J. Gen. Physiol. 59:659, 1972) or repeated by us. Experimental τ_c curves (6 ms gap width which is sufficient to prevent interference from activation development, compensated feedback) display an initial zero slope followed by a simple exponential both in full and reduced Na ASW (i.e. rather than an initial exponential decline there is an initial plateau). Delays are visible only for conditioning pulse durations for which g_{Na} is small. Reducing I_{Na} six fold (Tris substitution) does not reduce delays or affect τ_c. Delays are reduced with more positive conditioning potentials during which g_{Na} activates more rapidly and extensively, the opposite effect expected if delays are caused by R_s, but expected if activation and inactivation are sequential, as more rapid g_{Na} activation during the conditioning pulse delays inactivation onset less. Both Myxicola and squid exhibit delays in inactivation not due to obvious technical artifacts, with a longer delay in Myxicola. Supported by NIH Grant NS-07734.

T-PM-D9 SODIUM INACTIVATION IS A MULTI-STEP PROCESS IN CRAYFISH GIANT AXONS. M.D. Rayner, J.G. Starkus and B.D. Fellmeth. Dept. of Physiol., Univ. of Hawaii, Hon., HI 1962.

When both prepulse and test pulse are confined to a range of positive membrane potentials (+15 to +75mV), over which we demonstrate that the activation process becomes fully saturated shortly after peak sodium current is reached, test pulses imposed during the falling phase of prepulse sodium conductance can be used to study the voltage-sensitivity of the inactivation process. We observe that inactivation remains voltage-sensitive at all prepulse durations utilized here, with test pulse inactivation rates being identical to those observed in single pulse control steps to the same test pulse potential. This result seems to rule out any model in which inactivation is represented as a single, voltage-insensitive, reaction.

On the other hand, inactivation may itself involve multiple sequential steps (initiated either in parallel with, or sequential to, activation). The non-exponential voltage-dependence of inactivation rate suggests at least a two-step process, in which a "silent", voltage-sensitive, precursor reaction precedes a relatively voltage-insensitive inactivation-gating (pore-closing) reaction.

A model based on this two-step inactivation hypothesis correctly predicts the observed form of our test pulse transients. (Supported in part by BRSG Grant No. RR05599-13 and NIH Grant No. GM29263-01.)

T-PM-D10 SINGLE SODIUM CHANNEL CURRENTS IN EXCISED MEMBRANE PATCHES. **Richard Horn, Joseph Patlak, and Charles Stevens. Dept. of Physiology, Yale Univ., New Haven, CT 06510.**

Single Na channel currents in rat myoballs have recently been described (Sigworth and Neher, Nature 287:447,1980) using extracellular patch recording with gigohm seals. We have extended their work in the following ways: a) After making a gigohm seal, we have excised the membrane patch from the cell by withdrawing the electrode, containing the membrane fragment, from the surface of the cell (Horn and Patlak, PNAS 77#11, 1980). This method permits simultaneous control of the absolute, transmembrane potential and the internal (i.e. cytoplasmic-face) solution, which is continuous with the bathing solution in the experimental chamber. b) We have cooled the preparation to ~10° C in order to increase the duration of single channel events. Under our conditions, excised patches remained functional for up to 90 min, surviving through as many as four solution changes. The extracellular solution in the pipette was rat Ringer's (containing 150 mM NaCl). The standard internal solution was 160 mM CsF + 5 mM Cs-HEPES. Voltage steps from a holding potential, V_h, of -110 mV to a test potential of -40 mV produced ~1.6 pA inward currents. Decreasing V_h to -70 mV reduced the average number of channel openings during a depolarizing step, without affecting the single channel conductance. Substitution of tetramethylammonium for Cs^+ reduced the single channel current 37% at this potential. Internal application of 333 μM N-bromoacetamide (Oxford et al., JGP 71:227, 1978) caused an irreversible loss of Na channel inactivation in about 5 min, as determined by averaged single channel records. This treatment caused at least a 10-fold increase in open channel lifetime at -40 mV, suggesting that the inactivation gating process normally causes channel closing. This observation is inconsistent with simple H-H kinetics, which predict that the open channel lifetime at this potential is determined mainly by β_m, the rate constant for closing the activation gates.

T-PM-D11 Na-CURRENTS RECORDED FROM SMALL PATCHES OF SQUID AXON MEMBRANE. J.López-Barneo D.R. Matteson and C.M. Armstrong. Dept. of Physiology, Univ. of Pennsylvania, Philadelphia, PA, 19104

A new voltage clamp circuit for the squid axon has been designed to enable recording of currents through small areas of axon membrane. The primary modifications of previous, conventional voltage clamp designs are: (1) The internal voltage is held at virtual ground; membrane voltage is controlled by a feedback loop which supplies current to the membrane through external electrodes. (2) Membrane current generated by the clamped axon segment is recorded as the IR drop across a 100 ohm resistor in series with the external control amplifier. (3) Currents generated by small patches of membrane are recorded by placing an L-shaped pipette inside the axon and maneuvering its tip to the membrane surface (Conti and Neher, 1980).

For our purposes this configuration has two major advantages: (1) It avoids a low resistance shunt to ground of the I-V converter summing junction, thus minimizing input noise. (2) Capacity currents across the wall of the patch pipette are effectively eliminated, so that the frequency response of the patch recording is improved. Our particular chamber lacked guard electrodes and total membrane currents recorded with this clamp are therefore not highly accurate, since the ends of the preparation are not well controlled. We have recorded stable Na currents with the patch pipette. These currents are six to seven orders of magnitude smaller than total membrane currents, but have normal kinetics and voltage dependence and appear to reflect the activation of the population of Na channels contained in the membrane patch.

T-PM-D12 THE CUT-OPEN AXON. I.Llano* and F.Bezanilla. Dept. of Physiology, UCLA, CA, 90024.

A technique has been devised to cut open squid axons into sheets that can be voltage clamped and in which the internal side of the membrane is directly accesible. Axon segments from the squid L.pealei and L.opalescens ranging in diameter from 325 to 600 μm were transfered to a chamber consisting of two compartments separated by a plexiglass partition with a circular hole of either 150 or 250 μm. Both compartments were filled with ASW. The axons, cut into 2.0 to 2.5 mm segments, were held on top of the hole by negative pressure. The axonal membrane was cut longitudinally to obtain a membrane sheet, internal side facing up. ASW in the upper compartment was changed to isosmotic sucrose followed by a solution containing 400 mM KF, 230 mM Sucr. and 10 mM Tris. Membrane potential, V_m, was measured differentially with glass pipettes, i.d. 30 μm, positioned within 10 μm of the membrane; V_m was fed into a voltage clamp circuit which injected current through the axon sheet. The leakage resistance around the edge of the hole ranged from 300 to 600 KΩ. For depolarizing pulses, sodium and potassium currents had maximum amplitudes of 0.6 to 2.0 and 0.5 to 1.6 mA/cm^2, respectively. These currents exhibited normal voltage dependence but slightly distorted kinetics because current from the periphery, which is not under good potential control due to the shunt, is included in the measurement. Using current measuring pipettes, i.d. 10-30 μm, positioned close to the center of the axon sheet, I_{Na} and I_K showed normal voltage dependence and kinetics indicating that they are recorded from an area which is under accurate control. In this preparation Na gating currents can be easily resolved. Preliminary experiments using 4 μm i.d. suction pipettes to isolate electrically a patch of an enzyme treated cut-open axon indicate that seal resistances of at least 100 MΩ can be obtained. Thus, this preparation should prove useful for studying ionic currents, gating currents and channel-induced fluctuations.

Supported by MDA, PHS AM 25201 and E.I. duPont de Nemours & Co.

T-PM-D13 CARDIAC SODIUM CHANNELS ARE DIFFERENT FROM NERVE AND SKELETAL MUSCLE SODIUM CHANNELS. L.M. Hondeghem, K.R. Courtney, Pharmacology, University of California, San Francisco and Palo Alto Medical Research Foundation

Cardiac sodium channels are about a thousand-fold less sensitive to tetrodotoxin (TTX) than nerve and skeletal muscle sodium channels. In addition, the TTX block has been shown to be use and voltage dependent in heart, but not in nerve and muscle. That these differences may be caused by (1) non-linearities of the Vmax measurements in heart (unlikely). (2) The local anesthetic-like internal actions of TTX might be masked by a more potent specific external action. (3) The sodium channels are really different.

In order to discriminate between the latter two we voltage clamped skeletal muscle and nerve in a sucrose gap. The external pool was perfused and TTX was cut into the internal pool. Voltage clamps similar to the cardiac action potential were imposed at various rates and holding potentials. We were unable to document use or voltage dependent blockade by TTX in nerve or skeletal muscle. We therefore conclude that cardiac sodium channels are different from those in nerve and skeletal muscle. Supported by grants from NIH.

T-PM-E1 DIFFUSION AND CONVECTION OF SMALL PARTICLES ADHERING TO THE SURFACES OF MOVING CELLS. M. Dembo, Los Alamos Scientific Laboratory and A. K. Harris, University of North Carolina at Chapel Hill.

Time lapse films of particle motion on the leading lamella of chick heart fibroblasts and mouse peritoneal macrophages were analysed. The particles were composed of powdered glass or powdered aminated polystyrine and were 0.5 - 1.0 μ in radius. The statistics of the step size distribution of the particles was consistent with the motion of a Brownian particle in the presence of a constant force field. The two dimensional diffusion coefficient of different particles varied by more than an order of magnitude (10^{-11} - 10^{-10} cm^2/sec) even for particles composed of the same material and located very close to each other on the surface of the cell. This variation was not correlated with particle size but could be due to different numbers of adhesive bonds holding the particles to the cells. The constant force on the particles ($0.1 - 1.0 \times 10^{-8}$ dynes) was found to be inversely proportional to the diffusion constant for particles close to each other on the cell surface. This indicates that the particles are carried by the flow of the membrane as a whole or by flow of some submembrane material.

T-PM-E2 VIDEO ENHANCED CONTRAST MICROSCOPY STUDIES ON THE MOVEMENT OF INTRACELLULAR PARTICLES ALONG MICROTUBULES IN ALLOGROMIA.

Jeff Travis* and Robert D. Allen, Department of Biological Sciences, Dartmouth College, Hanover, NH, 03755

The reticulopodial network (RPN) of the benthic marine foraminifer Allogromia laticollaris displays constant, bidirectional streaming of ground cytoplasm and intracellular particles. The nature of these particle translocations is saltatory and movement occurs exclusively along microtubules, which course throughout the RPN. Surfaces coated with poly-cations such as protamine-sulfate or poly-l-lysine stimulate the development of extensive regions of hyaline cytoplasm at areas of pseudopodial contact with the substratum. Using a new method of video enhanced polarizing (AVEC-POL) and differential interference contrast (AVEC-DIC) microscopy which is remarkably insensitive to noise due to stray light, the presence of intracellular fibrils traversing these hyaline areas in detected. Cytoplasmic particles move along these fibrils and, in addition, the fibrils themselves move about relative to one another within these areas. Stereo electron micrographs of whole mounted-fixed and critical point dried specimens show that the fibrils that traverse the poly-cation induced hyaline regions are composed of microtubules, arranged either singly or in bundles. Numerous particles are alligned along the microtubules and are in contact with them. Even a single microtubule may have a cytoplasmic granule attached to it. Our results indicate that the microtubules play an active role in the movement of intracellular granules within the RPN.

Supported by grant GM22356 from the NIGMS and award from the ROWLAND Foundation to RDA.

T-PM-E3 MODEL FOR CILIARY TRANSPORT OF GAMETES IN A TRUMPET-SHAPED OVIDUCT. H.Winet[a] and J.R.Blake[b]*, [a]Dept. OB/GYN, University of Southern California, Los Angeles, CA 90033 and [b]Dept. Mathematics, University of Wollongong, Wollongong, Australia.

A complete hydromechanical model for oviductal gamete transport must account for the affect of vessel geometry and conformation, smooth muscle and ciliary contraction patterns, and the contributions of the gametes to their own transportability. As a first step beyond transport models of constant diameter tubes generating ciliary or peristaltic(recently shown to be absent) flows, we have developed a ciliated tapered tube model which includes the unobstructed and forcing pellet propulsive effects on both ova and dilute sperm suspensions between the ampullary isthmic and uterotubal junctions (AIJ and UTJ) around the time of fertilization. As the ovum approaches the AIJ and is sheared of its cumulus oophorus, its motion is increasingly explainable by lubrication theory for ciliated tubes. The transport of spermatozoa in the isthmus is more complex. Sperm near the walls are swept toward the UTJ at a maximum velocity U_m and those in the more central region of diameter D' where $U_m>0$ are refluxed toward the AIJ at $U(r') = \nabla P_i(r'^2 - D'^2/4)/4\eta + U_m$ with r' the distance from the tube axis, η the suspension viscosity and ∇P_i the average pressure gradient along the i^{th} tube segment. The change in ∇P_i with the approach of the ovum to the AIJ is the most significant feature of the new model because the battle between the uterad shear stress of the cilia pushing the ovum and the reflux ∇P_i first favors the latter enabling centrad spermatozoa to quickly reach the ovum and then favors the shear stress. As a result, the embryo moving toward the UTJ reverses the sign of ∇P_i and forces the lagging sperm back into the uterus. The key quantity in the successive recalculations of ∇P_i is the changing gap between the advancing ovum and the tube mucosa. Inclusion of the rugae in the model results in a predicted increase of reflux via their valleys.

Supported by NIH Grant #HD 15442.

T-PM-E4 FLUORESCENT MYOSIN S-1 LOCALIZATION OF ACTIN IN TOMATO PROTOPLASTS. M. Vahey, M. Titus* and C. Bowman, Department of Biological Sciences, Smith College, Northampton, MA 01063 and The Neurobiology Research Center, The University at Albany, Albany, NY 12222

Tomato protoplasts, prepared by incubating thin slices of the endocarp tissue from the fruit of red tomatoes in: 20% sucrose, 50 mM TRIS-HCl pH 7.2, 10 mM $MgSO_4$ and 20% hemicellulase, 20% pectinase, 20% cellulysin, exhibit rapid cytoplasmic streaming and are stable without wall regeneration for 10 hours. Intact protoplasts in: 20% sucrose, 50 mM TRIS-HCl pH 7.2, 1 mM $MgSO_4$, were allowed to settle on glass coverslips for observation with Nomarski and fluorescent optics. Fluorescent rabbit skeletal muscle myosin S-1 was prepared by the method of Sanger (Sanger, J., PNAS-USA, 72, 1975, p. 1913.) to remove uncoupled fluorescein from the fluorescent S-1 (Fl-S-1). The pure Fl-S-1 fractions used were tested for specificity and reversible binding by reaction with glycerinated rabbit myofibrils. A 5 mg/ml solution of Fl-S-1 in: 10 mM KCl, 5 mM potassium phosphate buffer pH 7.0, 1 mM $MgCl_2$, 1 mM EDTA was perfused over the settled protoplasts; the mix was allowed to stand for 10 min and unbound Fl-S-1 was rinsed off. Fl-S-1 treated protoplasts exhibit a large pool of fluorescent label. This structure is clearly visible within the protoplasts when viewed with Nomarski optics. Furthermore, this fluorescence is removed by: 1.) first treating the protoplasts with unlabelled S-1 and/or 2.) adding Mg^{++}ATP to a final concentration of 10 mM. Untreated protoplasts, which are derrived from non-photosynthetic tissue, exhibit no endogenous fluorescence.

We gratefully acknowledge the kindness of Dr. C. Edwards for use of his microscope; Dr. H. Tedeschi for use of his lab, and Mr. V. Laronga of AZI for use of the needed filters.

T-PM-E5 EXCHANGE OF 1, N^6-ETHENO-ATP WITH ACTIN-BOUND ATP AS A TOOL FOR FOLLOWING THE STEADY-STATE EXCHANGE OF SUBUNITS IN F-ACTIN SOLUTIONS. Yu-li Wang and D. Lansing Taylor, Cell and Developmental Biology, The Biological Laboratories, Harvard University, Cambridge, MA 02138.

The fluorescent analog of ATP, 1, N^6-etheno-ATP, exchanges readily with G-actin-associated ATP but not with F-actin-associated ADP. The exchange reaction can be followed by measuring the fluorescence intensity which increases significantly upon binding of the analog to actin. This reaction provides a convenient, non-perturbing way to follow the exchange of actin subunits in F-actin solutions. When excess 1, N^6-etheno-ATP is added to a solution of F-actin, a continuous increase in fluorescence intensity is observed, suggesting that the subunits in the F-state are exchanging extensively with those in the G-state. The kinetics of exchange consist of a fast phase and a slow phase. Both phases are stimulated by shearing, suggesting that the exchange occurs through the filament ends. Furthermore, pulse-chase experiments indicate that the exchange does not occur uniformly throughout the filaments; and that the assembly ends for the slow phase are probably different from the disassembly ends. Experiments with different ionic conditions further indicate that the slow phase of exchange requires millimolar concentrations of Mg^{++} ions. These observations provide useful information about the mechanism of subunit exchange in steady-state F-actin solutions. (Supported by NIH grant AM 18111 and NSF grant PCM-7822499.)

T-PM-E6 A POSSIBLE MECHANISM FOR CYTOCHALASIN-STIMULATED MONOMERIC ACTIN ATPase ACTIVITY. Stephen L. Brenner and Edward D. Korn, NHLBI, NIH, Bethesda, MD 20205.

Cytochalasins stimulate the ATPase activity of actin below its critical concentration in 0.5 mM $MgCl_2$ (Brenner and Korn (1980) JBC 255, 851) when no polymerization is detectable by viscometry, sedimentation or light scattering. Cytochalasin-stimulated ATPase activity is linear with actin concentration below the critical actin concentration and independent of the concentration of F-actin above the critical concentration which indicate that cytochalasin-stimulated ATPase activity is due to monomeric actin and does not require actin-actin interactions. For muscle and Acanthamoeba actins, the double reciprocal plots of ATPase activity vs cytochalasin concentration are linear for cytochalasins B, C, D and E. The Vmax values are similar for the four cytochalasins (9-10 and 12-24 mol P_i mol^{-1} actin h^{-1} for muscle and Acanthamoeba, respectively) while the Kapp values vary 400-fold (0.08 μM for CD and 33 μM for CE for muscle actin). These results require that essentially all of the cytochalasin be unbound even at Vmax. The simplest model (see scheme) consistent with these observations includes an initial first order transition, actin·ATP $\rightleftharpoons$ actin*·ATP (step 1), followed by very slow hydrolysis of ATP (step 2). If the cytochalasins bind weakly, rapidly and reversibly to monomeric actin (but with different K's for each cytochalasin), ATP hydrolysis (now step 3) could be accelerated until the cytochalasin-independent actin transition (step 1) became rate limiting (Vmax). The proposed actin $\rightleftharpoons$ actin* transition may also be an intermediate step in actin polymerization.

$$\begin{array}{ccccc} \text{Actin·ATP} & \overset{1}{\rightleftharpoons} & \text{Actin*·ATP} & \overset{2}{\rightleftharpoons} & \text{Actin·ADP + Pi} \\ \Downarrow & & \Downarrow & & \Downarrow \\ \text{Cyto·Actin*·ATP} & & \overset{3}{\rightleftharpoons} & & \text{Cyto·Actin·ADP + Pi} \end{array}$$

T-PM-E7 PROPERTIES OF BRAIN ACTIN DEPOLYMERIZING FACTOR (ADF). D. A. Amorese and J. R. Bamburg, Department of Biochemistry, Colorado State University, Fort Collins, Colorado 80523 (Intr. by J. Lett)

Using a modification of the DNase I inhibition assay for G-actin (Blikstad, et. al., Cell 15, 935 (1978)), we have isolated a protein from chick embryo brain which depolymerizes filamentous actin in vitro (Bamburg, et al., FEBS Lett., in press). Briefly, the procedure involves homogenization of brains in 10mM Tris, 1mM NaN_3, 0.2mM dithioerythritol (DTE), pH 7.8, centrifugation at 10^5Xg, passage of the extract through a column of DEAE-cellulose equilibrated in the same buffer, concentration by $(NH_4)_2SO_4$ fractionation (50-90%), and gel filtration on Sephadex G-75. The active component elutes from the column with an apparent mol. wt. of 35,000. Incubation of this material with an excess of F-actin, followed by centrifugation at 10^5Xg to remove excess F-actin, and gel filtration on Sephadex G-150 equilibrated in 20mM Tris, 0.2mM ATP, 0.2mM DTE, pH 8.0 resulted in the isolation of an ADF-actin complex which eluted with an apparent mol. wt. of 70,000. Rechromatography of this complex on Sephadex G-75 in 20mM Imidazole, 0.2mM DTE or on DEAE-cellulose in the 10mM Tris buffer resulted in the separation of the ADF from the actin. ADF so prepared was active in the depolymerization assay, had a polypeptide mol. wt. of about 19,000 on SDS-PAGE, and an isoelectric point of about 6.0 on focusing gels. Incubation of this ADF with ^{3}H-F-actin, prepared in vitro by reductive alkylation, resulted in the formation of an ADF-^{3}H-actin complex. Incubation of this complex with a large excess of unlabeled G-actin under assembly conditions (0.1M KCl, 4mM $MgCl_2$) resulted in 92% of the labeled actin being recovered with the F-actin following centrifugation at 170,000Xg. Thus, brain ADF meets the requirements for an actin assembly regulatory protein since it can form reversible complexes with actin and both components of the complex maintain biological activity. (Supported by NIH grant NS10429 and a BRS grant)

T-PM-E9 BIOCHEMICAL CHARACTERIZATION OF ACTIN FROM NORMAL AND LEUKEMIC LYMPHOCYTES. L. Liebes, R. Stark, D. Nevrla, P. Unger, D. Zucker-Franklin, and R. Silber, New York University School of Medicine, New York, NY 10016.

Actin was purified to homogeneity from lymphocytes isolated from normal (nl) donors and patients with chronic lymphocytic leukemia (CLL) according to a modification of the procedure of Gordon et al. (1). Characterization of the purified proteins revealed that the following were similar in nl and CLL actin: isoelectric point (β, 5.40; γ, 5.46), molecular weight (43,000), critical protein concentration in 2 mM $MgCl_2$ at 25°C and 4°C (0.025 mg/ml), intrinsic viscosity in 2 mM $MgCl_2$ (8.9 dl/g, 25°C; 4.0 dl/g, 4°C), ultrastructure of polymerized filaments and ratio of β/γ subcomponents (3:1). The activation of rabbit skeletal muscle (RSM) heavy meromyosin by nl lymphocyte actin resembled that of other non-muscle actins (2). The Vmax reached with nl lymphocyte actin was the same as obtained with RSM actin. A variable response was observed with CLL actin. In one case in which actin was prepared on three occasions, the Vmax was 50% that of nl lymphocyte and RSM actin, while actin from another patient was indistinguishable from nl lymphocyte actin in terms of its Vmax. The actin content as expressed in % total cellular protein in CLL lymphocytes (4.2 ± 1.1%, N=16) was lower than that of nl lymphocytes (6.8 ± 1.5%, N=16). Reduced actin levels were found in both B and T subsets in CLL lymphocytes (3.2 and 3.1% respectively, N=16) while nl B and T lymphocytes were found to have comparable levels (6.8 and 6.3% respectively N=6). The decreased level in both B and T subsets of CLL lymphocytes may contribute to the impaired motility and receptor mobility found in these cells.

1. Gordon et al. J. Biol. Chem. 251:4778, 1976.
2. Gordon et al. J. Biol. Chem. 252:8300, 1977.

T-PM-E10 POLYMORPHIC FORMS OF BRAIN TUBULIN. Henry J. George*, Lily Misra*, Deborah J. Field, and James C. Lee. Dept. of Biochemistry, St. Louis University, St. Louis, MO 63104.

Calf brain tubulin was subjected to isoelectric focusing and tryptic peptide map analysis. Results from isoelectric focusing experiments showed a total number of 17 well resolved protein peaks. The number of peaks and the mass distribution under each peak remained the same when the experiments were conducted as a function of protein or ampholyte concentration. When the protein was subjected to two dimensional isoelectric focusing, a diagonal pattern was observed indicating that the multiple peaks observed are not a manifestation of tubulin-ampholyte interaction. Further investigation by isolating these individual subspecies and subjecting them to isoelectric focusing yielded simple peaks corresponding to the original ones without generating the initial pattern of multiple peaks. Tryptic peptide maps showed that among the subspecies of the α-subunit tested there are 26 spots that are common among them. There are, however, 7±1 spots that are unique in each subspecies. Similar observations were obtained for the subspecies of the β-subunit tested although there are only 2±1 unique spots in each subspecies. These results suggest that tubulin subunits probably consist of polypeptides with both constant and variable regions in their sequences.

Identical results were obtained for canine and rabbit brain tubulin, indicating that tubulin polymorphism is common among brain tissues. Tubulin isolated by either the polymerization-depolymerization or the modified Weisenberg procedures yielded identical results. Thus, it may be concluded that the same subspecies of tubulin are extracted by both isolation procedures. (Supported by NIH grants NS 14269, AM 21489 and the Council for Tobacco Research, Inc.).

T-PM-E11 THE STRUCTURE AND FUNCTION OF MICROTUBULES R. Linck, D. Albertini*, G. Langevin*, G. Olson*† and D. Woodrum*. Departments of Anatomy, Harvard Medical School, Boston, MA 02115 and Vanderbilt School of Medicine†, Nashville, TN 37232.

We have taken a multidisciplinary approach to the study of microtubule structure and function. First, we have succeeded in polymerizing sea urchin sperm flagellar B(αβ)-tubulin, i.e., tubulin derived from the incomplete B-tubule of doublet microtubules. B-tubulin assembles in vitro into singlet microtubules whose morphology and chemical composition indicates that they are helically asymmetric. Second, ultrastructural studies and optical diffraction analysis of negatively stained flagellar singlet microtubules indicate that native microtubules are also helically asymmetric. Third, flagellar doublet microtubules decompose in the presence of 0.75% sarkosyl or 0.6 M KI to yield ribbons of 2 to 4 protofilaments which we refer to as "tektin" ribbons and filaments. Central pair singlet microtubules also decompose to yield stable tektin ribbons of 4 or more protofilaments. Finally, SDS-polyacrylamide gel electrophoresis indicates that doublet-microtubule- derived tektin ribbons possess tektin ribbon-specific proteins and that the tektin ribbons and filaments are composed of proteins with molecular weights unlike tubulin but rather similar to 10 nm (intermediate)-filament proteins. From our findings along with other available data, we conclude that these tektin filaments: (1) are a form of the so-called 10 nm (intermediate)-filaments; (2) form semipermanent longitudinal backbones in the microtubule wall; (3) are the sites of attachment for numerous tektin-associated proteins (TAPs) which function in the assembly and disassembly of microtubules; and (4) carry positional information to specify the attachment of numerous other cell components, e.g., polysomes and metabolic enzyme complexes. We further propose that tektin filaments have the ability to generate force by coiling in a mechanism which can account for chromosome movement in cell division.

T-PM-E12 EVIDENCE FOR TWO DIFFERENT EQUIMOLAR TUBULIN HETERODIMERS IN MICROTUBULES. R. E. Stephens, Marine Biological Laboratory, Woods Hole, Massachusetts 02543.

In most types of native microtubules but also in microtubules polymerized *in vitro*, free of accessory proteins, a prominent 16 nm repeat is seen in optical diffraction patterns. This spacing cannot be easily explained by the currently-accepted helical arrangement of a single, repeating 8 nm tubulin heterodimer. Based upon the presence of two equimolar α-chains in certain tubulin preparations, Bibring and coworkers (J. Cell Biol. 69: 301, 1976) suggest that two different heterodimers, alternating along the protofilament axis may produce the 16 nm periodicity. However, α-chain microheterogeneity and anomalous electrophoretic behavior leaves the biochemical evidence uncertain. On 5% acetic acid-6 M urea-6 mM Triton X-100-polyacrylamide (10T/1C) gels, various ciliary and flagellar tubulins are consistently resolved into two equimolar β-chains and one unresolved α-region, in 1:1:2 mole ratio, with the α-chain(s) trailing in cathodic migration. Conditions are optimized by running horizontal gradient gels in which urea, Triton X-100, gel strength, and crosslinkage are varied; optima are essentially the same as for histone separation (Zweidler, Meth. Chrom. Res. 1: 223, 1977). Chain identify is established by 2-D SDS-PAGE. Similar results are obtained on an alkaline (pH 9.8), discontinuous SDS-PAGE system with an acidic (pH 6.1) stacking gel (7.5T/1C running gel; 5T/5C stacking gel; Neville, J. Biol. Chem. 246: 6328, 1971). Here, multiple α-chains and two equimolar β-chains are obtained. The separation depends critically on the low pH-high crosslink stacking gel and on the composition of commercial "SDS". Since both electrophoretic separations occur through differential detergent binding, it appears that microtubules of various kinds contain two equimolar β-chains which differ in relative hydrophobicity. This finding lends independent support for the existence of two equimolar heterodimers, $\alpha_x\beta_1/\alpha_x\beta_2$. USPHS grant GM 20,644 from the NIGMS.

T-PM-F1 THE RESONANCE RAMAN SPECTRUM OF BACTERIORHODOPSIN'S PRIMARY PHOTOPRODUCT.
M. Braiman and R. Mathies, Chemistry Dept., University of California, Berkeley, CA. 94720

By spinning a purple membrane sample at liquid nitrogen temperature, we have obtained the resonance Raman spectrum of K, the primary photoproduct of bacteriorhodopsin. K is prepared in a photostationary steady-state by photolyzing the parent bacteriorhodopsin (bR) sample with a 514.5 nm "pump" beam. By using a red (676 nm) "probe" beam to excite the Raman spectrum, it is possible to selectively enhance the resonance Raman scattering from K. Spinning the sample eliminates two sources of background fluorescence that had made this red probe experiment difficult. First, it reduces the buildup of fluorescent photoproducts of bR generated by low quantum yield photoreactions. Spinning also permits the spatial separation of the pump and probe beams so that the fluorescence excited by the intense pump beam does not mask the scattering from the weaker red probe beam. The pump-and-probe Raman spectrum obtained in this fashion clearly shows several new lines which disappear reversibly when the pump beam is turned off; the probe-only Raman spectrum is the same as the room-temperature bR spectrum. The new lines, which must be due to K, contribute nearly half of the Raman intensity in the raw spectrum. It is thus possible to carry out a reliable subtraction to produce a pure K spectrum. This spectrum exhibits a single intense ethylenic stretching vibration at 1515 cm^{-1} and a "low wavenumber" line of comparable intensity at 955 cm^{-1}. The presence of anomalous Raman intensity in this low wavenumber region is a feature common to the primary photoproducts of both rhodopsin and bacteriorhodopsin. The 955 cm^{-1} line of K can thus be attributed to a hydrogen out-of-plane wag of a locally twisted retinal chromophore.
Supported by USPHS grant EY 02051

T-PM-F2 KINETIC RESONANCE RAMAN SPECTROSCOPY OF CHEMICALLY MODIFIED PURPLE MEMBRANE.
G. Gogel* and A. Lewis, Cornell Univ., Ithaca, N.Y. 14853.

We have been investigating the resonance Raman spectrum of purple membrane with selective chemical modifications such as a single deuteron on the retinal[1] or selective protein deuteration[2]. We now present a kinetic resonance Raman investigation of purple membrane modified by iodination[3], a procedure which modifies predominantly tyrosines. Resonance Raman spectra of the initial bacteriorhodopsin species in these chemically modified membranes demonstrate that even though the absorption of this species has been altered from 570 nm to 550 nm, the C=N-H⊕ stretching frequency is unaltered. These data suggest as previously noted[2] that tyrosine may be interacting with the chromophore in addition to the protein group previously postulated to be complexed to the Schiff base proton. However, all our data are only consistent with a through space rather than a chemically bonded secondary interaction.

Even though the C=N-H⊕ frequency of bacteriorhodopsin is unaltered by this modification, kinetic resonance Raman spectroscopy demonstrates that in these membranes the rate of Schiff base deprotonation on the μsec time scale is seriously altered. The data are consistent with an hypothesis that the deprotonation of tyrosine is involved in effecting the pK of Schiff base deprotonation. This pK has previously been determined to be 10.2±0.3 by Ehrenberg and Lewis[4] using kinetic resonance Raman spectroscopy of naturally occuring bacteriorhodopsin as a function of pH. Thus our data for the first time implicates tyrosine in the deprotonation of the Schiff base. (Supported in part by NIH grant EY01377. G. Gogel is an NIH Postdoctoral Fellow.) 1. B. Ehrenberg et al. (1980) Biochem. Biophys. Acta 592, 441. 2. A. Lewis et al. (1978) Proc. Natl. Acad. Sci. 75, 4642. 3. W. Hunter and F. Greenwood (1962) Nature 194, 495. 4. B. Ehrenberg and A. Lewis (1978) Biochem. Biophys. Res. Commun. 82, 1154.

T-PM-F3 KINETIC RESONANCE RAMAN SPECTRA OF 11-D-, 15-D- and 11-15-diD- PURPLE MEMBRANE AND ^{15}N PURPLE MEMBRANE.
T. K. Porta, J. Aldern, G. Gogel, A. Lewis and H. Crespi (introduced by H. A. Scheraga). Cornell Univ., Ithaca, NY 14853 and Argonne Natl Lab., Argonne, Ill. 60435.

Resonance Raman spectra of selectively deuterated Schiff bases of retinal will be discussed. These spectra will be compared to kinetic resonance Raman spectra of 11-D, 15-D and 11-15-di-D retinal incorporated into native and ^{15}N enriched purple membrane. The data clarifies the assignment of the Schiff base vibrational modes and other modes in the resonance Raman spectra of the purple membrane. These kinetic resonance Raman spectra of isotopically labelled membranes will also be used to verify the rate of Schiff base deprotonation, and comparisons will be made to the kinetic resonance Raman spectra of native[1] and fully deuterated purple membrane in H_2O.[2] Furthermore, it will be shown that the data supports the concept of retinal isomerization in the L and X (?) intermediates as previously noted.[3] In addition to the above, alterations in the concentration of purple membrane intermediates as a function of deuteration of non-exchangeable protons on the retinal and protein will be discussed. Finally, the data will be compared to spectra of purple membrane, with another form of isoprenoid chain alteration, a benzene ring between carbon atoms 9 and 12.

1. M. A. Marcus and A. Lewis, Science 195, 1328 (1977).
2. B. Ehrenberg, A. Lewis, H. Crespi, Biochem. Biophys. Acta 592, 454 (1980).
3. M. A. Marcus and A. Lewis, Biochemistry 17, 4722 (1978).

T-PM-F4 SALT DEPENDENT SPECTRAL TRANSITION OF HALOBACTERIUM PIGMENT P_{588}. R.A. Bogomolni, J.W. Belliveau, and H.J. Weber. University of California, San Francisco California 94143.

P_{588} is a second retinal containing pigment in Halobacteria that absorbs maximally at 588 nm. in 2-4 M salt solutions (P^S_{588}). Lowering of the ionic strength leads to a reversible spectral shift of the absorption spectrum from λ^S_{max}=588nm to λ^W_{max}=565nm. The new pigment, P^W_{565} undergoes a photochemical cycle significantly different from that of P^S_{588}. Excitation of membrane fragments of H. halobium ET-15 in aqueous suspension by a laser pulse (7 nsec. 580nm; pH 7, 22°C) causes a decrease in pigment absorption (λ_{min}= 560nm) and a transient absorption increase with a maximum at around 640 nm, P^W_{640}. The decay of P^W_{640}($t_{½}$=2.5 msec.) matches the recovery of pigment absorption at 560nm. Illumination of P^W_{565} at 77 °K with 500nm light causes a bathochromic shift in the absorption spectrum (λ_{max}= 630nm ,isosbestic point at 580nm).The bathoform, P^W_{630}, fully reverses to the initial state on illumination with light of wavelength longer than 650nm. The P^S_{588} to P^W_{565} transition is reversed by addition of NaCl with a conversion midpoint around 300mM concentration. KCl or $MgCl_2$ are also effective to regenerate P^S_{588}. The photo and salt dependent transitions of P^S_{588} are summarized in the following scheme:

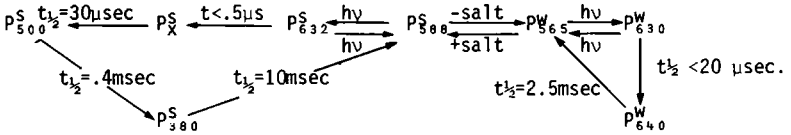

Supported by NIH grants GM-27057 and GM-28767

T-PM-F5 CHIRALLY ASYMMETRIC REVERSIBLE PHOTO BLEACHING IN PURPLE MEMBRANE FILMS. N. A. Clark, Univ. of Colorado, Boulder, CO 80309, and K. J. Rothschild, Boston Univ. School of Medicine, Boston, MA 02118.

Multilayer arrays of Purple Membrane (PM) fragments were deposited on glass substrates in the form of (2-5µ thick x 1cm across) dried films, with membrane planes oriented parallel to the glass, and membrane E faces oriented randomly toward and away from the glass. These samples were photo bleached (570nm ⇄ 412nm) with polarized 568nm Kr^+ laser light and the optical anisotropy induced was probed. We find an effective optical rotary dispersion and circular dichroism to be associated with the bleaching, which is several orders of magnitude larger than that observed for either the 570nm or 412nm PM states. (Supported in part by the Army Research Office).

T-PM-F6 PROTON FLUX CONTROLS THE LIGHT-REGULATED PROTEIN PHOSPHORYLATION SYSTEM IN HALOBACTERIUM HALOBIUM. Elena N. Spudich and John L. Spudich, Department of Anatomy, Albert Einstein College of Medicine, Bronx, NY 10461.

We have recently described a retinal-dependent, light-regulated reversible phosphorylation of two specific proteins in H. halobium (Spudich, J.L. and Stoeckenius, W. (1980) J. Biol. Chem. 255: 5501-5503). We have now investigated the relationship of this protein phosphorylation system to the light-driven transmembrane ion pumps of this organism. The sensitivity of the phosphorylation system to light correlates with the cellular content of the proton pump, bacteriorhodopsin (bR), at varying stages of culture growth; the action spectrum of protein dephosphorylation by light is similar to the action spectrum for proton efflux through bR; and the protein phosphorylation system of a mutant which lacks bR (but contains the light-driven sodium ion pump) is insensitive to light. From these results we conclude the protein phosphorylation system is regulated by the proton efflux through bR. Ionophores which collapse the transmembrane proton gradient (carbonyl cyanide-m-chlorophenylhydrazone, nigericin, and triphenyltin chloride) prevent the light-induced dephosphorylation, and furthermore will induce rephosphorylation when delivered in the light. An increase of the cellular transmembrane proton gradient induced by decreasing the extracellular pH in darkness mimics the effect of light on the phosphoproteins. These results and the interactions between the effects of light, ionophores, and imposed proton gradients implicate the transmembrane electrochemical potential of protons as the protein phosphorylation system regulator.

T-PM-F7 EVIDENCE THAT THE LIGHT-DRIVEN SODIUM ION PUMP IS A PHOTOTAXIS RECEPTOR IN HALOBACTERIUM HALOBIUM. Vic Narurkar and John L. Spudich, Department of Anatomy, Albert Einstein College of Medicine, Bronx, NY 10461.

A strain of the bacteriorhodopsin-deficient mutant ET15 was selected for enhanced chemotactic migration rate. The good motility of the selected strain (ET15S) permitted detailed examination of its tactic responses to light. ET15S has a repellent sensitivity to short wavelength light (less than 500nm) and an attractant sensitivity to long wavelength light (greater than 520nm). The repellent and attractant responses of ET15S are similar in magnitude to those of its similarly selected parent ET1001S, which contains bacteriorhodopsin. We determined photoattraction action spectra for both ET15S and ET1001S by measuring the duration of swimming reversal inhibition (1) caused by increases in light intensity at 10nm wavelength intervals through narrow band interference filters. The ET15S action spectrum has a single peak at 590nm. The action spectrum of ET1001S has two maxima, one at 570nm and one at 590nm. We interpret the results as indicating bacteriorhodopsin is the attractant photoreceptor responsible for the 570nm peak, thus supporting Hildebrand and Dencher's conclusion that bacteriorhodopsin is a phototaxis receptor (2). The dependence of the ET15S attractant response on retinal and the action spectrum maximum near 590nm suggest that also the retinal-dependent light-driven sodium ion pump (P588)(3,4), known to be present in ET15, is an attractant phototaxis receptor in H. halobium.

(1) Spudich, J.L. and Stoeckenius, W. (1979) Photobiochem. Photobiophys. 1: 43-53.
(2) Hildebrand, E. and Dencher, N. (1975) Nature 257: 46-48.
(3) Lindley, E.V. and MacDonald, R.E. (1979) BBRC 88: 491-499.
(4) Lanyi, J.K. and Weber, H.J. (1980) J. Biol. Chem. 255: 243-250.

T-PM-F8 EVIDENCE FOR β STRUCTURE IN BACTERIORHODOPSIN. R.M. Glaeser, Department of Biophysics, B.K. Jap and M.F. Maestre, Donner Laboratory, University of California, Berkeley, 94720, and S.B. Hayward, Department of Biochemistry and Biophysics, University of California, San Francisco, 94143.

A Fourier map of the projection of the structure of bacteriorhodopsin (in the plane of the membrane) has recently been obtained by Hayward at a resolution of about 4 Å. This map is consistent with earlier ones obtained at about 7 Å, but certain pronounced features now suggest that there could be as few as four α-helical regions of the peptide chain, rather than seven regions as had been proposed previously. Circular dichroism spectra have been obtained in the UV, using both the "fluorscat" cell and the fluorescence-detected CD technique, to avoid the need for any theoretical corrections due to light scattering. The resulting CD spectra cannot be fitted well by standard basis functions (for α-helix, β-sheet and random coil) except by the inclusion of substantial β-sheet. The interpretation of the spectra is made ambiguous, however, by uncertainty whether a correction is needed for "absorption flattening," and by uncertainty concerning the form that such a correction should take for a highly anisotopic structure such as the purple membrane. The IR absorption spectra of air-dried films of purple membrane show a strong band at about 1665 cm^{-1} and a pronounced shoulder at about 1630 cm^{-1}. The IR spectra thus provide strong evidence that a significant fraction of the peptide chain is in a β-sheet conformation, which is consistent with the high resolution Fourier map and with the UV circular dichroism spectra.

T-PM-G1 IDENTIFICATION AND CHARACTERIZATION OF A K-SALT ELECTRONEUTRAL PATHWAY IN MEMBRANES DERIVED FROM THE APICAL POLE OF THE STIMULATED OXYNTIC CELL. J.M. Wolosin & J.G. Forte. Dept. of Physiology-Anatomy, Univ. of California, Berkeley, CA 94720.

Large membrane (LM) vesicles rich in (K^+-H^+)-ATPase, an enzyme that has been localized in the apical-intracellular canaliculus of the oxyntic cell, were obtained from homogenates of "in vivo" stimulated gastric fundic mucosa. These vesicles display functional properties compatible with the requirements for those of the stimulated apical membrane as outlined in various reports (Ann. Rev. Physiol. (1980), 42:111; Am. J. Physiol. (1980), 238:6165). These LM vesicles will, in a medium containing K^+, Mg^{+2}, ATP and one of a number of anions, accumulate H^+ against a large chemical gradient. Unlike the case of the well-known smaller microsomal vesicles obtained from non-stimulated mucosae the rate of H^+ uptake is insensitive to valinomycin or to pre-exposure of the vesicles to K^+-salt medium. The dependence of H^+ transport on K^+, Cl^- or KCl concentration and temperature in LM vesicles differ drastically from that of the microsomal vesicles. These results as well as independent measurements of rates of salt flux demonstrate the presence of a passive K^+ permeability in this new membrane preparation. Its features identify it as an anion-linked electroneutral K^+ pathway in which Cl^-, NO_3^- and $CH_3SO_3^-$, but not carboxylate ions, could function as the co-transporting anions. Incubation of the LM vesicles at physiological temperature in a medium such that $[Cl^-]>[K^+]$ results in the fast and, to date, irreversible closure of the salt pathway, but not if NO_3^- or $MeSO_3^-$ replace Cl^- or if $[Cl^-]\leq[K^+]$. Once the salt-channel is lost the LM vesicles become functionally similar to the microsomal vesicles. It is postulated that this last property is a reflection of a putative "in vivo" modulation of this pathway.

T-PM-G2 POLARIZATION OF DOGFISH GASTRIC MUCOSA. C. Adrian M. Hogben, Mount Desert Island Biological Laboratory, Salsbury Cove, Maine 04672 and Dept. of Physiology & Biophys., U. of Iowa, Iowa City, Iowa 52242.

Having voltage clamped the isolated dogfish gastric mucosa at ± 60 mV, pO_2 1 atm, Hogben reported that H+ secretion was not modified (Bull. Mt. Desert Isl. Biol. Lab. 15:45, '75) but Kidder, pO_2 1.9 atm, elicited a "Rehm" effect (ibid 17:25, '77). Again mucosae were isolated in a flux chamber. The bicarbonate-free mucosal solution was gassed with 100% O_2 and 'stat' titrated to pH 4.5 or 7.0. With extended protocols and pO_2 1 atm, mucosae were clamped for 1 hour at -45 or -60 mV (lumen in reference to ECF), 'hyperpolarized' and at +45 or +60 mV, 'hypopolarized.' Both hyper- and hypo-polarization reduce H+ secretion. The discrepancy between the present results and former findings and between the earlier reports arise from the restricted protocols of the latter and/or variation among dogfish. There is no reason to suppose that the gastric mucosa of Squalus is hypoxic at pO_2 1 atm and 15°C. Similar results were obtained whether the mucosal solution was titrated to pH 4.5 rather than pH 7.0. Bathing the serosal surface with a bicarbonate-free buffered elasmobranch saline, 30 mM TES-100% O_2, rather than the customary 30 mM HCO_3-5% CO_2 saline did not notably change the polarization response. Conductance was increased by protracted hyper- and hypo-polarization, revealing a hitherto unsuspected long-long electrical "transient." Sporadically, 3 of 21 mucosae hyperpolarized at -45 mV and 'stat' titrated to pH 4.5 developed a "base" secretion, whose rate, 13.0, exceeded the voltage clamp current, 11.3 μ Eq cm^{-2}. hr^{-1}. The open-circuit PD of a few millivolts and conductance were not exceptional, implying that the anamalous "base" secretion arose from a forced ion exchange.

T-PM-G3 K^+- ATPase DEPENDENT ACCUMULATION OF H^+ BY GASTRIC MICROSOMAL VESICLES: EFFECTS OF HYPERTONIC KCl AND SCN^-. T.K. RAY AND Z. MENG-AI*, Dept. of Surgery, SUNY Upstate Medical Center, Syracuse, NY 13210.

We used the technique of fluorescence quenching of acridine orange (AO) for the measurement of intravesicular accumulation of H^+ by pig gastric microsomes. The normal incubation system was an isotonic medium consisting of sucrose/pipes/EDTA buffer (pH 6.8), 150 mM KCl, 1 mM $MgCl_2$, 2 mM ATP, 10^{-5} M valinomycin, 10 x 10^{-6} M AO and 0.1 mg membrane protein. About 80% of fluorescence produced by AO was quenched within 7 min under the conditions mentioned above. Increasing the concentration of KCl as high as 300 mM did not have any effect on dye uptake. The initial rate as well as the net uptake of H^+ was considerably reduced in presence of SCN^- (20-50 mM). Thus the rate of H^+ uptake was decreased by 3 fold in presence of 50 mM SCN^- and the net uptake by about 50%. Preincubation of the vesicles for 48 h at 0°C with 100 mM KCl and different combinations of 0-50 mM NaCl and NaSCN followed by pelleting and resuspension in isotonic sucrose/pipes/EDTA buffer reduced the dye uptake ability of the SCN^--loaded vesicles. The dye uptake by K^+ (100 mM)-loaded vesicles was comparable to that of the 100, K^+- val system (no preincubation) but was significantly less than the 150, K^+- val system. However, further addition of 150 mM K^+- val to the K^+ (100 mM)-preloaded vesicles produced a rapid quenching response. The SCN^- loaded vesicles on the other hand showed a dose related decrease in the second dye uptake (rapid) phase upon addition of 150, K^+- val; the uptake being completely abolished with 40 mM SCN^-. SCN^- did not have any effect on the K^+- stimulated ATPase activity of the gastric microsomes. Our data suggest that the SCN^- may induce some kind of conformational aberration in the K^+/H^+ exchange system of the gastric microsomes. (Supported by USPHS, AM 25544 and AM 00623)

T-PM-G4 IDENTIFICATION OF THE TRANSPORTING CELL TYPE, THE CHLORIDE CELL, IN A HETEROGENEOUS EPITHELIUM, THE TELEOST OPERCULAR MEMBRANE. Carl Scheffey, J. Kevin Foskett, and T.E. Machen, Depts. of Physiology-Anatomy and Zoology and Cancer Research Laboratory, Univ. of California, Berkeley, CA 94720.

Opercular membranes isolated from the seawater-adapted teleost, Sarotherodon mossambicus, possess mitochondria-rich "chloride cells" and generate short-circuit currents equal to net basal to apical secretion. Correlative data has implicated chloride cells as the cell type responsible for the transport activity in this and the branchial epithelium. To test this hypothesis, we have measured the distribution of current density immediately above the apical surface of the epithelium using the vibrating probe technique (Jaffe and Nuccitelli, 1974, J. Cell Biol. 63:614). Current sources on the apical surface were located with a spatial resolution of 20 microns. With opercular membranes at short circuit, sources of negative current of variable size were seen over 90-95% of chloride cells, but not over other cell types. The size of the sources was estimated as 2-8 nA, in good agreement with previous indirect estimates for the short-circuit current per chloride cell (total epithelial current / no. cells). The transepithelial conductance at these sources of current was much higher than that of the surrounding membrane. Momentary steps in transepithelial voltage from zero to values in the range -150 to +150 mV demonstrated a rectified voltage dependence of the current density over the chloride cells, similar to that observed for the total current across the epithelium. We conclude that chloride cells in the opercular membrane are sites of high transepithelial conductance and active chloride transport. (Supported in part by NRSA traineeships CA-09041 to J.K.F. and GM 07048-06 to C.S., by NSF grant PCM-7725205 to T.E.M., and by NIH grant NS15114.)

T-PM-G5 THE EFFECTS OF METABOLIC INHIBITORS ON SODIUM, PHOSPHATE, AND GLUCOSE ABSORPTION IN THE PROXIMAL RENAL TUBULE. S.R. Gullans, P.C. Brazy, V.W. Dennis, and L.J. Mandel. Depts. Physiology and Medicine, Duke University Medical Center, Durham, N.C. 27710

ATP generated by oxidative metabolism has been implicated as the primary, direct energy source for sodium reabsorption in the proximal tubule. However, due to technical limitations, previous studies using metabolic inhibitors have been unable to confirm this idea. In this study, isolated, perfused rabbit proximal convoluted tubules were used to measure net absorption rates for sodium (Jv), phosphate (J-Phos), and glucose (J-Gluc) during inhibition of oxidative metabolism. Transport rates were determined with radioisotopes. In addition, metabolic events were monitored in suspensions of rabbit cortical tubules by measuring oxygen consumption rates (QO_2) and mitochondrial NADH fluorescence. Metabolism was altered with either rotenone or Antimycin A, specific inhibitors of mitochondrial oxidative phosphorylation. Using dextran as the oncotic agent, 10^{-5} M rotenone or 10^{-6} M Antimycin A abolished all net transport. Furthermore, rotenone and Antimycin A inhibited QO_2 with K_i's equal to 1.6 x 10^{-7} M and 1 x 10^{-7} M, respectively. In the presence of albumin, higher doses of these inhibitors were required for equivalent effects, presumably due to the binding of the inhibitors to the albumin. These data indicate that maximal inhibition of mitochondrial ATP synthesis abolishes net transport of sodium, phosphate, and glucose. A sub-maximal dose of rotenone (10^{-6} M) inhibited Jv, J-Phos, and QO_2 by 84±4, 85±5, and 79±3 percent, respectively, and increased NADH fluorescence by 76±6 percent indicating that a direct relationship exists between these processes. J-Gluc, however, was inhibited only 59±6 percent and was thus significantly less sensitive to graded metabolic inhibition. Hence, variability appears to exist in the response of sodium-dependent transport processes to graded reductions in oxidative phosphorylation. (Supported by NIH grants AM 26201 and AM 26815).

T-PM-G6 STIMULATION OF RESPIRATION IN ISOLATED RENAL CORTICAL TUBULES BY NYSTATIN. Stuart I. Harris and Lazaro J. Mandel. Department of Physiology, Duke University Medical Center, Durham, N.C. 27710. (introduced by Melvyn Lieberman).

The spontaneous rate of respiration in isolated renal cortical tubules respiring on glucose, lactate, and alanine at 37° C is 19.0 nmol O_2 per min per mg protein. The rate may be stimulated by a factor of 1.45 by the addition of the polyene antibiotic, Nystatin (.02 mg per mg protein). The respiratory stimulation is secondary to Nystatin mediated stimulation of the Na^+,K^+-ATPase as the respiratory response is completely inhibited by ouabain. When the metabolic substrate regimen is supplemented with ketone bodies or fats prior to Nystatin addition, the degree to which Nystatin is able to stimulate respiration is significantly enhanced as follows: acetoacetate, 1.68; butyrate 1.80; valerate, 1.73. Respiratory rates in the Nystatin stimulated state were converted to mitochondrial respiratory chain turnover as follows: glucose, lactate and alanine, 634 nmol O per cyt a per min; + acetoacetate, 771; + butyrate, 1,045; + valerate, 1,002. Respiratory chain turnover for ADP stimulated respiration (state 3) in digitonin treated tubules respiring on glutamate and malate was 827 nmol O per cyt a per min; 1,008 for tubules respiring on glutamate, malate and butyrate; 986 for tubules respiring on glutamate, malate and valerate. These results indicate Nystatin mediated stimulation of respiration in intact tubules results in complete or nearly complete utilization of cellular respiratory capacity (state 3) in all substrate regimens employed with the exception of glucose, lactate and alanine alone. This finding suggests that cellular respiration becomes substrate limited during Nystatin mediated stimulation of respiration unless fats or ketone bodies are present in the substrate regimen. (Supported by NIH grants AM 26815 and GMO - 7171).

T-PM-G7 MEASUREMENT OF LIQUID JUNCTION POTENTIALS AND DETERMINATION OF PROXIMAL TUBULE TRANSEPITHELIAL POTENTIALS. Raynald Laprade, Jean Cardinal. Centre de Recherche, Hôpital Maisonneuve-Rosemont; Département de Physique and Département de Médecine, Université de Montréal, Montréal, Québec, Canada. H3C 3J7

Transepithelial potential difference measurements in the isolated proximal tubule involve the presence of liquid junction potentials (LJP) between perfusate (P) and bath (B) solutions or between these and the electrodes whenever P and B differ in ionic composition. Due to their importance relative to the actual potentials, these LJP must be appropriately corrected for in order to determine the driving force for ions and solutes transport or to evaluate the relative ionic permeabilities in the presence of gradients. Theoretical evaluations of these LJP using Henderson's equation are most often unsatisfactory while measurements with the usual saturated KCl reference electrode introduce important errors. We therefore describe a more accurate method of measurement, using Ag/AgCl electrodes and a liquid junction formed across the tip of a micropipette. The value of the LJP can be evaluated from the measured potential across the whole circuit and the concentration of Cl ions in the two solutions forming the junction, taking into account in the presence of proteins, Cl binding and protein volume. Depending on the solutions involved, values of LJP measured with this method are between 30% and 60% higher than those measured with a saturated KCl electrode. For the case of normal perfusate and bath serum (containing 6g/100 ml albumin) the correction for the B-P junction is 2.6 mV, implying that the actual potential difference in the proximal convoluted tubule with these artificial solutions is close to zero. In the presence of a 50 mM NaCl gradient, we show that the correction is more than 2 mV higher than that used in previous studies, indicating that in the latter, the sodium to chloride permeability ratio has been overestimated.

T-PM-G8 POTENTIAL-DEPENDENT D-GLUCOSE UPTAKE BY RENAL BRUSH BORDER MEMBRANES IN THE ABSENCE OF Na^+. Shirley Hilden, Laboratory of Molecular Aging, Gerontology Research Ctr., National Institute on Aging, NIH, Baltimore City Hospitals, Baltimore, MD 21224.

D-Glucose transport in brush border membranes has been proven to be Na^+-dependent. This paper reports the existence of glucose uptake in the absence of Na^+ which is believed to be an alternative mode of operation of the Na^+ dependent glucose transport system. This Na^+-independent glucose uptake is 1) stereospecific, 2) phloridzin sensitive, 3) phloretin and cytochalasin insensitive and 4) membrane potential dependent. This glucose uptake shows characteristics which include a) saturability, b) accelerative exchange diffusion, c) osmotic sensitivity, d) substrate specificity and 3) temperature dependence. These results have implications for the following aspects of the Na^+/glucose cotransport: A) What is the order of substrate addition?, B) How are the kinetic parameters for glucose transport effected by Na^+? and C) How does membrane potential effect Na^+ dependent glucose transport?

T-PM-G9 EFFECTS OF pH AND VFA ON RABBIT URINARY BLADDER. MARK IFSHIN AND DOUGLAS C. EATON, UNIVERSITY OF TEXAS MEDICAL BRANCH, GALVESTON, TEXAS.

Large changes in the transport properties of the rabbit urinary bladder can be seen when the mucosal solution contains a volatile fatty acid (VFA) and the pH of the mucosal solution is changed to a pH of less than 5. Both serosal and mucosal solutions were symmetrical except for pH and were buffered by HEPES at pH 7.4 and by the VFA at the test pH. Most experiments were performed using acetate although propionate was also used. Mucosal pH was monitored using a Corning pH electrode in the mucosal chamber. The transepithelial potential was measured using calomel electrodes while current was passed through Ag/AgCl electrodes. Microelectrodes were used to determine the voltage divider ratio (alpha). The response caused a large increase in the short circuit current, a large increase in the transepithelial conductance, and a large drop in alpha. The response is abolished when either mucosal sodium or mucosal chloride is removed. The response apparently requires the sodium/potassium ATPase at the basolateral membrane since the response is not present with serosal ouabain or zero serosal potassium. Attempts at eliciting a response by simply acidifying the intracellular pH by ammonium, increased carbon dioxide, and high acetate at a higher pH failed ruling out the possibility that the response is simply due to intracellular acidification facillitated by the VFA and the low pH.

T-PM-G10 CHLORIDE INDUCED CHANGES IN SHORT CIRCUITING CURRENT IN TURTLE BLADDER. J.H. Durham, C. Matons, and W.A. Brodsky. Dept. Physiol., Mt. Sinai Sch. Med.,N.Y.,N.Y.

In turtle bladders bathed on both surfaces by identical Na-free media containing HCO_3 and Cl, Isc exceeded net reabsorptive Cl flux (I^{Cl}_{net}); and when the mucosal HCO_3 was reduced to vanishingly low levels Isc approximated I^{Cl}_{net}, suggesting that active Cl reabsorption is an electrogenic process (Gonzalez et al.,AJP,1967). However I^{Cl}_{net} approximated the rate of alkali entry into a HCO_3-free mucosal fluid from a HCO_3-rich serosal fluid suggesting that Cl reabsorption occurs via a one-for-one transepithelial exchange of Cl for bicarbonate secretion (Leslie et al.,AJP,1973). Because the transepithelial electrochemical potential gradients (notably HCO_3) were not zero in those studies, we therefore studied the effects of Cl removal from and addition to (HCO_3+Cl)-containing bathing fluids under steady state conditions of zero transepithelial electrochemical potential gradients. In 7 such experiments, addition of Cl increased the PD and Isc from 27±5 to 46±7 mV and from 15±2 to 41±10 μA, respectively. In another 11 bladders under the same conditions, it was found that the mean Cl-induced increase in Isc (19.6±8.1 μA) and I^{Cl}_{net} (19.3±7.5 μA) were not statistically different. These results are predicted by the hypothesis holding that active Cl transport occurs by an electrogenic process, but are not predicted by any kind of transepithelial electroneutral exchange of Cl for HCO_3. (Supported in part by NSF grant PCM 76-02344 and NIH grant AM-16928)

T-PM-G11 INTERFERENCE OF FUROSEMIDE AND OTHER ANION TRANSPORT INHIBITORS WITH LIQUID CL-EXCHANGER ELECTRODES. E. Heinz and S. Grassl, Cornell University Med. Coll., New York, NY 10021

To test the liquid Cl-exchanger (Corning Code No. 477315), which is widely used for Cl-microelectrodes, as to sensitivity and interferences, a Cl-electrode was made by soaking a Celgard TM membrane with the above exchanger, using a Ag-AgCl electrode in 0.1 N KCl. The electrode was found to respond rapidly but to be very unspecific with respect to anions. For instance, it is more than 3 times more sensitive towards NO_3^- and Br^- than to Cl^-, but it also responds to various organic ions, such as lactate, according to their lipid solubilities. These interferences can easily be corrected for, as plotting $\bar{S}$, the exponential function of the PD vs. the Cl^- activity yields a straight line, the slope of which is not altered by the presence of interfering anions at constant concentrations. The Cl-electrode was strongly but reversibly disturbed by inhibitors of Cl-transport, such as furosemide and the stilbene derivatives, SITS and DIDS, which at physiologically effective concentrations slowly and steadily shift the readings towards seemingly higher Cl^- activities. The effect of furosemide could be identified as that of an anion towards which the electrode is 16 times more sensitive than towards Cl^- but which does not appreciably alter the selectivity of the exchanger towards Cl^-. Hence [Cl] in biological fluids could be monitored satisfactorily even in the presence of 0.1 mM furosemide, once the electrode had equilibrated with the latter. The effect of the stilbene derivatives, however, appear to affect the electrode in a more profound manner, which has not been elucidated.

T-PM-G12 MEMBRANE ASYMMETRY IN EPITHELIA: IS THE TIGHT JUNCTION A BARRIER TO DIFFUSION IN THE PLASMA MEMBRANE? P.R. Dragsten[1], R. Blumenthal, Laboratory of Theoretical Biology, DCBD, NCI, NIH, and J.S. Handler, Laboratory of Kidney and Electrolyte Metabolism, NHLBI, NIH, Bethesda, MD 20205

We investigated the maintenance of cellular asymmetry in confluent epithelia in culture by direct observation of fluorescent probes labeling either the apical or basolateral surface. This asymmetric labeling was maintained for lectin probes, which were immobile on the cell surface, and also for some fluorescent lipid probes, which freely diffused. The initial asymmetric distribution was not maintained with other lipid probes. The barrier to penetration between apical and basolateral membranes appears to be at the tight junction, thus demonstrating that the tight junction may act as a barrier segregating certain lipids to either the apical or basolateral surface. Accessibility of the lipid probes to quenching and measurements of lateral diffusion coefficients by fluorescence photobleaching recovery indicate differences in interaction with the membrane between the lipid probes which do and do not pass the tight junction. The distinguishing feature of those probes capable of passing the tight junction may be related to their ability to "flip-flop" to the inner monolayer of the cell membrane.

[1]Current address: The Procter and Gamble Company, Miami Valley Laboratory, P.O. Box 39175, Cincinnati, OH 45247

T-PM-H1 VARIATION OF DIFFRACTED LIGHT INTENSITY WITH ANGLE OF INCIDENCE DURING TETANIC CONTRACTION. Barry D. Lindley, David Goldthwait, Jr.*, and Evalyn Pelander*. Department of Physiology, Case Western Reserve University, Cleveland, Ohio.

The approach of Rüdel and Zite-Ferenczy (J. Physiol. 290:317,1979) was extended to allow dynamic resolution of lengths of sarcomere populations during twitches and tetanic contractions. Single fibers were dissected from m. semitendinosus of R. pipiens and mounted in a chamber, with cover-slip sides, fixed to a rotating platform. A 1 mm HeNe laser beam was passed through the fiber and the intensity of the first order diffraction line monitored by a photodiode. Records of the time course of intensity were digitized and stored on disk during successive contractions at different angles of deflection of the fiber axis from the direction normal to the laser beam. From these records "isochronal"sections could be reconstructed and, following correction for refraction at the air/Ringer interface, assessment made from such profiles of intensity versus angle of deflection of the apparent subpopulations of sarcomere length and tilt during contraction and relaxation. During the plateau of a 0.3 s tetanus the intensity of the diffracted light was greatly reduced at all angles. As the fiber relaxed, the intensity returned to resting levels or greater and a variable number of distinct peaks appeared. The return to a smaller number of peaks characteristic of the resting fiber required a few seconds. Peaks which could be matched in left and right first order lines indicated shorter sarcomeres during contraction and relaxation than at rest.

Supported by NS10196,HL19848, and the Northeast Ohio Affiliate,AHA.

T-PM-H2 THE USE OF LASER DIFFRACTION TO MEASURE SARCOMERE LENGTH by Richard L. Lieber, Yin Yeh, and Ronald J. Baskin, Departments of Zoology and Applied Science, University of California, Davis, CA 95616.

For several years, laser diffraction has been used as a non-invasive tool for measuring sarcomere length in skeletal muscle. The simplicity and supposed degree of accuracy of the technique has made it available for use in a variety of physiological settings. However, recent studies (Rudel & Zite-Ferenczy, J. Physiol. 290:317, Biophys. J. 30:507, and Baskin, Lieber, Oba, & Yeh, Fed. Proc. 39:1729) have shown that three dimensional diffraction effects (e.g., Bragg diffraction) can be observed under certain conditions. This demonstration has suggested that the grating equation ($n\lambda = d \sin\theta$) may not accurately describe the position of a diffracted order.

We have addressed this question by considering diffraction from a muscle fiber to be the result of the superposition of grating and three dimensional diffraction. Based on this premise, and the theory which we recently presented (Yeh, Baskin, Lieber, & Roos, Biophys. J. 29:509), experimental conditions are set forth under which grating information (i.e., sarcomere length) can be expected to dominate the diffraction pattern. These conditions are examined by performing angle scans (measuring intensity variations while varying incident angle) of fibers with different diameters with two different beam widths. With the smaller beam, more fine structure is observed. This may indicate an increased contribution of Bragg or thick grating diffraction to the angle scan profile.

T-PM-H3 REAL TIME HIGH SPEED SARCOMERE LENGTH MEASUREMENTS FROM OPTICAL IMAGE. Robert C. Jacobson , Reuven Tirosh, Michael J. Delay and Gerald H. Pollack, University of Washington, Seattle, WA 98195.

We have reported stepwise shortening behavior in contracting muscle based on high speed measurements of the sarcomere length using laser diffraction. These results have been questioned due to the possibility of artefact arising from Bragg effects. We have therefore developed the following technique which is not subject to the limitations of diffraction. The microscopic image of the muscle obtained with Xe illumination was projected onto a photodiode array. The field of view of the device was a thin strip approximately 5 μm wide by 30 striations. The video signal was processed by a phase-locked loop, and sarcomere length was computed every 250 μs. The resulting sarcomere length signals were of very high quality, in some cases having r.m.s. noise levels less than 0.75 nm. Many records showed clear stepwise behavior. Statistical analysis of the latter data confirmed that sarcomere shortening alternated abruptly between periods of constant high velocity and near zero velocity. In general, steps seemed to occur in greater abundance and regularity with the optical imaging method than with laser diffraction. This may be due to the fact that the volume of muscle examined using the optical imaging method is much smaller, thus providing a signal which is more representative of localized events.

T-PM-H4 CONTRACTING MUSCLE GENERATES SOUND BURSTS. F. V. Brozovich and G.H. Pollack, Dept. of Anesthesiology, Div. of Bioengineering (RN-10), University of Washington, Seattle, WA 98195.

It has been reported (1,2) that muscle contracts in a stepwise fashion, in which periods of high velocity shortening alternate with pauses. This phenomenon has been observed using optical diffraction and also by analysis of the muscle striation pattern. Stepwise changes of muscle length might be accompanied by stepwise changes in diameter. If so, each stepwise change of fiber diameter should produce a short, high-frequency shock wave, which may be detectable as a sound burst. The present study tests this hypothesis. Sartorius muscle of Rana pipiens was stimulated to twitch isotonically. Shortening averaged 20-25% of resting length. Sounds were recorded with a piezoelectric transducer (resonant at 1.8 MHz) which was placed close to the muscle. A series of discrete bursts of high frequency sound was generated during each contraction. Subthreshold stimulation did not produce sound. This suggests that the sound was not produced by the experimental apparatus. The pattern of sound was repeatable from contraction to contraction, and similar recordings were obtained in eight muscles. At 1.5°C, bursts were produced approximately every 50 msec; at 13.5°C, the interval between bursts decreased to 10-15 msec. The time intervals between sound bursts are consistent with the pause durations expected from optical observations.

(1) Pollack, G.H., et al. (1977). Sarcomere shortening in striated muscle occurs in stepwise fashion. Nature (Lond.), 268: 757-59.
(2) Tirosh, R., et al. (1980). Stepwise sarcomere shortening: confirmation by high speed cinemicrography. Fed. Proc., 39:1730.

T-PM-H5 DIFFERENTIAL SHORTENING OF MYOFIBRILS DURING DEVELOPMENT OF FATIGUE. Gonzalez-Serratos, H., Garcia, Maria del Carmen*, Somlyo, Avril+, Somlyo, A. P.+ and McClellan, G.+ Dept. Biophysics, Univ. of Maryland, Baltimore, MD, 21201, *Dept. Physiology, Centro de Investigacion, Mexico 14, D.F., +Dept. of Pathology and Physiology, Univ. of Pennsylvania, Philadelphia, Penn., 19104.

In a previous report we have shown that during fatigue a) the T.C. calcium content is above normal b) the transverse tubules are swollen in several places (Proc. Nat. Acad. Sci. (USA) 75, 1329, 1978) and c) the duration of the active state increases during the repetitive stimulation before the development of fatigue and well within it (Proc. Int. Union Physiol. Sci. XIV, 440, 1980). The above findings led us to suppose that during fatigue some myofibrils or groups of them might be either less or not activated at all as compared to the rest of them.

We have investigated this possibility in isolated muscle fibres by giving them repetitive (500 msec stimulation period repeated every 3 sec.) tetanic stimulations (60 Hz) until fatigue developed. Before stimulation started the average sarcomere space was set to 2.2μm. The isometric force was recorded all along the experiment. During some cycles, before and after fatigue developed, the muscle fibre was allowed to shorten during the plateau of the tetanic stimulation to an average sarcomere space of around 1.6μm. The behavior of myofibrils during isotonic contractions was followed by taking cine-microphotographic recordings. Before fatigue, no indication of lack of shortening of myofibrils could be found. In contrast, during fatigue groups of myofibrils became wavy indicating that either they did not shorten or shorten less during the contraction. The existance of non-activated myofibrils may explain in part the development of fatigue. (Supported by grants from NIH: NS13420-05 and Muscular Dystrophy Assoc. of America. GMC supported by a fellowship from CONACYT).

T-PM-H6 SPECKLE BEHAVIOR, ACTIVATION, AND ISOMETRIC RELAXATION IN CARDIAC MUSCLE. J. Krueger & R. Glassman, The Albert Einstein College of Medicine, Bronx, N.Y. 10461

We used a kymographic technic to determine the basis for the behavior of the speckle spots comprising the pattern of light diffracted from cardiac muscle. Thin (<250μm) trabeculae from rat hearts were bathed in oxygenated Ringers solution containing 1.9 mM $CaCl_2$ @ 27° C and electrically stimulated to contract at 24/min. Force and sarcomere length were measured, the latter by light diffraction (λ=0.6328μm). The speckled pattern of the zero light was scanned every ms with a narrow (16μm) photodiode array. The array's video output was deflected across the face of an oscilloscope to create a 'streak-photo' of the speckle behavior. (This simple technic distinguishes between speckle motion and fluctuation, and could detect ~ 5ms speckle fluctuations in resting muscles in the presence of 1 mM Ouabain + 0.25 mM $CaCl_2$ (Lappe & Lakatta, 1980).) The speckle pattern was quiescent during the latent period, the onset fluctuations coincided (within 2 ms) to the onset of sarcomere shortening in contractions in which the ends of the muscle were held isometric. However, when contractile shortening of the sarcomeres was prevented by direct feedback control, contractile force increased and the speckle spots persisted as streaks 100 to 300 ms in duration. Thus speckle fluctuation is associated with neither force nor activation processes in cardiac muscle. When sarcomere length was controlled throughout contraction, speckle fluctuations and motion coincided with a sudden 'give' in tension occurring at midrelaxation. This event resembles the 'give' and subsequent yielding described in single skeletal muscles fibers (Cleworth & Edman, 1969; Huxley & Simmons, 1970) except that here the length of the cardiac muscle preparation is shortened to keep sarcomere length constant. (Supported, in part, by the New York Heart Association and N.I.H. grant HL 21325-04.)

T-PM-H7 STIFFNESS OF FROG SINGLE MUSCLE FIBERS DURING TENSION TRANSIENTS AND CONSTANT VELOCITY SHORTENING. David L. Morgan and Fred J. Julian, Dept. of Muscle Research, Boston Biomedical Research Institute, 20 Staniford St., Boston, MA 02114

The length change of a central segment of a frog muscle fiber was measured during and after a quick shortening was applied to the end of the fiber, by attaching markers and using a spot follower apparatus to monitor the length change between them. In this way it was shown that the stiffness of tetanised single frog fibers as mounted in our apparatus is located predominantly in the sarcomeres, and that the ends are comparatively stiff. The stiffness of tetanised frog single fibers at 0°C was measured by applying a small 4 kHz sinusoidal length change, and measuring the resultant tension change. This was done during the first few milliseconds after a quick release, and while the fiber was shortening at constant velocity. As reported previously, Biophys. J. 25, 271a, the stiffness during the fast tension transient after a quick release was always less than the stiffness before release, supporting the idea that the fast recovery is not due to attachment of extra cross-bridges. The stiffness during steady shortening was always less than when isometric, and a line fitted to this stiffness-tension plot, when extended, intercepted the stiffness axis at less than half the isometric value. The slope of the stiffness-force plot during the fast tension transient was consistently and significantly less than the slope of the force-stiffness plot during steady shortening, further supporting the conclusion that only a small part of the decrease seen during shortening could be due to nonlinear end compliance. These results suggest that X-ray diffraction results, which has shown little if any change in intensity ratios during steady shortening, may not be a suitable method of measuring numbers of attached cross-bridges under these conditions, perhaps due to the effects of changes in cross-bridge orientation. (Supported by USPHS HL-16606, AHA 77-616 and MDA)

T-PM-H8 TENSION, STIFFNESS, UNLOADED SHORTENING VELOCITY AND POTENTIATION OF FROG MUSCLE FIBERS AT SARCOMERE LENGTHS BELOW OPTIMUM. David L. Morgan and Fred J. Julian, Dept. of Muscle Research, Boston Biomedical Research Institute, 20 Staniford St., Boston, MA 02114

The plot of isometric tetanic tension against sarcomere length for frog single fibers, (Gordon, Huxley and Julian, 1966 J. Physiol. 184, 170-192) includes a shallow ascending limb from 1.65 to 2.0 um, where filament overlap is maximal, but tension is submaximal. In order to determine whether this submaximal force is caused by the existence of some force opposing shortening, or by a reduction in the number of active cross-bridges, unloaded shortening velocity and stiffness were measured in this region. The velocity of externally unloaded shortening was found to be constant over most of this range, certainly not changing as predicted by the force-velocity curve and the assumption of an internal force opposing shortening. Stiffness was found not to vary in proportion with tension between sarcomere lengths 1.65 um and 2.0 um, nor to be constant between 2.0 and 2.2 um, where tension is constant. By assuming a small filament compliance, the observations could be adequately modelled on the hypothesis that the variation in tension was caused by variations in the number of attached cross-bridges. In order to determine whether this decrease was caused by structural effects or failure of spread of activation, the effects of various agents on the sarcomere length-tetanic tension curve were investigated. The twitch potentiators Zn^{++}, tetra-ethyl-ammonium (T.E.A.), nitrate and caffeine were found not to change the shape of the sarcomere length-tension diagram. Absolute tetanic potentiation was less than 3% in all experiments. It is concluded that the shallow ascending limb of the sarcomere length-tension curve is probably caused by a reduced number of attached cross-bridges, due to mechanical interference, as no evidence of incomplete activation could be found in these fibers at these lengths. (Supported by USPHS HL-16606, AHA 77-616 and MDA)

T-PM-H9 THE EFFECT OF RAPID SHORTENING ON ATP UTILIZATION AND ENERGY LIBERATION OF FROG SKELETAL MUSCLE. M. Irving, E. Homsher & A. Wallner (Intr. by W.K. Chandler) Dept. of Physiology, U.C.L.A., Los Angeles, CA 90024.

Pairs of sartorius muscles were tetanically stimulated for 3 s. at 0°C. Chemical changes associated with a period (S) from 2 to 2.3 s., during which the muscles shortened rapidly at constant velocity from sarcomere length 2.6 μm to 1.8 μm, were determined by freezing one muscle of a pair at 2 s. and the other at 2.3 s. (Sarcomere lengths were measured in resting muscles). The 0.7 s. period (PS) immediately following such shortening and the period (I) from 2 to 3s. in an isometric tetanus at 1.8 μm were studied similarly. The design eliminates some ambiguities of earlier experiments in which shortening began at the start of stimulation and progressed to very short sarcomere lengths. The levels of ATP, ADP and AMP did not change significantly in any contraction period; the only measurable reaction occurring was phosphocreatine splitting. The calculated mean rate of ATP utilization (per muscle wet weight) in period S was 0.48 ± 0.24 μmole/g/s (mean ± S.E.M., n = 29), which was not significantly different from that, 0.32 ± 0.11 μmole/g/s (n = 17) in period I. The rate in period PS, 0.71 ± 0.10 μmole/g/s (n = 22) was however significantly greater than that in I. In contrast the mean rate of energy (heat plus work) liberation was much higher in S than in either PS or I. Energy liberation in S was significantly in excess of that expected from the simultaneous chemical reactions, by 6.5 ± 2.6 mJ/g (mean ± S.E.M.). The discrepancy was in the opposite direction in PS, when the liberated energy was 6.2 ± 2.6 mJ/g less than that expected from the corresponding chemical changes. There was no significant discrepancy in the isometric period. The results will be discussed in terms of a change in the distribution of cross-bridge states during rapid shortening. (Supported by U.S.P.H.S. grant HL-11351 and S.R.C., England).

T-PM-H10 INTERFILAMENTARY FORCES IN RELAXED DETERGENT-SKINNED FROG SKELETAL MUSCLE. Alan Magid, Dept. of Anatomy, Duke Univ. Med. Ctr.,Durham,NC 27710.

The forces which stabilize the A band filament lattice are incompletely known. Therefore, I have studied radial filament movements in Triton-skinned sartorius and semitendinosus muscles by X-ray diffraction. Demembranation under relaxing conditions permits expression of lattice forces unhindered by osmotic constraints imposed by the plasmalemma or mechanical constraints by attached crossbridges (Magid & Reedy,Biophys.J.30:27,1980).Using osmotic pressure (up to 500 torr) provided by PVP-40 (polyvinylpyrollidone, 40000 MW) to oppose lattice swelling pressure, interaxial thick filament spacing ($d_{m,m}$) showed a hyperbolic dependence on applied pressure. At SL 2.2 μm, $d_{m,m}$ approached 32 nm. This asymptote is about 10 nm greater than would be expected from close-packing of thin and thick filaments. When stretched, sartorius muscles showed a small decrease in $d_{m,m}$ with SL until ~2.7 μm, where a sharp increase in slope appeared. Radial compression with PVP caused this slope to flatten. Combining osmotic pressure (300 torr) and tensile stress (SL 3.0 μm) brought the thick filaments closer ($d_{m,m}$ 29 nm) than either treatment alone. Semitendinosus muscles, mechanically more compliant than sartorius, also differed in $d_{m,m}$ vs SL. The breakpoint occured at SL 3.2 μm and then fell less steeply. Lattice compression produced by tensile stress continued beyond filament overlap, reaching 33.5 nm at SL 5.0 μm, the longest SL obtained. These results will be discussed in terms of a new structural model for striated muscle (Magid, ms submitted) which proposes two new elastic elements: "third filaments" which connect the ends of each thick filament to the Z line, and "struts" which link thick filaments transversely along their length. The former bear the tensile stress when muscles are stretched while the latter resist radial lattice movements. (Supported by NIH grants to M.K. Reedy and MDA grants to A. Magid.)

T-PM-H11 MYOSIN PHOSPHORYLATION AND TWITCH POTENTIATION IN RAT FAST- AND SLOW-TWITCH SKELETAL MUSCLE. David R. Manning and James T. Stull. Dept. Pharmacol., U. Tx. Hlth. Sci. Ctr., Dallas, TX 75235

Phosphorylation of the 18,500-dalton light chain subunit (P-LC) of vertebrate fast-twitch skeletal muscle myosin has been characterized in intact fast-twitch skeletal muscle. In previous studies utilizing rat extensor digitorum longus (EDL) muscle, we found a positive correlation to exist between P-LC phosphate content and potentiation of peak twitch tension at 23°. Values for both increased transiently at comparable rates following tetanic stimulation and were similarly dependent upon the frequency and duration of stimulation. In order to determine the extent to which this correlation persisted, the occurrences of P-LC phosphorylation and twitch potentiation were examined at 35° in rat EDL and soleus muscles, fast- and slow-twitch skeletal muscles, respectively. In EDL muscle, pre-tetanic resting P-LC phosphate content was 0.21 mol phosphate/mol P-LC. At 10 sec following a 1-sec tetanic stimulation (200 c/s), P-LC phosphate content had increased to a maximum of 0.50 mol phosphate/mol P-LC and peak twitch tension was 1.6-times that of pre-tetanic controls. Thereafter, both declined similarly in slow, monoexponential manners. In soleus muscle, the phosphate content of the P-LC was <0.01 and 0.11 mol phosphate/mol P-LC prior to and 10 sec following a 1-sec tetanic stimulation (200 c/s); there was no measurable potentiation of twitch. However, at 10 sec following a prolonged (10 sec) tetanic stimulation, P-LC phosphate content had increased to 0.37 mol phosphate/mol LC2 and peak twitch tension was 1.25-times that of pre-tetanic controls. These results corroborated previously established correlations between P-LC phosphate content and potentiation of peak twitch tension, and were consistent with a role for P-LC phosphorylation in modulation of muscle contraction.

T-PM-H12 RESPONSES OF ISOLATED GOLGI TENDON ORGANS TO SINUSOIDAL STRETCH. Y. Fukami and R.S. Wilkinson, Dept. Physiology and Biophysics, Washington University School of Medicine, St. Louis, Mo. 63110.

Isolated cat tendon organs (GTOs) were placed in a chamber containing Locke's solution with their muscle end tied to an electromechanical transducer and their tendon end tied to a force transducer. The afferent axon was raised on a recording pipette into mineral oil. After impulse block by tetrodotoxin, receptor potential was recorded together with displacement and tension in response to steady-state sinusoidal stretch over the frequency range from 0.1 Hz to 100 Hz. The gain, A_R and A_T, and phase, ϕ_R and ϕ_T of receptor potential and tension (with respect to displacement, $D=D_o\cos 2\pi ft$) were computed by Fourier analysis of digitized responses.

Both A_R and A_T showed compressive nonlinearity in their amplitude dependence. With the GTO just taut, A_R was constant or decreased slightly as D_o was increased up to ≈ 9 μm; for larger D_o, A_R decreased as a power function, $A_R \sim D_o^{-.21}$ (average of 10 GTOs tested). The power law slope relating A_R and D_o became more negative when initial tension in the preparation was increased. A_T showed similar but less severe amplitude nonlinearity.

In frequency response measurements, A_T increased slightly with f as an approximate power function, $A_T \sim f^{.07}$; ϕ_T averaged 8° for 8 GTOs tested. A_R was nearly constant for f < 1 Hz, increased with f in the range from 1 to ~20 Hz, then fell. Maximum ϕ_R averaged 23°. Generally, GTOs showed less frequency dependence than spindle secondary endings, indicative of lesser dynamic sensitivity. Supported by grants from NSF (BNS77-21801) and the Muscular Dystrophy Association.

T-PM-Po1 MULTIPLE ACTIONS OF ANIONS WHICH CAUSE Ca RELEASE FROM SARCOPLASMIC RETICULUM. M.M. Sorenson and L. de Meis. Departments of Neurology, Columbia University, New York, and Biochemistry, Federal University of Rio de Janeiro, Brazil.

Salicylate (Sal) and thiocyanate (SCN) inhibit ATP-dependent Ca uptake and cause Ca release from isolated sarcoplasmic reticulum (SR) vesicles. Experiments show that effects on ATP hydrolysis as well as on the passive permeability are involved. As reported for SCN (The & Hasselbach,1975), in the presence of a precipitating anion (pH 7, 25°), substitution of 100mM KSCN or KSal for KCl reversibly inhibits Ca uptake rates by 76% and 97% in comparison with controls (100mM KCl). Without a precipitating anion, both rate and capacity for Ca uptake are reduced. Addition of 50mM SCN or Sal to a control which has reached a steady state leads to a similar reduction in capacity as 38% or 55% of the accumulated Ca is released. Both release and reduced uptake can be attributed in part to inhibition of the pump, since under similar conditions activity of solubilized ATPase is inhibited 18% by SCN and 50% by Sal. A second factor in release and reduced Ca uptake is enhanced permeability to Ca^{2+}. Net efflux of Ca into EGTA (10mM, 25°) was measured using SR passively loaded with 40mM $CaCl_2$. Half of the Ca in the SR (19 of 39 nmol/mg prot) is released in 50-60 sec by 50mM Sal or 100mM SCN, compared with a loss of only 8 nmol/mg in 100mM Cl. The permeability increase caused by SCN may involve the pump, since (a) it is blocked by addition of Mg + Pi (phosphorylating conditions), and (b) it is specific for Ca (^{14}C sucrose permeability is not affected). In the case of Sal, only part of the increased Ca permeability is blocked by Mg + Pi, and the permeability to sucrose is also enhanced. Data which appeared in abstract but were not presented (Fed. Proc. 39:2037, 1980) will be summarized as required to define conditions for measurements of passive efflux. Supported by NIH, MDA, FINEP, CNPq, and the Fulbright Commission.

T-PM-Po2 TRYPSIN-STIMULATED LEAKAGE AND CALCIUM TRANSINHIBITION IN SARCOPLASMIC RETICULUM. K. C. Toogood, M. K. T. Dolejsi, H. J. McCutchan, and A. K. Dunker; Biochemistry/Biophysics Program and Chemistry Department, Washington State University, Pullman, WA 99164

Previous studies on trypsin digestion of sarcoplasmic reticulum membranes have focused on the degradative aspects of trypsin. Surface projections observable in the electron microscope become removed by trypsin digestion, the membranes no longer pump calcium, the ATPase activity of the membrane becomes diminished, and the ATPase molecule becomes degraded.

In marked contrast, we report here the creation of two new trypsin associated activities, trypsin-stimulated leakage and calcium transinhibition of calcium leakage. If sarcoplasmic reticulum vesicles are loaded with calcium and then subjected to digestion, the calcium is found by filtration to leak out rapidly after a lag period. This trypsin-stimulated leakage is stopped by a shift to pH 5.0, and this low pH inhibition is reversed without a lag if the pH is raised back to 6.8. The low pH inhibition curve follows that expected for the titration of a single group of pK = 5.0. These results are consistent with the titration of a single carboxyl group leading to the closing of the calcium leakage pathway.

If calcium is added to the external medium along with the trypsin, subsequent leakage from the inside is completely inhibited. Subsequent addition of soy bean trypsin inhibitor, to stop further trypsin digestion, followed by addition of EDTA, to remove the external calcium, leads to immediate calcium leakage. Thus, external calcium added at the time of trypsin digestion is blocking holes, not simply altering the trypsin digestion. Since calcium on the outside blocks leakage of calcium from the inside, we call this phenomenon calcium transinhibition. Strontium also blocks leakage, but appears to be less effective than calcium; barium is still less effective and magnesium has no measurable affect on the initial leakage rate. Thus, calcium transinhibition is highly calcium specific.

T-PM-Po3 CROSSLINKING OF CARDIAC MUSCLE SARCOPLASMIC RETICULUM PROTEINS. Charles F. Louis and Bruce Jarvis. Department of Veterinary Biology, University of Minnesota, St Paul, Minnesota 55108.

Chemical crosslinking, which can indicate the arrangement of protein subunits, was used to examine the organisation of the different proteins that are present in cardiac sarcoplasmic reticulum vesicles (SR) isolated from canine ventricular muscle. SR (4 mg/ml) was crosslinked with either cupric phenanthrolate or dithiobis (succinimidyl propionate) in 20 mM HEPES (pH 7.0) for 5 minutes at 25°C. Low concentrations of cupric phenanthrolate (0.2 mM $CuSO_4$/0.4 mM phenanthroline) crosslinked only the 100,000 dalton Ca-ATPase monomers; the several lower molecular weight components in SR remained uncrosslinked. Analysis of crosslinked samples by two-dimensional slab gel electrophoresis that contained sodium dodecyl sulfate and 2-mercaptoethanol (a gel system that reveals the monomers from which the crosslinked species are derived) indicated that the Ca-ATPase was crosslinked to form homopolymers. Similar results were obtained when SR was crosslinked with 1 mM dithiobis (succinimidyl propionate). That the cardiac SR Ca-ATPase can only form crosslinked homopolymers (even when there are are many other proteins in this membrane) suggests that as in skeletal muscle SR, the Ca-ATPase may exist as a homopolymer in the cardiac SR membrane. (Supported by the American Heart Association Minnesota Affiliate, the Graduate School of the University of Minnesota, and HL-25880 from NIH)

T-PM-Po4 THE PROFILE STRUCTURE OF THE Ca^{2+} PUMP PROTEIN MOLECULE IN THE ISOLATED SARCOPLASMIC RETICULUM MEMBRANE. J.K. Blasie[+], L. Herbette[°], P.H. DeFoor[∓] and Sidney Fleischer[∓], Univ. of Penn.[+], Philadelphia, PA 19104, Univ. of Conn. Health Center[°], Farmington, CT 06032, Vanderbilt Univ.[∓], Nashville, TN 37325, Brookhaven Natl. Lab.[+°], Upton, NY 11973.

The electron density profile has been previously derived for the isolated sarcoplasmic reticulum (SR) membrane to ~10Å resolution utilizing lamellar X-ray diffraction from functional hydrated oriented membrane multilayers. The contributions of water and lipid to this profile have now been determined directly utilizing appropriate neutron scattering difference profiles together with H_2O/D_2O exchange and the exchange of deuterated SR lipids for protonated SR lipids in the isolated SR membrane. This exchange of deuterated SR lipids (prepared biosynthetically) into the isolated SR membranes using exchange proteins did not affect the Ca^{2+} transport activity (using lecithin exchange protein), the particle distributions as observed by freeze-fracture electron microscopy or the electron density profile at ~10Å resolution of the isolated SR membrane. The direct determination of the water and lipid contributions to the SR membrane profile has permitted the determination of the Ca^{2+} pump protein molecular profile by simple difference methods to ~10Å resolution since the Ca^{2+} pump protein comprises over 90% of the total protein in these isolated SR membranes and the Ca^{2+} pump protein is distributed in a unidirectional manner in these membrane profiles. This approach represents the first time that the profile structure of an isolated membrane has been directly separated into the contributions from its individual components. (Supported by NIH grants HL18708 and AM 14632 and an AHA Invest. Award - TN affiliate to P.H.D.)

T-PM-Po5 TIME-RESOLVED X-RAY DIFFRACTION STUDIES OF THE SARCOPLASMIC RETICULUM MEMBRANE USING SYNCHROTRON RADIATION. L. Herbette[+] and J.K. Blasie[∓], Univ. of Conn. Health Center[+], Farmington, CT 06032; Univ. of Penn.[∓], Philadelphia, PA 19104; Stanford Synchrotron Rad. Lab., Stanford, CA 94305.

Lamellar X-ray diffraction using rotating-anode sources has provided the "static" (i.e. in absence of Ca^{2+} transport) profile structure of the sarcoplamic reticulum membrane at 10Å resolution. This work was extended to obtain time-resolved X-ray diffraction with which the profile structure was determined for the SR membrane during Ca^{2+} transport as averaged over 15-30 turnovers of the Ca^{2+} pump protein using rotating anode sources together with an area image-intensifier X-ray detector. Recently, this study was further extended to an investigation of conformational changes in the SR membrane profile associated with Ca^{2+} transport as averaged over only 1-3 turnovers of the pump protein utilizing intense highly monochromatic synchrotron X-radiation (E=8048±2eV). The X-ray beam was allowed to intersect curved specimens of a fully-functional hydrated oriented multilayer of SR membranes containing 100μM Ca^{2+} and 2.5mM caged ATP. Ca^{2+} transport was initiated with a flash of UV light (λ_{max} = 330 nm, $\Delta\lambda$= ± 60 nm) and the diffraction was recorded in serial time windows of 100, 200, and 500 msec. Changes in the lamellar diffraction were obtained for the lower order reflections for all three time frames. These changes relaxed over a period of approximately 1 minute. Appropriate controls carried out under identical conditions using 1:1 molar mixture of "caged" ADP and "caged" Pi revealed no changes in the lamellar diffraction. Analysis of these data suggests that conformational changes in the sarcoplasmic reticulum membrane profile are correlated with a single turnover of the Ca^{2+} pump protein which is associated with the transport of Ca^{2+} and that these changes may be related to dynamic conformational states of the Ca^{2+} pump protein itself. (Supported by NIH grant HL18708).

T-PM-Po6 SURFACE CHARGE DENSITY OF SARCOPLASMIC RETICULUM VESICLES. Joel A. Cohen and Mario M. Moronne, Laboratory of Physiology and Biophysics, University of the Pacific, San Francisco, California 94115.

The electrophoretic mobilities of individual vesicles of fragmented skeletal sarcoplasmic reticulum in aqueous solution were measured by use of a particle electrophoresis apparatus with laser illumination. Mobilities were measured at pH 7.0 in solutions of KCℓ and other monovalent electrolytes at concentrations ranging from 1 mM to 100 mM. The zeta potentials were then determined by use of the theory of Wiersema et al., assuming spherical vesicles of 750 Å radius. Values ranged from -42 mV in 1.6 mM KCℓ to -13 mV in 100 mM KCℓ. From the zeta potentials and the location of the hydrodynamic surface of shear, taken at 2 Å from the vesicle surface, the electrostatic surface potentials and surface-charge densities were determined by use of an excellent approximate solution of the spherical Poisson-Boltzmann equation formulated by Bentz. The calculated apparent surface-charge densities ranged from one negative charge per 3500 $Å^2$ in 1.6 mM KCℓ to one negative charge per 1400 $Å^2$ in 100 mM KCℓ. The lack of constancy of these values is suggestive of ion binding and/or ion-induced structural alteration of charged membrane components. Trypsin-treated vesicles and large multilamellar SR vesicles were also investigated. Zeta-potential shifts resulting from pH and Ca^{2+} titrations were observed and permit elucidation of H^+ and Ca^{2+} binding phenomena at the membrane surface.

Supported by NIH (HL-16607 and Biomedical Research Support Grant).

T-PM-Po7 Ca AFFINITY CHANGE OF SR-ATPase DURING ENZYME CYCLE IN THE PRESENCE OF ORGANIC SOLVENTS. Takahide Watanabe and Giuseppe Inesi. Laboratory of Physiology and Biophysics, University of the Pacific, San Francisco, CA 94115.

The transport of Ca by SR-ATPase may involve a change in affinity for Ca during the enzyme cycle. Using membrane filtration and spectroscopic methods, we detected a low affinity form of Ca-ATPase in the presence of organic solvents (∿30% dimethylsulfoxide (DMSO), dimethylformamide, etc., with purified ATPase prepared according to MacLennan. The low affinity form was also observed with ITP, p-nitrophenyl phosphate and acetyl phosphate. The low affinity form could not be detected in the absence of organic solvents. The low affinity form of ATPase returned to a high affinity form after exhaustion of substrate. The amount of Ca bound to the high affinity site is not changed in the presence of DMSO. The low affinity form was also detected with fragmented SR vesicles in the presence of DMSO and a calcium ionophore (A-23187). Because SR still has Ca uptake ability in the presence of DMSO, this low affinity form may be the intermediate form which releases the Ca inside the vesicle during the enzyme cycle. (Supported by NIH Grant HL 16607)

T-PM-Po8 Ca INFLUX AND ATP HYDROLYSIS IN Ca-FILLED SARCOPLASMIC RETICULUM VESICLES. H. Takenaka, F.C. Messineo, C. Favreau, P. Nash-Adler, P.B. Pinto, and A.M. Katz, Department of Medicine, University of Connecticut Health Center, Farmington, CT 06032

Ca transport by rabbit white skeletal sarcoplasmic reticulum vesicles (SR) was studied with relation to Ca uptake, Ca influx, ATP hydrolysis, and EP decomposition. Reactions were carried out at 25° C with 0.1 mg/ml SR in 0.12 M KCl, 20 μM ATP, 50 μM $CaCl_2$, 1 mM $MgCl_2$ and 40 mM histidine (pH 6.8). Ca content reached a maximum after approximately 1 min. followed by a slow spontaneous Ca release. Ca influx rates measured by pulse-labelling the external medium with ^{45}Ca at 20 sec. and 1 min. were similar to the initial Ca uptake rate, whereas at 3 min., Ca influx rate had slowed considerably. At least 80% of the Ca inside the SR exchanged with external Ca during the first 1 min. after ^{45}Ca was added at 20 sec. and 1 min., but less than 50% of the Ca exchanged at 3 min. The amount of Pi liberated from ATP reached a plateau at approximately 1.5 min., after which there was little net hydrolysis of ATP. In contrast, ATP hydrolysis rates, obtained by pulse-labelling the external medium with (γ-^{32}P) ATP at 20 sec. and 1 min. were similar to the initial rate of Pi liberation. At 3 min., when net Pi liberation from ATP had virtually ceased, hydrolysis of added (γ-^{32}P) ATP was still observed, although at a slow rate. The amount of acid-stable phosphoenzyme (EP) steadily decreased over time, falling to < 10% of the initial level at 2 min. These results suggest that Ca-Ca and ATP-Pi exchanges in Ca-filled SR vesicles may occur with little net ATP hydrolysis, but the rates of exchange do not correlate closely with EP levels. (Sponsored by NIH Grants HL-22135 and HL-21812.)

T-PM-Po9 DISPLACEMENT OF ATPase PUMP UNITS AND ENHANCEMENT OF CALCIUM UPTAKE IN SR BY DIETHYLETHER. Donald Scales, Parris Kidd and Giuseppe Inesi, Laboratory of Physiology and Biophysics, University of the Pacific, San Francisco, CA 94115.

The velocity and maximum levels of calcium uptake by SR vesicles are increased in the presence of 5 - 7% v:v diethylether. In addition the rate of turnover, but not the amount, of the phosphoenzyme is increased. However, if the vesicles are exposed to diethylether, centrifuged, resuspended and then placed in the reaction mixture, no net calcium uptake is measured upon addition of ATP. A similar effect is noted in experiments done in the presence of oxalate. There is no net accumulation of calcium after addition of ether, centrifugation and resuspension. Consistent with this observation, we find that calcium dependent hydrolysis of the ATPase proceeds at constant rates until the substrate is depleted. We have studied the ultrastructure of the SR vesicles after simple exposure to diethylether and find no differences from control vesicles. Tannic acid fixed vesicles show the usual fuzzy coat corresponding to the hydrophilic portion of the ATPase. Freeze fracture replicas show normal asymmetry of intramembranous particles: most particles are associated with concave faces. However, vesicles exposed to diethylether, centrifuged and resuspended before fixation show evidence of vesicle deformation and disruption of the fuzzy coat. Freeze fracture replicas reveal a loss of intramembranous particle asymmetry: particles appear on concave and convex faces and some concave faces are completely depleted of particles. We conclude that diethylether weakens lipid-lipid and lipid-protein interactions such that protein movements involved in calcium transport are facilitated but at the same time the integrity of the membrane as a whole is weakened. Supported by HL 16607.

T-PM-Po10 DEVELOPMENTAL STUDIES ON SARCOPLASMIC RETICULUM FROM DYSTROPHIC CHICKEN MUSCLE. Danuta Kosk-Kosicka and Giuseppe Inesi, Laboratory of Physiology and Biophysics, University of the Pacific, San Francisco, CA 94115.

Developmental studies were carried out on sarcoplasmic reticulum prepared from the breast muscle of chickens with a genetic muscular dystrophy (line 413), and normal chickens (line 412). Parameters investigated included 1) levels of acid stable phosphoprotein, 2) rates of Ca^{+2} uptake with oxalate, 3) maximum Ca^{+2} loading, and 4) rates of Pi production. Development was studied in chickens from 1 to 8 weeks old. Levels of phosphoprotein in SR from normal muscle were constant over the development period, while phosphoprotein in SR from dystrophic muscle decreased. Corresponding changes were also noticed in rates of Ca^{+2} uptake and levels of maximal loading. Steady state rates of Pi production were measured in the presence of triton X-100. The SR exhibited varying responses to triton depending on age of the chicken. (Supported by the Muscular Dystrophy Association of America)

T-PM-Po11 Ca•ATPase OF SARCOPLASMIC RETICULUM IS THE CONTAMINATING ATPase IN STANDARD MYOSIN PREPARATION - David D. Hackney, Department of Biological Sciences, Carnegie-Mellon University, Pittsburgh, PA 15213

Standard myosin preparations have been shown to contain a contaminating ATPase whose presence accounts for some anomalous ^{18}O-oxygen exchange results obtained with myosin in the absence of actin [Sleep, J.A., Hackney, D.D. and Boyer, P.D., J. Biol. Chem. 255, 4094 (1980)]. The Ca•ATPase of sarcoplasmic reticulum (SR) was initially excluded from being this contaminating ATPase on the basis of the high Km for ATP of the contaminating enzyme and its lack of significant inhibition by EGTA. It is now shown that this was a result of the assay conditions (0.5 M KCl, 5 mM ATP), which were optimized for the reactions with myosin. When a partially purified preparation of the contaminating enzyme is assayed under conditions more optimal for the SR enzyme (0.1 M KCl, variable ATP), it displays properties expected for the SR Ca•ATPase:

1) The extent of inhibition by EGTA in the presence of 10 μM $CaCl_2$ and 3 mM $MgCl_2$ is dependent on the Mg•ATP concentration. The Ca-sensitive component has a Km of 6 μM for Mg•ATP, while the basal component (not inhibited by EGTA) has a Km of 650 μM and a Vm 2.8 fold greater than that for the Ca-sensitive component. The dominance of the basal component at high ATP concentrations was responsible for the low inhibition by EGTA observed previously.

2) The contaminating enzyme is inhibited by quinidine sulfate and chloropromazine, but not by ouabain, oligomycin or azide.

3) The contaminating enzyme is inhibited and partially solubilized by Triton X-100.

4) Standard myosin contains a polypeptide of molecular weight 100,000 (by SDS polyacrylamide gel electrophoresis) which is enriched in the partially purified preparation of the contaminating ATPase.

T-PM-Po12 INCREASED PHOSPHATE (P_i) BURST AMPLITUDE IN FROG MYOSIN AND SUBFRAGMENT-1 INDUCED BY F-ACTIN AND LOWERED IONIC STRENGTH. M.A. Ferenczi and E. Homsher. Dept. of Biochemistry, Univ. of Pennsylvania, Philadelphia, PA 19104 and Dept. Physiology, UCLA, Los Angeles CA 90024.

Studies of frog myosin (M) at 0.5 M KCl and frog subfragment-1 (S-1) at 0.1 M KCl have shown that, based on the amplitude of the P_i burst, only 30-50% of the protein is active; further, enzyme activity is lost at a rate of 25%/day (Ferenczi, et al., Biochem. J. 171: 165-175). In studies of transient kinetics of frog acto-S-1 ATPase, we found that the amplitude of the S-1 P_i burst in the presence of f-actin (A) was as great as 0.9 mol P_i/mol S-1 when the stiochiometry of A:S-1 was 1:1 or more. Reduction of the A:S-1 ratio to values < 1 caused the P_i burst amplitude to decline to 0.3 mol P_i:mol S-1 at zero added A. To learn if actin activation of S-1-P_i burst amplitude was physiological, similar experiments were made on frog myosin. At 0.3 M KCl or greater the P_i burst ratio was 0.3 mol P_i:mol S-1 head and was not altered by actin addition. However, as the ionic strength is lowered in the absence of actin the amplitude of the P_i burst rises, reaching a value of 0.95 mol P_i: mol S-1 head at 0.1 M KCl. If the myosin is stored at 0.1 M KCl and 0°C, loss of protein activity is < 10%/day. These results suggest that 1) highly active and stable preparations of frog myosin can be obtained if exposure to elevated ionic strength is minimized and 2) the actin-activation of S-1 P_i burst amplitude is probably an artifact induced by the proteolytic digestion necessary for its preparation. (Supported by NIH HL11351 and MDAA C781030).

T-PM-Po13 COOPERATIVE EFFECTS OF REGULATED ACTIN. K. M. Trybus and E. W. Taylor, University of Chicago, Chicago, Illinois 60637.

The steady state kinetics of the regulated acto-SF-1 ATPase were investigated. With SF-1 in excess of actin (30/1), the observed V_{max} with actin-tropomyosin (A-TM) and actin-tropomyosin-troponin (A-TM-TN) in the presence of calcium was 24 sec^{-1} (20°C, 5 mM KCl, 5 mM $MgCl_2$, pH7), while that of pure actin and A-TM-TN (-calcium) was 7-8 sec^{-1}. The approach to V_{max} at a slightly higher ionic strength (30 mM KCl) was markedly sigmoidal for A-TM and A-TM-TN (-calcium) and slightly sigmoidal for regulated actin in the presence of calcium. The binding of SF-1·ADP to these actin species shows qualitatively similar cooperativity. Modification of tropomyosin by the procedure of Johnson & Smillie (Biochem. 16, 2264, 1977) to prevent end to end interactions decreased the steepness (cooperativity) of the transition relative to unmodified TM. With actin in excess of SF-1 (30/1), the maximum rate obtained with A-TM was 20-30% of the maximum rate obtained with pure actin, while the degree of inhibition obtained with A-TM-TN in the absence of calcium was 90-95%. The approach to saturation of the rate was not sigmoidal. Both A-TM and A-TM-TN (-calcium) appear to be predominantly in an inhibited state when the SF-1 concentration is low. When the concentration of SF-1 intermediate states is in excess of regulated actin or A-TM, the ATPase is cooperatively activated. The results are consistent with a TM shift model in which SF-1 interacts with the TM in both the inhibited and active states. (Supported by grants from MDA and NIH HL 20592).

T-PM-Po14 FURTHER STUDIES ON THE BINDING OF MYOSIN SUBFRAGMENT-1 TO REGULATED F-ACTIN IN THE PRESENCE OF ATP. J. M. Chalovich and E. Eisenberg, NHLBI NIH, Bethesda, MD 20205.

According to the steric blocking model, the troponin-tropomyosin complex inhibits actin activation of the myosin subfragment (S-1) ATPase at low [Ca^{2+}] by physically blocking the binding of S-1 to actin. Using stopped-flow absorbance as a measure of binding, we have previously shown that at low [Ca^{2+}], where the ATPase rate is 96% inhibited, the binding of S-1·ATP or S-1·ADP·Pi to regulated actin is similar to the binding at high [Ca^{2+}] or in the absence of regulatory proteins where the ATPase rate is much higher (Chalovich, Eisenberg and Chock (1980) Fed. Proc. 39, 1106). We have now confirmed this finding using sedimentation in the Airfuge to directly measure the binding at pH 7.0, 25°C, and μ = 18 mM. In the presence of Ca^{2+} or in the absence of troponin-tropomyosin, the binding constant of S-1·ATP or S-1·ADP·Pi to actin is 1.5×10^4 M^{-1} (compared to 2.3×10^4 M^{-1} determined by stopped-flow). In the absence of Ca^{2+} the binding constant is 1.4×10^4 M^{-1} (compared to 1.3×10^4 M^{-1} determined by stopped-flow). Under identical conditions the maximum steady state S-1 ATPase activities are 20 s^{-1} with unregulated actin, 18 s^{-1} with regulated actin +Ca^{2+}, and 0.08 s^{-1} with regulated actin -Ca^{2+}. The small change in binding constant which occurs in the presence and absence of Ca^{2+} and the corresponding large difference in ATPase rates is not consistant with the steric blocking model. Furthermore, we have obtained similar results at higher ionic strength (μ = 50 mM). These results can be explained by assuming that, in the absence of Ca^{2+}, troponin-tropomyosin markedly decreases the rate of Pi release from the acto-S-1·ADP·Pi complex, perhaps by blocking the transition from the 90° to the 45° state.

T-PM-Po15 BINDING OF MYOSIN SUBFRAGMENT ONE TO F-ACTIN AND REGULATED ACTIN IN THE PRESENCE OF ATP. Paul D. Wagner and Edward Giniger (Intr. by D.B. Stone) CVRI, School of Medicine, University of California, San Francisco, CA 94143

The alkali-1 light chain was labeled with ^{3}H-iodoacetic acid and exchanged into subfragment-one, S1, using recombination in 4.7 M NH_4Cl. The labeled S1 was purified by ion exchange. The actin activated ATPase of the modified S1 had the same K_m and V_{max} values as control S1. The dissociation constants of this labeled S1 with F-actin and with regulated actin were determined in the presence of ATP, using a preperative ultracentrifuge to separate free from bound S1. At 20° and I = 0.025 M, the K_d for the binding of S1 to F-actin was only slightly larger than the K_m of the actin activated ATPase, 45 µM and 30 µM respectively. Similarly, in the presence of calcium, the K_d for the binding of S1 to regulated actin was 55 µM compared to K_m of 40 µM. In the absence of calcium, while the ATPase was 95% inhibited, K_d for the binding of S1 to regulated actin was 65 µM. This small difference in the affinity of S1 for regulated actin in the presence and absence of calcium is similar to that reported by J.M. Chalovich and E. Eisenberg, Fed. Proc. 39, abs. 1106 (1980), who used changes in turbidity to determine the extent of binding, and supports their conclusion that regulation may not result from an inhibition of S1 binding but rather by prevention of some subsequent step, perhaps the rotation of the myosin cross-bridge on actin, which is thought to occur during force generation.

This investigation was supported by USPHS Program Project Grant HL-16683 and NSF Grant PCM-75-22698.

T-PM-Po16 EFFECT OF NUCLEOTIDE AND CALCIUM ON THE ABILITY OF S-1 TO BIND TO REGULATED ACTIN. L. E. Greene, T. L. Hill and E. Eisenberg, NHLBI, NIH, Bethesda, MD 20205.

We previously found that troponin-tropomyosin strongly inhibits the binding of S-1·ADP to actin in the absence of Ca^{2+} and to a lesser extent in the presence of Ca^{2+}. In contrast, other studies in our laboratory have shown that troponin-tropomyosin has almost no effect on the binding of S-1·ATP or S-1·ADP·Pi to actin either in the presence or absence of Ca^{2+}. These results suggest that the nucleotide bound to S-1 affects the ability of S-1 to bind to regulated actin. This was tested by directly comparing the effect of troponin-tropomyosin on the binding of S-1, S-1·ADP, and S-1·AMP-PNP to actin in the presence and absence of Ca^{2+}. We found that troponin-tropomyosin strongly inhibits the binding of both S-1 and S-1·ADP to actin, but inhibits the binding of S-1·AMP-PNP much less. In addition, in all three cases, Ca^{2+} further reduced the inhibitory effect of troponin-tropomyosin. We first analyzed these data using our earlier cooperative model of troponin-tropomyosin action where we postulated that the regulated actin could exist in two forms, one binding S-1 weakly and the other strongly. However, we found that for this model to account for our data, AMP-PNP would have to affect the equilibrium between the two forms, even in the absence of S-1. This is not possible because the equilibrium in the absence of S-1 must be an intrinsic property of the regulated actin filament. Therefore, we developed a slightly modified model in which both the position of troponin-tropomyosin on actin and the configuration of the acto-S-1 complex determines the inhibitory effect of troponin-tropomyosin. On this basis, Ca^{2+} would act by changing the position of tropomyosin on actin, while AMP-PNP would act by changing the configuration of the acto-S-1 complex, perhaps by changing the angle at which S-1 binds to actin from 45° to an angle closer to 90°.

T-PM-Po17 MICROCALORIMETERIC MEASUREMENT OF THE ENTHALPY OF RABBIT SKELETAL MYOSIN-S1 AND HMM BINDING TO F-ACTIN.

Susan Smith*[a], Howard White, and Roger Woledge*[a], Dept. of Biochemistry, University of Arizona, Tucson, Arizona and Department of Physiology, University College, London[a].
(Sponsored by Duane P. Flamig)

The heat of binding of rabbit skeletal myosin-S1 and HMM to f-actin has been measured by batch microcalorimetry. The heat of association in 100 mM KCL, 5 mM MgCl, 10 mM Tris, pH 8.0, 13°C is +20 ± 2 kJ/mole for S1 and +36 ± 4 kJ/mole for HMM (+18 ± 2 kJ/mole HMM head). Proton release measurements in unbuffered solutions indicate that less than 0.1 mole of protons are absorbed or released during the reaction. Hence the measured heats are equal to the enthalpy of the acto-myosin-S1 and acto-HMM association reactions. The entropies of the reactions, calculated from literature values for the equilibrium constants (3×10^3 M^{-1} for HMM and 5×10^6 M^{-1} for S1)[1] and the enthalpies determined here are +54 J/mole/K° for HMM and +59 J/mole/K° for S1. These results are consistant with models in which each myosin head in HMM is able to interact independently with f-actin.
(Supported by the MRC of Great Britain, PHS #AM25113-02, and the Muscular Dystrophy Association of America).

1. L.E. Greene and E. Eisenberg, JBC, 255, 549-554 (1980)

T-PM-Po18 ESTIMATION OF THE BINDING OF MYOSIN HEADS TO ACTIN BY EPR SATURATION TRANSFER (ST) AND CONVENTIONAL EPR. B.A. Manuck, J.C. Seidel and J. Gergely, Dept. of Muscle Res., Boston Biomed. Res. Inst.; Dept. Neurol., Mass. Gen. Hosp.; and Dept. Biol. Chem. and Neurol., Harvard Med. School, Boston, MA 02114.

Results of Ishiwata et al. (Biophys. J. 25,19a,1979) suggest that rotation of myosin heads can be used to estimate the fraction of heads bound to actin. In the present work ST-EPR and conventional saturation (CS) techniques, both reflecting rotation, and sedimentation, providing a direct estimate of binding, were used to study the binding of maleimide spin-labeled HMM to F-actin at various PP_i or AMPPNP concentrations. The fraction of bound heads was estimated with ST-EPR from the motional parameter L"/L (Thomas et al., J. Chem. Phys. 65,3006,1976) and with CS from the decrease in the signal amplitude, assuming that L,L", and the decrease of the saturated signal, are linear functions of the fraction of heads bound. Spectral parameters for bound heads (τ_2 10^{-8} s) and free heads (τ_2 10^{-9} s) were obtained from spectra of acto-HMM and HMM, respectively. The binding data obtained by EPR and sedimentation methods agreed well. The agreement can be explained if i) there are few or no HMM's bound by one head or ii) the binding of one head immobilizes the other. A plot of bound heads against either [PP_i] or [AMPPNP] had the shape of a simple binding isotherm. We could not fit the data with models in which the binding of two ligands is required for dissociation of HMM, but agreement could be obtained assuming that one ligand per HMM produces dissociation or that only one head plays a functional role in binding to actin. (Supported by grants from the National Science Foundation (PCM 801-3005); the National Institutes of Health (HL-5949, HL-07266, HL-15391, and HL-23249), and the Muscular Dystrophy Association.)

T-PM-Po19 ENERGETICS OF THE INTERCONVERSION OF TWO MYOSIN CONFORMATIONS VIEWED BY ^{31}P NMR John W. Shriver and Brian D. Sykes. MRC Group on Protein Structure and Function, Department of Biochemistry, University of Alberta, Edmonton, Alberta, Canada T6G 2H7.

^{31}P NMR spectra of ADP and AMP.PNP bound to myosin subfragment-1 (0.1 M KCl, 5 mM $MgCl_2$, pH 7) indicate that both exist in two interconvertible conformations, M^*_RN and M^*_TN, with a highly temperature dependent equilibrium constant K_3:

$$M + N \overset{1}{\rightleftharpoons} M.N \overset{2}{\rightleftharpoons} M^*_TN \overset{3}{\rightleftharpoons} M^*_RN$$

(M.N is a transitory recognition complex in fast exchange with M). From the temperature dependence of K_3 for ADP we calculate for reaction 3 that ΔH° = 14 kcal/mole and ΔS° = 52 cal/deg/mole, implying a large conformational change is associated with the T → R conversion. ΔG° = 0 at approximately 271°K. Comparison of the temperature dependence of K_3 with transient kinetics data (Trybus and Taylor, Biophysical J.25,21a (1979)) and the temperature dependence of intrinsic fluorescence intensities indicates that the R form is more fluorescent than the T form and reaction 3 (T → R) is exothermic for ADP, i.e. at 298°K M^*_RADP is not significantly populated. The ADP binding enthalpy observed by Swenson and Ritchie (Biochemistry, 18, 3654, (1979)) may be assigned to reactions 1 and 2.

Similar experiments with AMP.PNP indicate that it significantly populates M^*_RN at 293°K (K_3 = 1), consistent with the higher intrinsic fluorescence of S-1.AMP.PNP complexes. Temperature variation experiments show that reaction 3 (T → R) is endothermic for AMP.PNP and is presumably the conformational change proposed by Swenson and Ritchie to explain the near zero binding enthalpy of AMP.PNP. Preliminary results with fluorine labelled S-1 indicate that two forms, M_T and M_R, exist in the absence of nucleotide with ΔH° = 24 kcal/mole and ΔS° = 85 cal/deg/mole. ΔG° = 0 at 288°K. (Supported by MDA and MRC of Canada)

T-PM-Po20 LYSOLECITHIN PHOSPHOLIPASE ACTIVITIES OF MUSCLES FROM CONTROL AND DUCHENNE MUSCULAR DYSTROPHY SUBJECTS. L.H. Schliselfeld, M. Bárány, M.J. Danon*, E. Abraham* and R.A. Kleps*. University of Illinois at the Medical Center, Chicago, IL 60612

This laboratory has previously shown that control human muscles have a high level of glycerol 3-phosphorylcholine (GPC) whereas muscles from Duchenne Muscular Dystrophy subjects have significantly lower levels (Ann. N.Y. Acad. Sci. 317, 649, 1979). Human muscle extracts were assayed for lysolecithin phospholipase activity to see if this enzyme could be responsible for the GPC levels in these muscles. Normal muscles, non-dystrophic abnormal muscles and one Becker's Muscular Dystrophy muscle had similar activity values of 13.9 ± 1.1, 11.5 ± 0.5, and 16.2 nmoles lysolecithin hydrolyzed/min per g muscle, respectively, at 200 µM lysolecithin. No abnormality of these activities was observed in these muscle groups.

Muscle from Duchenne Dystrophy patients contained significant lysolecithin phospholipase activity at 200 µM lysolecithin. One of these muscles had a 1 hr. time lag for hydrolysis; another muscle had decreasing activity with increasing amounts of muscle extract. One Duchenne Dystrophy muscle was provided by the youngest patient, a 5 year old boy. At 0.75 - 2.0 µM lysolecithin this muscle had 1/16th or less activity than was found in control muscles under identical conditions. Increasing the lysolecithin concentration above 57 µM produced normal levels of activity in this Duchenne Dystrophy muscle. This result suggests that there may be a significant problem with the affinity of this enzyme for lysolecithin in Duchenne Muscular Dystrophy. At 200 µM lysolecithin the pH activity curves for control muscle, Becker's Dystrophy muscle, and Duchenne Dystrophy muscle were identical. (Supported by MDA).

T-PM-Po21 PARAMETERS AFFECTING VERTEBRATE ACTOMYOSIN ATPase ACTIVITY. Dallas L. Pulliam, Vitaly Sawyna and Rhea J. C. Levine. The Medical College of Pennsylvania, Philadelphia, PA 19129.

Previously, we demonstrated that a reconstituted system composed of rabbit skeletal muscle actin and myosin was calcium sensitive (enzyme activity was inhibited up to 52% in the absence of calcium) when assayed for ATPase activity in an increased ionic strength medium (120mM KCl), and was inhibited by calcium in the same medium containing only 15mM KCl. In the presence of troponin and tropomyosin both the lower and higher ionic strength assays demonstrated calcium sensitivity: inhibition of enzyme activity was 90% in the absence of calcium. The possibility of troponin and tropomyosin contamination of actin preparations has been ruled out by SDS polyacrylamide slab gel electrophoresis. Additionally, calcium sensitivity of higher ionic strength actomyosin ATPase assays is evident only with freshly prepared myosin. Myosin, stored for as little as 48 hours at 4°C no longer demonstrates calcium sensitivity in the absence of troponin and tropomyosin. Interestingly, when myosin was run in a two dimensional polyacrylamide gel system, using isoelectric focusing on urea gels in a pH range of 3.5-7.0 as the first dimension, and SDS 13% polyacrylamide slab gels in the second dimension, we observed that the degree of LC_{II} phosphorylation decreases markedly during the same time period. Studies are underway to determine if a correlation exists between the degree of LC_{II} phosphorylation and the percent calcium sensitivity of actomyosin at the higher ionic strength.

Supported by USPHS grants NS 05615 and BRSG RR 05418

T-PM-Po22 EFFECT OF MYOSIN LC_2 PHOSPHORYLATION ON HIGH-ENERGY PHOSPHATE USAGE IN CONTRACTING SKELETAL MUSCLE. R.J. Barsotti and T.M. Butler, Thomas Jefferson Univ., Phila., Pa. 19107.

Studies on the extensor digitorum longus (EDL) of female Sprague Dawley rats (50-70 gm) showed that phosphorylation of LC_2 as measured by IEF-SDS two-dimensional gel electrophoresis increased from 4±1% (mean±SE) at rest to 17±2% and 58±1% during isometric tetani (100 Hz) of 1 and 10 sec durations respectively. Even after relaxation from a 1 sec tetanus, LC_2 phosphorylation continued to rise to a maximum of 45±4% at 6.5 sec. High-energy phosphate usage was measured directly as changes in phosphorylcreatine (PCr) and ATP in the rat EDL in which respiration and glycolysis were blocked by incubation in an anaerobic glucose-free Krebs solution containing 0.5 mM iodoacetate and 2 mM NaCN at 23°C for 5 min. This treatment did not affect isometric force development or resting ATP contents, but did stop glycolysis since there was no significant lactate production (0.005±0.008 mole/mole total creatine, Ct= 21 µmole/g) in muscles hammer frozen 10 sec after a 10 sec isometric tetanus. Chemical energy usage under conditions of low LC_2 phosphorylation was determined by isometric stimulation of a muscle for 1 sec at l_o compared to a paired unstimulated control. In this case phosphorylation was initially 4% and $\Delta\sim P$ was 0.074±0.008 mole/mole Ct, N=13. In the second design both muscles were stimulated for 1 sec and allowed to relax for 6.5 sec. The experimental muscle was then given an additional 1 sec stimulation. In this case, phosphorylation of LC_2 was initially 45% but $\Delta\sim P$ (0.070±0.009 mole/mole Ct, N=13) was nearly identical to that under low LC_2 phosphorylation conditions. It thus seems that phosphorylation of LC_2 does not affect rate of crossbridge cycling as evidenced by rate of ATP utilization during the development phase of an isometric tetanus in this fast mammalian skeletal muscle. (Supported in part by HL 15835 to the Pa. Muscle Institute and NSFPCM 791618).

T-PM-Po23 PHOSPHORYLATION OF MYOSIN LIGHT CHAIN KINASE BY C-SUBUNIT AND ITS EFFECTS ON SMOOTH MUSCLE. R.L. Bridenbaugh, P.E. Hoar and W.G.L. Kerrick. Dept. of Physiology and Biophysics, University of Washington, Seattle, WA 98195.

The phosphorylation of myosin light chain kinase (MLCK) in Triton X-100 skinned smooth muscle fibers (chicken gizzard) was monitored by using [γ-^{32}P]ATP as the substrate for the catalytic subunit of a cAMP-dependent protein kinase (C-subunit). The phosphorylation level of MLCK increased with time when exogenous C-subunit was present, while the phosphorylation level of the 20,000 dalton light chain (LC_{20}) decreased. The addition of calmodulin to the skinned fibers (where the MLCK was phosphorylated) reversed the low phosphorylation levels of LC_{20}. These results are consistent with those observed from tension measurements, where the presence of C-subunit caused maximally Ca^{2+}-activated (pCa = 3.6) skinned fibers to relax, while the addition of calmodulin to these relaxed fibers returned tension to control values at pCa = 3.6. These results support the contention that phosphorylation of MLCK decreases the formation of the Ca^{2+}-calmodulin-MLCK complex such that phosphorylation of LC_{20} and tension are inhibited. Consistent with this hypothesis is that additional calmodulin should increase the formation of the Ca^{2+}-calmodulin-MLCK complex, which should return LC_{20} phosphorylation and tension to control levels. Thus, smooth muscle contraction can be inhibited by cAMP levels through the action of a cAMP-dependent protein kinase phosphorylating MLCK. These data are also in agreement with a model of smooth muscle regulation where MLCK is responsible for the phosphorylation of LC_{20} and thus the activation of contraction. (This research was supported by NIH training grant HL 07090 to Dr. Bridenbaugh, a Muscular Dystrophy Assn. fellowship to Dr. Hoar, and grants to Dr. Kerrick from the American Heart Assn. (79-664) and the Muscular Dystrophy Assn.)

T-PM-Po24 EFFECTS OF PHOSPHORYLATION ON THE AGGREGATION BEHAVIOR OF PORCINE AORTIC MUSCLE MYOSIN. Jane F. Koretz, Dept. of Biology, RPI, Troy, NY, 12181 and Dixie W. Frederiksen, Dept. of Biochemistry, Vanderbilt U. School of Medicine, Nashville, TN 37232.

The importance of phosphorylation of myosin as a control mechanism in the activation of actomyosin ATPase in porcine aortic smooth muscle myosin has recently been shown (Rees and Frederiksen, JBC, in press). Complementary studies of the possible effects of phosphorylation on aortic myosin aggregation were undertaken to determine whether this mechanism might also be related to the presence and/or nature of the thick filaments in vivo, as has been shown to be true for thymus and platelet myosin (Scholey et al., 1980). Turbidity and electron microscope results show:

1. Without phosphorylation, dialyzed aortic myosin forms small ($\sim$.5μ) filaments, while phosphorylated aortic myosin under the same formative conditions aggregates into long, aligned multifilament bundles.
2. These results are not dependent upon calcium concentration; magnesium, however, must be present in at least micromolar concentrations to prevent denaturation.
3. Column-purified rabbit skeletal myosin aggregation is unaffected by changes in divalent cation concentrations.

These results indicate the importance of phosphorylation in the aortic myosin aggregation mechanism, and suggest an explanation for the heterogeneity of in vivo myosin aggregate structures observed in fixed sections.

T-PM-Po25 THE FUNCTION OF MYOSIN LIGHT CHAIN PHOSPHORYLATION IN SKELETAL MUSCLE. R. Cooke, K. Franks, C.J. Ritz-Gold & T. Toste, University of California, San Francisco, Ca 94143 and D.K. Blumenthal & J.T. Stull, University of Texas, Dallas, Tx 75235

We phosphorylated the P-light chain of rabbit skeletal myosin using purified light chain kinase and Ca^{++}-dependent regulation protein (CDR). More than 0.9 Pi per light chain was incorporated as determined by PAGE in urea. The ATPase activity of phosphorylated myosin was measured as a function of actin concentration (0.5 to 5 μM) at 25°C, and contrary to recent reports no significant effect on ATPase activity was found. We also phosphorylated the P-light chain of myosin in myofibrils and found no effect on ATPase activity as a function of pCa (pCa4 to 7). In addition thiophosphorylation of glycerinated rabbit psoas fibers was achieved by incubating small bundles (3-6 fibers) at 23°C for 10 min in kinase, CDR and ATP-γS. Approximately 0.75 thiophosphate per light chain was incorporated as determined by PAGE; only the P-light chain incorporated significant activity from ATP γ-^{32}P. At 10°C neither the pCa dependence of isometric tension nor the fiber force-velocity relation was affected by thiophosphorylation. Recently we have found that the ATPase activity of fibers in isometric contractions at 37°C (0.81±.09 s^{-1} per head) is diminished to 0.44±.04 s^{-1} by thiophosphorylation of the P-light chain. Myosin was not thiophosphorylated and ATPase activity was not changed if either kinase, CDR or ATP-γS was omitted during incubation. Thus, phosphorylation of myosin decreases the cycling rate of the actomyosin interaction during isometric contraction. It may therefore play a role in the potentiation of twitch tension following a tetanus or in decreasing the rate of energy output during long tetani in vivo. Supported by NIH HL16683 to R.C. and a Cal. Heart Fellowship to C.J.R-G.

T-PM-Po26 LIGHT CHAIN PHOSPHORYLATION AND MUSCLE ENERGETICS. Michael Crow and Martin J. Kushmerick, Harvard Medical School, Department of Physiology, 25 Shattuck St., Boston, Mass. 02115.

The pattern of energy utilization in mouse fast twitch (extensor digitorum longus, EDL) muscle and slow twitch (soleus, SOL) muscle measured at 20° is different in two respects: (1) the initial rate of ~P splitting per unit force per cross-sectional area during steady isometric contractions is about 3-fold higher in EDL than in SOL; (2) this rate in EDL decreases to 1/3 of the initial rate after about 4 sec of stimulation whereas comparable contractile activity induced no change in the rate of ~P utilization in SOL for tetani up to 20 sec in duration. The change in energy utilization rate in EDL corresponds temporally with phosphorylation of the 18,000 dalton light chain. The extent of LC-2 phosphorylation was measured by the appearance of a more acidic form of LC-2 on 2-dimensional polyacrylamide gel electrophoresis (IEF→SDS). Also, when muscles were incubated with ^{32}P orthophosphate to steady specific activity of ATPγ, only EDL muscles incorporated ^{32}Pi into LC-2 upon stimulation. The hypothesis that covalent modification of myosin light chains is causally related to decreased actomyosin ATPase rate predicts that the steady-state force velocity curve should be altered (decrease V_{max}) during continued stimulation in EDL but not in SOL. Thus myosin light chain-2 phosphorylation may represent a mechanism for the modulation of myosin turnover rate in continuously active, actin-filament regulated muscles, but only in fast-twitch types. Supported by NIH 14485, KO4 AM00178 and T32 6M07258.

T-PM-Po27 INTERACTION OF CALMODULIN WITH RABBIT SKELETAL MUSCLE MYOSIN LIGHT CHAIN KINASE. T.H. Crouch, J.D. Johnson, M.J. Holroyde, J.H. Collins, R.J. Solaro and J.D. Potter. Departments of Pharmacology and Cell Biophysics and Physiology. University of Cincinnati, College of Medicine, Cincinnati, Ohio 45267.

Myosin Light Chain Kinase (MLCK) isolated from rabbit skeletal muscle has an apparent molecular weight of 81,000 daltons and a sedimentation coefficient of 3.2 Svedbergs. Gel filtration chromatography with ^{3}H labeled calmodulin (CAM) shows that MLCK binds one mole of CAM per enzyme molecule with an affinity of $(1.9\pm.5) \times 10^{7}M^{-1}$. The calcium dependence of MLCK activation is characterized by a Hill coefficient of 2 with 50% activation occurring at pCa 6.2 at 3 mM total $MgCl_2$ concentration. Binding of MLCK in the presence of Ca^{2+} produces a 30% enhancement of MLCK tryptophan fluorescence which is half maximal at pCa 6.2. This technique shows an affinity of $2.6\pm0.7 \times 10^{7}M^{-1}$ of CAM for MLCK with one mole CAM bound per mole of MLCK. Stopped flow fluorescence studies show that upon mixing with Ca^{2+} the CAM induced increase in MLCK tryptophan fluorescence occurs as a biphasic process with rates of 65 sec^{-1} and 6 sec^{-1}. The fluorescence decrease upon Ca^{2+} removal is monophasic with a rate of 2 sec^{-1}. The conclusions from these studies are that the interaction of CAM·MLCK is dependent on $[Ca^{2+}]$ and independent of $[Mg^{2+}]$, occurs with Ca^{2+} binding to any one of the four Ca^{2+}-specific sites on CAM ($K_{Ca} = 4.2 \times 10^{5}M^{-1}$), is specific for CAM over S-TnC and is directly related to the activation of MLCK for LC_2 phosphorylation. Supported by grants from the NIH (HL 22619-3A, B, E), the Muscular Dystrophy Association and the American Heart Association (78-1167 79-1001).

T-PM-Po28 THE EFFECT OF DISRUPTING THE TROPOMYOSIN (TM) STRAND ON TM DEPENDENT FUNCTIONS. C.E. Trueblood*, T.P. Walsh*, and A. Weber, Dept. of Biochemistry and Biophysics, Univ. of Pennsylvania, Philadelphia, PA.

TM molecules, through end to end overlap, form a continuous strand on the actin filament such that movement of a single TM molecule may be constrained. If the constraints on lateral diffusion or rotational flexing of TM imposed by strand formation should be the structural basis for part or all of the cooperativity observed during the transition from relaxation to contraction or from the non-potentiated to the potentiated state, then disconnecting the TM molecules should produce major changes in cooperativity. Carboxypeptidase A digestion of αα TM eliminates end to end overlap, yielding low viscosity 'digested' TM. As predicted by Wegner's analysis of TM binding to actin, we observed that digested TM binds actin very weakly. This lowered binding affinity allowed us to avoid artifacts due to residual undigested TM by extracting it with actin. Lack of binding of digested TM to actin may explain why digested TM in the absence of troponin (TN) did not cause the TM inhibition of acto-S-1 ATPase that is observed at high actin/S-1 ratio. We confirmed, with digested TM, the observation by Wegner and Walsh that even Ca saturated TN greatly enhances TM binding to actin. With digested TM, the high degree of cooperativity of the Ca-dependence of ATPase was reduced to that predicted by a requirement for simultaneous binding of two Ca ions. However, under some conditions such a reduction can also occur with high viscosity TM. Potentiation appeared unaltered at very low ATP concentrations and seemed reduced at ATP concentrations above 0.1 mM.

T-PM-Po29 THE EFFECT OF MALEIMIDE SPIN LABELS ON METAL BINDING TO TROPONIN-C. C.-L.A. Wang, P.C. Leavis, J.C. Seidel and J. Gergely. Dept. of Muscle Research, Boston Biomedical Res. Inst., Dept. of Biol. Chemistry and Neurology, Harvard Med. School, and Dept. of Neurology, Mass. General Hospital, Boston, MA 02114.

We have attached N-(1-oxyl-2,2,6,6-tetramethyl-4-piperidinyl)-maleimide (MSL) to the single cysteine residue (Cys-98) of skeletal muscle troponin-C (TnC). Binding of Ca^{2+} to MSL-TnC alters the shape of the EPR spectrum, indicating decreased mobility of the probe. The endpoint of the spectral titration was 1:1, instead of 2:1, as expected from the existence of two high affinity metal ion binding sites. The same results were obtained with lanthanide ions, La^{3+}, Gd^{3+} and Tb^{3+}. In the case of Tb^{3+}, the enhanced metal luminescence resulting from energy transfer from a tyrosine group (Tyr-109) was monitored. The enhanced metal luminescence was slightly quenched by the nitroxide free radical. After labeling with iodoacetamide spin labels, titrations exhibit an endpoint of 2:1 as for the unlabeled protein. We also examined the binding of Eu^{3+} to MSL-TnC by directly exciting the metal ions using a pulsed dye laser. The first equivalent of added Eu^{3+} preferentially binds to one of the two high affinity sites and gives rise to a peak in the excitation spectrum; subsequent addition of Eu^{3+} results in another peak corresponding to the low affinity sites. These results suggest that the binding affinity of either site III or site IV is altered by the maleimide moiety in the spin label bound to Cys-98. (Supported by NIH, AHA and MDA.)

T-PM-Po30 STUDY OF THE STRUCTURE OF TROPONIN-I BY MEASURING THE RELATIVE REACTIVITY OF LYSINES WITH ACETIC ANHYDRIDE. Sarah E. Hitchcock-DeGregori, Dept. of Biological Sciences, Carnegie-Mellon University, Pittsburgh, PA 15213.

A topological "map" of rabbit skeletal muscle troponin-I has been made by measuring the relative reactivities of lysines with acetic anhydride using a competitive labeling procedure (Kaplan et al., 1971, Biochem. J. 124, 289). Troponin-I was trace labeled free, in native troponin, and in binary complexes with TN-C and TN-T with ^{3}H-acetic anhydride. The ^{3}H-TN-I was combined with ^{14}C-TN-I that had been acetylated in 6M guanidine HCl, and chemically labeled in 6M guanidine HCl. Following digestion with trypsin and S. aureus protease, the peptides were separated on columns and paper and located using autoradiography. The labeled peptides were eluted, counted for $^{3}H/^{14}C$, analyzed for amino acid composition, and N-terminal residue, and identified in the sequence (Wilkinson & Grand, 1975, Biochem. J. 149, 493). Twenty-two of 24 lysines have been identified in 13 peptides (missing lys 18 and 31). In free TN-I, lys 70 is the most reactive; the remaining have similar reactivities. In the native troponin complex, lys 40, 65, 70, and 78 become less reactive, lys (84, 87) becomes more reactive. Lys 40 may be less reactive $+Ca^{2+}$ (with 2mM $MgCl_2$); lys 78 may be more reactive $+Ca^{2+}$. In the troponin-IT complex, there are large reductions in the reactivities of lys 40, 65, 78. In TN-IC, lys 70 and lys 78 (to a small extent) are reduced in reactivity. The reactivities of the lysines in the IC complex are not sensitive to Ca^{2+} (+2mM $MgCl_2$). The present results suggest that the region in TN-I including res. 40-78 may be involved in complex formation with TN-C and TN-T. This research was supported by grants from NIH and MDA.

T-PM-Po31 A COMPARATIVE STUDY OF C-PROTEINS FROM HEART AND SKELETAL MUSCLES. K. Yamamoto & C. Moos, Biochem. Dept., SUNY, Stony Brook, NY 11794.

C-protein has been found not only in white skeletal muscle but also in red muscle (Callaway & Bechtel, Fed. Proc. 39, 2167 (1980)). We have studied the C-protein of rabbit heart in comparison to that of skeletal muscles. Heart C-protein can be separated from crude myosin by DEAE-Sephadex chromatography in the same manner as skeletal muscle C-protein. The molecular weights of heart, red and white C-proteins, estimated by SDS PAGE, are 150,000, 145,000 and 135,000, respectively. Antibody against mixed skeletal muscle C-protein forms a strong precipitin line with white C-protein in Ouchterlony double-diffusion plates, and it also forms a second weaker line with red or heart C-protein. The lines for red and heart C-proteins are continuous, but they both cross the line for white C-protein. Absorption of the antibody with either heart or red muscle myofibrils abolishes the precipitin reaction with both red and heart C-proteins while the reaction with white C-protein remains. Thus, red muscle C-protein is immunologically more similar to heart C-protein than to white muscle C-protein. On the other hand, preliminary analyses of tryptic and chymotryptic fragments on SDS gels show distinct patterns for C-proteins from red muscle and heart as well as from white muscle. We conclude, therefore, that at least three structurally distinct variants of C-protein are present in the rabbit. We have not observed any functional differences between the C-proteins, however. All three bind similarly to myosins from white, red or cardiac muscle, with a limiting stoichiometry of about 1 mole/mole, and all three have quantitatively similar inhibitory effects on white muscle actomyosin ATPase at low ionic strength.

Supported by grants from NSF (PCM 7726785) and Muscular Dystrophy Assoc.

T-PM-Po32 CALCIUM INDUCED FOLDING OF SYNTHETIC Ca^{2+} BINDING PEPTIDES - A PROTON MAGNETIC RESONANCE STUDY. J. Gariépy, A.K. Saund, B.D. Sykes, R.E. Reid and R.S. Hodges. MRC Group in Protein Structure and Function, Dept. of Biochemistry, University of Alberta, Edmonton, Alberta, Canada T6G 2H7.

The amino acid sequences of the Ca^{2+} binding units of troponin C's, parvalbumins and calmodulins are highly homologous. To study the Ca^{2+} induced folding of these proteins, synthetic analogs corresponding to the high affinity site III of rabbit skeletal muscle troponin C have been prepared. In this presentation we have used proton magnetic resonance to monitor the changes occurring in the environment of specific side chains upon Ca^{2+} addition to the 26-residue (98-123) and 34-residue (90-123) apopeptides. The aromatic region involves a single tyrosine (109) present in the Ca^{2+} binding loop and 3 phenylalanines located in the C-terminal (119) and N-terminal helical regions (99 and 102). The nmr spectra of the iodinated peptides in the presence and absence of Ca^{2+} were determined to aid in the assignment of resonances in the aromatic region. Chemically induced dynamic nuclear polarization (CIDNP) was used to monitor the exposure of the tyrosine residue in the presence of calcium. Chemical shifts of resonances during Ca^{2+} titration were used to determined the Ca^{2+} binding constants for the peptides. The synthetic peptide data are compared to TnC and the native CNBr fragment CB9.

T-PM-Po33 A THREE DIMENSIONAL NMR VIEW OF THE EF CALCIUM BINDING SITE OF CARP PARVALBUMIN: A ^1H NMR STUDY OF THE LANTHANIDE INDUCED SHIFTS OF YTTERBIUM SUBSTITUTED PARVALBUMIN AND THE ELUCIDATION OF THE PRINCIPAL ELEMENTS AND ORIENTATION OF THE MAGNETIC SUSCEPTIBILITY TENSOR OF THE METAL ION. L. Lee and B.D. Sykes, M.R.C. Group on Protein Structure and Function, The University of Alberta, Biochemistry Department, Edmonton, Alberta, Canada T6G 2H7.

The interaction of the lanthanide ion ytterbium for the calcium ion in the EF binding site of carp parvalbumin results in high resolution ^1H NMR spectra exhibiting a series of resonances with chemical shifts spread over the range 32 to -19 ppm. The paramagnetic induced shifts are sensitive monitors of the precise geometrical orientation of each proton nucleus relative to the metal. The orientation and principal elements of the ytterbium magnetic susceptibility tensor have been determined using the three assigned NMR resonances of the His 26 C-2 and C-4 protons, the amino terminal acetyl protons, and seven methyl groups nuclei with known geometry relative to the EF metal binding site. The elucidation of these parameters has allowed us to view the coordination geometry of the metal binding site and to compare the observed spectrum of the nuclei surrounding the EF metal binding site of parvalbumin with that spectrum calculated from the X-ray crystallographic structure. The X-ray based proton coordinates have been refined by using the geometric information contained in the lanthanide shifted NMR spectrum in conjunction with a graphical analysis of the chemical shift contours as a function of three dimensional space.

T-PM-Po34 REACTIVITY OF TYROSYL SIDECHAINS IN NATIVE RABBIT TROPOMYOSIN. Béla Nagy and Henryka Bialkowska. Department of Neurology, Department of Pharmacology and Cell Biophysics University of Cincinnati College of Medicine, Cincinnati, Ohio 45267.

In previous studies our data suggested that the tyrosine residues in native tropomyosin (TM) are located between the interacting subunits within the hydrophobic crest forming the interacting area. Solvent perturbation difference spectra with use of compounds that do not affect the conformation of TM indicated partial accessibility of the tyrosine sidechains. (Nagy, B.: J. Biol. Chem. 252, 4557 (1977)). The juxtaposed tyrosine residues in TM double helix can be conveniently crosslinked with use of peroxidase mediated reaction or by u.v. irradiation centered at 275 nm at pH 8-9 to yield 3,3'-bityrosines probable through a mechanism involving free radicals. Dityrosine linked TM can be detected at pH 11 by a red shift in absorption spectrum from 294 to 310 nm and by a strong fluorescence spectrum at 420 nm when excited at 310 nm. Dithiothreitol reduced TM in SDS gel electrophoresis shows only the subunit and dityrosine linked dimer bands of 34,000 and 68,000 daltons respectively, indicating intramolecular links only. The 68,000 dalton band eluted from the gel posses the spectral characteristics of dityrosine. The determination of the numbers of tyrosines involved in crosslinks are in progress. The tyrosine sidechains in TM can be fully nitrated with use of tetranitromethane indicating an access for this highly hydrophobic reagent. Neither dityrosine formation nor nitration of tyrosines does introduce significant changes in the α-helix content of TM as CD measurements indicated. Dityrosine linked TM was able to inhibit the Mg^{2+}-stimulated ATPase of desenzitised actomyosin by about 80% in presence of 1 mM EGTA and troponin complex while nitrated TM lost the inhibitory activity. (This work was suppoted by MDA research grants.)

T-PM-Po35 A NEW HETEROBIFUNCTIONAL CROSSLINKING REAGENT FOR THE STUDY OF BIOLOGICAL INTERACTIONS IN PROTEINS. TROPONIN C - TROPONIN I BINDING SITE. P.C.S. Chong and R.S. Hodges. MRC Group in Protein Structure & Function, Dept of Biochemistry, University of Alberta, Edmonton, Alberta, Canada T6G 2H7.

In the muscle system SH groups have been shown to be in the proximity of the sites of interaction of the following proteins: troponin C-troponin I, troponin T-tropomyosin, actin-myosin, tropomyosin-actin and actin-actin. Therefore a bifunctional crosslinking reagent that could be specifically attached to these SH groups would be invaluable in the identification of the sites of interaction. The present work describes the synthesis and characterization of a new heterobifunctional photoaffinity probe, N-(4-azidobenzoylglycyl)-S-(2-thiopyridyl) cysteine (AGTC) and its general utility in the study of biological interactions in proteins by determining the site of interaction between troponin C and troponin I. Radioactive AGTC was specifically attached to cysteine 98 of troponin C with 90% incorporation as determined from the release of pyridine-2-thione and incorporation of radioactivity. After complex formation and photolysis in the presence of Ca^{2+} the covalently crosslinked TnI-TnC complex was isolated under conditions which completely dissociate the non-covalent complex (DEAE-chromatography in 6 M urea, 1 mM EGTA buffer). The radioactively labelled TnI was isolated from the complex by DEAE-chromatography in DTT-urea buffer which reduces the disulfide attachment to TnC.

T-PM-Po36 FLUORESCENCE STUDIES OF THE BINDING OF TWO CHYMOTRYPTIC FRAGMENTS OF TROPONIN-T TO TROPOMYOSIN. E.P. Morris and S.S. Lehrer, Department of Muscle Research, Boston Biomedical Research Institute, 20 Staniford Street, Boston, MA 02114.

The binding of two chymotryptic fragments of troponin-T to tropomyosin was studied by means of a fluorescent probe, N-(1-anilinonaphthyl-4)maleimide, attached to the cysteine 190 residues of tropomyosin in order to determine which regions of troponin-T and tropomyosin interact with each other. Purification and characterization yielded 2 fragments of troponin-T (which contains 259 residues): an N-terminal fragment troponin-T_1 (residues 1-155 and/or 1-158) and a C-terminal fragment troponin-T_2 (residues 156-259 and 159-259). Troponin-T_1 binds strongly to tropomyosin but has little effect upon the fluorescence of the label. Conversely, troponin-T_2 binds to tropomyosin rather weakly, but on binding enhances the fluorescence to a similar extent as whole troponin-T (~100%). Similar effects were observed with actin-tropomyosin filaments. A simple interpretation of these observations is that troponin-T binds to tropomyosin in such a way that its C-terminal region is close to Cys 190 of tropomyosin but that its N-terminal region is further away. This is in agreement with the elongated manner in which troponin-T attaches to the thin filament, determined by electron microscopy of thin filaments labeled with antibodies to troponin-T_1 and troponin-T_2 (Ohtsuki (1979) J. Biochem. 86, 491). (Supported by the Muscular Dystrophy Association and by NIH grant HL 22461.)

T-PM-Po37 FLUORESCENCE LIFETIME STUDIES OF THE CONFORMATIONAL DYNAMICS OF TROPOMYOSIN. D.R. Betteridge and S.S. Lehrer (Intr. by P. Graceffa), Dept. of Muscle Research, Boston Biomedical Research Institute, 20 Staniford St., Boston, MA 02114.

Earlier fluorescence studies indicated that the coiled-coil α-helix of tropomyosin (Tm) undergoes localized chain separation in the region of Cys 190 (Betcher-Lange and Lehrer (1978) J.B.C. 253, 3757; Graceffa and Lehrer (1980) J.B.C., to be published). Further evidence for this selective instability was obtained from parallel CD and fluorescence measurements (steady-state and lifetime) on rabbit cardiac Tm labeled specifically at Cys 190 with didansyl cystine (DDC). CD studies showed 2-step thermal unfolding profiles for both DDC-Tm and unlabeled Tm at pH 7 in 1M NaCl, indicating the presence of a partially unfolded intermediate, first proposed by Woods ((1979), Aust. J. Biol. Sci. 29, 405). Lifetime analyses gave 2 components despite the specific attachment to Cys 190: a short-lived component (a_1) of 6 nsec and a long-lived component (a_2) of 18 nsec. During the first step of unfolding, a_2 increased from 5 to 15% between 25° and 42°, before decreasing to 2% during the second unfolding stage. The spectrum shifted 3 nm to the blue and then 8 nm to the red during the first and second unfolding stages, respectively. The 2 different lifetimes and spectra suggest that the probe equilibrates between 2 different environment polarities: the short lifetime and "red" spectrum indicating high probe exposure to solvent, the long lifetime and "blue" spectrum indicating low probe exposure to solvent. The increase in a_2 during the first step is due to an increase in the fraction of the probes that interact with the hydrophobic ridge between the chains as the chains locally separate. These data show that between 25° and 40° Tm exists in equilibrium between a folded and an intermediate state, which is partially unfolded in the region of Cys 190. (Supported by NIH grant HL 22461 and the Muscular Dystrophy Association.)

T-PM-Po38 LOCALIZATION OF THE TROPONIN BINDING SITE IN TROPOMYOSIN BY FLUORESCENCE TECHNIQUES. T. Tao, D.R. Betteridge, M. Lamkin, and S.S. Lehrer, Dept. of Muscle Research, Boston Biomedical Research Institute, 20 Staniford St., Boston, MA 02114, and Dept. of Neurology, Harvard Medical School, Boston, MA.

The binding of troponin (Tn) to rabbit skeletal α,α-tropomyosin (Tm) labeled with 1,5-IAEDANS at Cys-190 was studied by fluorescence quenching measurements (using acrylamide as the quencher). The results are summarized in the table on the right, wherein K'_{sv} is the apparent Stern-Volmer constant, τ is the fluorescence lifetime, and k_q is the quenching rate constant. Whereas the presence of Tn increases the fluorescence lifetime of the AEDANS moiety, its accessibility is markedly decreased. A binding stoichiometry of 0.9 Tn:Tm and a binding constant of $1.5 \times 10^7 M^{-1}$ were obtained by titration. Similar observations were obtained using α,α-Tm labeled with didansyl cystine at Cys-190. The directly excited fluorescence yield was increased by 50% upon the binding of Tn. Energy transfer measurements between the tryptophans of Tn and the dansyl group indicated that one of the 3 tryptophans is within 40 Å of the label. The most straightforward interpretation of all these findings is that Tn binds to labeled Tm's near the labeling site, viz. Cys-190. This conclusion is consistent with that drawn from structural studies (McLachlan and Stewart (1976) J. Mol. Biol. 106, 1017). (Supported by NIH AM-21673, NIH HL 22461 and the MDAA.)

	K'_{sv} (M^{-1})	τ (ns)	$k_q \times 10^{-8}$ ($M^{-1}s^{-1}$)
- Tn	7.32	13.4	4.09
+ Tn[a]	5.25	19.2	0.57

[a] 1.7 μM Tn added to 1.7 μM Tm, in .1M NaCl, 0.1 mM $CaCl_2$, 5 mM $MgCl_2$, 10 mM Hepes, pH 7.5.

T-PM-Po39 The Effect of Cytochalasin D on Actin Nucleation. James E. Estes, Lynn A. Selden and Lewis C. Gershman. Research Service, US Veterans Administration Medical Center, Albany, and Department of Physiology, Albany Medical College, Albany, N.Y. 12208.

We have previously proposed that the effect of cytochalasin D (CD) on muscle F-actin is two-fold: 1) to cause a slight increase in the rate constant of depolymerization, k_-, and 2) to destabilize actin polymers to produce a greater number of polymer fragments (B.B.R.C. 95, 1854 (1980)). If this proposed mechanism is correct, then the presence of CD should increase the ATP hydrolysis by actin, or the cycling rate of monomers on and off the polymer ends, by increasing the number of polymer ends. We determined if this was the case by examining the nucleation of various concentrations of column-purified G-actin which had been labelled with ATP^{32} as the bound nucleotide. At very low ionic strength and 25°C, the time course of P^{32} liberation was proceeded by a lag period which was shorter in the presence of 0.2 μM CD than without CD. After the lag period, a slow but steadily increasing rate of P^{32} liberation was observed in both the presence and absence of CD, with the ATPase rate 2 to 4 times higher with CD than without CD. If 0.2 mM $MgCl_2$ was also present, the cycling rate increased over 10-fold. These ATPase rates did not depend in a linear manner on [actin]. Throughout the time course, the pattern of ATP hydrolysis rates, both with and without CD, were as would be expected for a nucleation reaction, with higher magnitudes always obtained with CD present. We thus consider that the CD-induced ATPase activity of monomer actin reported by Brenner and Korn (J.B.C. 255, 84 (1980; Fed. Proc. 39, 2045 (1980)) to be due to actin nuclei formation and the equilibrium of monomer actin with these nuclei. Supported by the Veterans Administration and NIH Grant AM 21573.

T-PM-Po40 ANOMALOUS BINDING OF NBD-Cℓ TO ACTIN. T. William Houk, S. Karipides, M. Ovnic, Department of Physics, Miami University, Oxford, Ohio 45056.

The fluorescent probe 4-chloro-7-nitrobenz-2-oxa-1,3 diazole (NBD-Cℓ) has been used in a number of studies involving various proteins. The probe appears to exhibit reactivity toward different amino acid residues depending on the protein to which it is conjugated as well as the reaction conditions employed. [Birkett, D.J. et al, FEBS Letters, (1970) 6, 346-348; Allen, G and G. Lowe, Biochem J., (1973) 133, 679-686; Aboderin, A. A. and E. Boedefeld, Biochem. Biophys. Acta (1976) 420, 177-185.] We report and compare the spectroscopic properties exhibited by NBD-Cℓ complexed with actin by two methods of labelling; addition of NBD-Cℓ dissolved in organic solvent and addition of the crystalline compound directly, which exhibit marked differences in the quantum yield of the complex. We have also investigated the effects of the treatment of actin solution with various ion-exchange reagents normally used to remove free ATP from solutions of F-and G-Actin. Spectroscopic evidence suggests that certain of the reagents either alter the conformation of the protein or catalyze a change in the probe molecules' site of attachment.
(Supported in part by a grant-in-aid from the American Heart Association with funds contributed in part by the Ohio Affiliate, AHA, Inc. and by the Miami University Faculty Research Committee.)

T-PM-Po41 ISOLATION AND CHARACTERIZATION OF COVALENTLY CROSS-LINKED ACTIN DIMER.
Stephen C. Mockrin and Edward D. Korn, NHLBI, NIH, Bethesda, MD 20205.

Rabbit skeletal muscle F-actin was cross-linked with p-N,N'-phenylenebismaleimide (Knight and Offer (1978) Biochem. J. 175, 1023). Sephadex G-200 column chromatography of depolymerized cross-linked F-actin and cycles of polymerization-depolymerization were used to separate dimer from other oligomers and monomer. All buffers contained 0.2 mM ATP. Polymerization competent dimer was more than 96% pure, with less than 2% monomer by weight and no detectable higher molecular weight oligomers. Although initially the F-actin contained ADP, the isolated dimer contained 2 moles of ATP (1 mol nucleotide/actin subunit). These two nucleotide sites exchanged with free ATP at very different rates in G-buffer at 25°. The first site had an exchange half-life of 55 min, while the second site exchanged almost no ATP after 11 h. When dimer was separated from free ATP in G-buffer, the first site contained a mixture of ATP and ADP•P_i (about 10-14% ADP•P_i). When polymerization was initiated by adding $MgCl_2$, 1 mol P_i was released from this site for each mol of dimer entering a filament. The filaments made from cross-linked dimer appeared normal in electron microscopy and activated muscle myosin S-1 ATPase activity normally. The critical concentration of dimer at 25° in 0.5 mM and 2 mM $MgCl_2$ was, at most, twice that of monomeric actin. Monomer and dimer copolymerized. Like actin monomer, the ATPase activity of actin dimer below its critical concentration in 0.5 mM $MgCl_2$ was stimulated by cytochalasin D. This ATPase activity was directly proportional to actin dimer concentration in the presence and absence of cytochalasin. In addition, the cytochalasin-stimulated ATPase activity of a mixture of actin monomer and dimer was the same as the sum of their separate rates. These results, taken together, indicate that the cytochalasin-stimulated ATPase activity of actin dimer, as was previously shown for actin monomer, does not require actin-actin interactions.

T-PM-Po42 A FLUORESCENT PROBE SENSITIVE TO SKELETAL MUSCLE ACTIN POLYMERIZATION. Robert P. Liburdy, ESD/SGPM, Hanscom AFB, MA 01731.

N-(3-pyrene)maleimide (PM) is a covalent affinity label that is specific for -SH groups at pH<7.5. Fluorescent properties of a simple model compound, PM-mercaptoethanol, were recently characterized and PM is sensitive to hydrogen ion concentration, microviscosity, and solvent permittivity(J.Chem. Phys. 82(1978)870). PM was therefore used to characterize microenvironmental changes in G-actin monomers during their polymerization to filamentous, double-stranded F-actin. PM-G-actin (0.8 moles PM/actin) was polymerized by addition of KCl to 0.1M in the presence of trace amounts of $MgCl_2$,$CaCl_2$, and ATP. An approximate five fold increase in fluorescence (λ_{ex} 345nm; $\lambda_{em,max}$ 350nm) was observed during the time course of polymerization with no spectral shift. Bulk solvent effects appeared negligible since in control studies PM-aldolase exhibited no fluorescence enhancement in the presence of G-actin during its polymerization. Also since a spectral shift to longer wavelengths was not observed, as is characteristic for PM at pH > 7.5, and since fluorescence quenching is expected in microenvironments less than pH 7.5, hydrogen ion effects appear excluded. The observed enhancement of PM fluorescence during G-actin polymerization is most likely associated with a microenvironmental decrease in permittivity. One hypothesis is that PM moeities are internalized near aromatic side chains or a hydrophobic domain as a consequence of intermolecular binding during formation of F-actin.

T-PM-Po43 AGGREGATION STUDIES OF MYOSIN ROD AS A FUNCTION OF IONIC STRENGTH AT pH 7.0.
Anne M. Bertasso, Jeanne Herbst*, and Jane F. Koretz, Dept. of Biology, RPI, Troy, NY 12181.

Myosin rod, the largest aggregating fragment of myosin, was prepared from column-purified rabbit skeletal myosin according to the method of Harrison et al., 1971, then dialyzed against 10mM imidazole, pH 7.0, and either .05M, .10M, or .15M KCl. Electron micrographs of the resultant aggregates, negatively stained with 2% uranyl acetate, were taken at 62,300X (1mm $\triangleq$ 12.5nm); optical diffraction from 1:1 contact transparencies was also performed.

Rod appears to aggregate into flat or curling sheets, which exhibit a 14.3nm stripe pattern. These stripes are almost invisible at .05M KCl, but are clearly discernible at higher ionic strenghs. Optical diffraction of these sheets shows meridional periodicities of 14.3 and 7.2nm^{-1}. No other periods are observed, in contrast to certain forms of LMM paracrystals whose reflections index on orders of 43nm. These results indicate that the subfragment-2 portion of the myosin rod limits the rod-rod interaction such that one degree of freedom is lost relative to LMM. When combined with LMM and myosin structural studies, these results suggest a possible mechanism for in vitro myosin aggregation at pH 7.0.

(Supported in part by NIH grant NS14377).

*Dept. of Physics, Siena College, Loudenville, NY. Supported through NSF Undergraduate Research Participation Program, SPI79-26887, awarded to Dept. of Physics, RPI, 1980.

T-PM-Po44 ASSEMBLY AND KINETIC PROPERTIES OF MINIFILAMENTS FORMED FROM MYOSIN A1 AND A2 ISOENZYMES. S.C. Pastra-Landis, T.W. Huiatt and S. Lowey. Rosenstiel Center, Brandeis University, Waltham, Massachusetts 02254.

Potential functional effects of the alkali light chains of myosin have been sought in the actin-activated MG^{++}ATPase. Studies on the subfragment-1 isoenzymes at low ionic strength (Wagner & Weeds, 1977) have shown a two-fold difference: the S-1(A2) enzyme exhibits a higher Vmax and actin Km than S-1(A1). Our measurements on chicken pectoralis muscle myosin A1 and A2 isoenzymes, isolated by immunoadsorption methods, show only minor differences in the actin-activated ATPase. However, double reciprocal plots of actomyosin activities contain considerable experimental error, due in part to the uncertain aggregation state of the myosin, and this error may mask possible small kinetic differences. Recently, Reisler et al. (1980) have shown that myosin is capable of assembly into stable short bipolar filaments, termed minifilaments, under carefully defined conditions. Due to the known state of aggregation of the myosin, such minifilament preparations provide a useful tool for obtaining much more reliable actin-activated Mg^{++}ATPase activities. Minifilaments prepared from purified chicken myosin A1 or A2 homodimers were examined by analytical ultracentrifugation using a photoelectric scanner, and by electron microscopy of both negatively stained and shadowed preparations. Chicken myosin assembles into minifilaments at the low protein concentrations (0.2 mg/ml) used in these studies. These minifilaments appear similar to those described by Reisler from the rabbit myosin. Steady-state kinetic studies on the A1 or A2 myosin minifilament preparations exhibit identical actomyosin ATPase activities measured in 10mM citrate - 35mM tris, pH 8.0 and 25mM KCl. These results show that the type of alkali light chain present in myosin does not affect its kinetic properties at moderate ionic strengths, in agreement with the earlier observations on the S-1 isoenzymes.

T-PM-Po45 STRUCTURE OF LIMULUS THICK FILAMENTS. Robert W. Kensler and Rhea J. C. Levine. The Medical College of Pennsylvania, Philadelphia, PA 19129.

Long thick filaments ($\sim$ 4.0 μm) rapidly and gently isolated from fresh, relaxed, Limulus muscle by an improved procedure have been examined by high resolution electron microscopy and optical diffraction. Images of negatively stained filaments appear highly periodic with improved myosin cross-bridge preservation. Optical diffraction patterns of the electron micrographs are detailed and superior to those previously obtained (Levine and Dewey, Biophys. J. 21:62a, '78). The patterns show strong meridional reflections at 14.5^{-1}, 7.2^{-1}, and 4.8^{-1} nm. Off meridional layer lines appear to index at 43.5^{-1}, 21.9^{-1} and 10.9^{-1} nm. This pattern appears qualitatively similar to the X-ray data of Wray et al. (J. Mol. Biol. 88:343, '74).

Paramyosin cores were prepared by brief extraction of long filaments adsorbed onto carbon-coated grids with 0.4M KCl, 7mM phosphate buffer, pH 6.0. Cores appear relatively aperiodic and have smooth contours. Optical diffraction patterns of cores reveal weak meridional 14.5^{-1} and 7.2^{-1}nm reflections. No Bear-Selby nets are seen. This appearance may be expected of the paramyosin cores of thick filaments with diameters less than those of molluscan smooth muscles.

Similar studies are underway using short thick filaments isolated from stimulated Limulus muscle.

Supported in part by USPHS grants GM 07475 and HL 15835 to The Pennsylvania Muscle Institute.

T-PM-Po46 MONOCLONAL ANTIBODIES TO LIGHT CHAIN 2 OF BREAST MYOSIN FROM ADULT CHICKEN. T. Shimizu, T. Masaki and D.A. Fischman. Department of Anatomy and Cell Biology, SUNY-Downstate Medical Center, Brooklyn, New York 11203.

After fusion of P3U-1 mouse myeloma cells with splenocytes of C3H mice immunized with native myosin from breast muscle of adult chicken, 24 hybridoma lines have been established which secrete immunoglobulin reactive with breast myosin, its proteolytic subfragments or genetic subunits. By solid phase, indirect RIA it was established that four lines secrete IgG binding at high affinity to native breast myosin, HMM, an alkaline released light chain fraction and column purified DTNB light chain (LC_2). Indirect RIA of SDS-PAGE fractionated breast myosin revealed binding to LC_2. No binding was obtained with LMM, chymotryptic rod, S_2 or a chymotryptic S_1 fraction lacking LC_2. High affinity of this IgG was evident when assayed against myosins from adult heart (ventricle), anterior latissimus dorsi (ALD) and embryonic breast muscles of the chicken and extensor digitorum longus (EDL) of the rat. Lower affinity, but definite cross-reactivity was observed with rat soleus myosin. Indirect immunofluorescent staining of glycerinated myofibrils from breast muscle was negative with native myofibrils, but strongly positive in the cross-bridge bearing zone of the A-band after acetone fixation. We conclude that this monoclonal antibody recognizes a determinant (possibly an amino acid sequence) on LC_2 which is shared by chick cardiac, ALD and rat EDL myosins, and a related but non-identical determinant in rat soleus myosin. Supported by grants from Muscular Dystrophy and New York Heart Associations.

T-PM-Po47 FORMATION OF SYNTHETIC MYOSIN FILAMENTS FROM MYOSIN MINIFILAMENTS. E. Reisler, C. Oriol-Audit* and J.A. Lake, Departments of Chemistry and Biology and the Molecular Biology Institute, UCLA, Los Angeles, CA 90024.

Dialysis of myosin from vertebrate striated muscle into 10mM citrate-tris buffer (pH 8.0 at 5° C) containing no other salt results in formation of minifilaments (short filaments ∿ 0.3 μ long). In solution the minifilaments are homogeneous in terms of size distribution, and no other myosin forms can be detected in their presence by analytical ultracentrifugation. Addition of KCl to solutions of minifilaments results in formation of regular size synthetic myosin filaments. The rate of this process is determined by the total protein concentration, the monovalent salt concentration, and the pH of the solution. When examined in the ultracentrifuge the "growing filament system" is composed of three types of species: dissociated myosin (monomer-dimer), minifilaments and filaments. As evidenced by light scattering studies and stop flow experiments, the partial dissociation of minifilaments precedes the growth of filaments. This research was supported by grants from MDAA and USPHS (AM 22021).

T-PM-Po48 EFFECT OF PHOSPHATE ON THE STABILITY OF MYOSIN HEAVY CHAIN-HEAVY CHAIN INTERACTION Walter F. Stafford, III and Sarkis S. Margossian, Department of Muscle Research, Boston Biomedical Research Institute, Boston, MA 02114; and Montefiore Hospital and Medical Center, Division of Cardiology, Bronx, NY 10467.

Very little is known about the precise nature of forces which stabilize the asymmetric structure of myosin and other coiled-coil α-helical proteins under native conditions. We report the results of an investigation into the effects of phosphate ion on the chemical equilibrium between rabbit skeletal myosin heavy chains in both myosin and its proteolytic subfragments, LMM and rod. Dissociation of myosin heavy chains was first reported by Pollard, Stafford and Porter (JBC 253,4798,1978) in myosin from Acanthamoeba. Since then we have been able to demonstrate dissociation of rabbit skeletal muscle myosin in a relatively benign medium consisting of 0.6M KCl, 0.5M phosphate, 10 mM EDTA at pH 8.5 as well as in 0.6M KCl, 0.2M phosphate, 10 mM EDTA at pH 7.3. Dissociation was observed both in equilibrium and sedimentation velocity experiments. The equilibrium constant for association of myosin heavy chains (including light chains) to form whole myosin was found to be ∿ 2 x $10^6 M^{-1}$ at 4°C in the 0.5M phosphate system. A value for the second virial coefficient (BM_1) of ∿ 0.06 L/g consistent with the expected excluded volume effects was obtained by curve fitting. At low concentrations (0.03<c<0.5 g/L) plots of 1/s vs. c extrapolated to a value of $s^\circ_{20,w}$ less than 4.5 S (corresponding to a Stokes' radius of less than 12 nm) suggesting that the dissociated single chain of myosin is partially folded. Sedimentation coefficients measured at higher concentrations (c>1.0 g/L) extrapolated to an infinite dilution value of 6.4S as expected for whole myosin. (Supported in part by MHLBI grant HL 25397 to W.F.S.; grant from NYHA to S.S.M. during tenure of Est. Invest. AHA to S.S.M.)

T-PM-Po49 FRACTIONATION AND CHARACTERIZATION OF MYOSINS FROM EMBRYONIC CHICKEN PECTORALIS MUSCLE. Pamela A. Benfield, Susan Lowey and Denise D. LeBlanc.* Rosenstiel Center, Brandeis University, Waltham, Massachusetts 02254.

At 11-12 days' incubation, myosin isolated from embryonic chicken pectoralis, a fast twitch muscle in the adult, has enzymatic properties (Ca^{2+}, K^+ and actin-activated Mg^{2+} ATPases) which are very similar to those obtained for adult pectoralis myosin. This is inconsistent with the view that the slow speed of contraction of embryonic muscles is due in part to a low myosin ATPase activity. At this stage of development embryonic pectoralis myosin contains approximately 10% slow light chains, and the muscle stains with fluorescent antibodies specific for both adult fast (pectoralis) and adult slow (ALD) myosins. Antibody which is specific for adult slow (ALD) myosin heavy chain still cross reacts with embryonic pectoralis myosin. Therefore, some slow determinants in the embryo are also present on heavy chains. Using immunoadsorbents prepared from anti-ALD myosin heavy chain and anti-pectoralis myosin, we have achieved a preliminary fractionation of embryonic myosin. The fractionated species have been characterized by a) light chain composition, b) radioimmunoassay and c) heavy chain peptide mapping. The latter was achieved by two-dimensional gel electrophoresis of partial chymotryptic digests. Detection of the small amounts of material required the use of a highly sensitive silver stain. Our results indicate that embryonic pectoralis myosin is distinct from adult myosins, and that the cross-reactivity with anti-ALD heavy chain is not due to the presence of small amounts of adult slow heavy chain. The material retained by the anti ALD-heavy chain column is enriched in slow light chains which suggests a minimum of two myosin heavy chain species in the embryonic chicken pectoralis. (Supported by grants from NIH, NSF and Muscular Dystrophy Association.)

T-PM-Po50 THE EFFECT OF CYCLOHEXIMIDE ON PROTEIN DEGRADATION IN CULTURED RAT AND HUMAN SKELETAL MUSCLE. H.E. Neville, M.C. Neville and R. Farrell. Department of Neurology and Physiology, University of Colorado, School of Medicine and the Veterans Administration Medical Center, Denver, Colorado 80262.

We have studied the effect of cycloheximide on protein synthesis and degradation in cultured human and rat muscle. Specimens of biopsied human and rat muscle were dissociated with collagenase and grown in culture until extensive myotube formation had taken place (10-14 days). Proteins in the cultured cells were labeled with (^{14}C) or (^{3}H)-tyrosine by incubation for 48 hours in medium containing 1-5 uCi/ml. Both human and rat cultures incorporated between 25 and 40 nmol labeled tyrosine/mg. protein. Measurements of the rate of labeled tyrosine loss after removal of the isotope from the medium suggested that the culture contained two pools of protein: a small (less than 5% of total protein) rapidly degrading pool, turning over with a half-time of about 2 hours and a large, slowly degrading pool with a half-time of 2-3 days. Cycloheximide (0.5 mM) abolished protein synthesis in these cultures. The effect of the agent on degradation was estimated by determining the specific activity of labeled tyrosine remaining in cultured cells at various times after removal of isotope. After four hours the specific activity of labeled tyrosine in cycloheximide treated cultures had declined 13% (control wells showed a decline of 23%) but over the next 21 hours there was no further decline (controls declined an additional 24%). Thus, cycloheximide after four hours completely blocked protein degradation in these cultures. This may result from a direct effect of cycloheximide on protein degradation, from the loss of a rapidly degraded enzyme responsible for protein turnover, or to interactions between control of protein synthesis and degradation. (Supported by a research grant from the Veterans Administration).

T-PM-Po51 ABNORMAL HEART DEVELOPMENT IN VALIUM-TREATED EMBRYOS. William E. Renehan and Robert R. Kulikowski, Departments of Anatomy and Physiology, The Milton S. Hershey Medical Center, Hershey, PA 17033 USA

In an effort to further elucidate the role of myofibrillogenesis as a regulatory factor during the ontogenetic time period of looping in the embryonic vertebrate heart, we have used diazepam (Valium, Roche), a putative inhibitor of myosin heavy chain synthesis, to attempt to block myofibril formation. Chick embryos, grown in New culture, were incubated in the presence of 100 μM diazepam. Controls were similarly grown in Tyrode's solution without diazepam. Light and scanning electron microscopic (SEM) observations of treated embryos revealed a variety of abnormalities, including absence of looping, aberrant loop formation, abnormally formed outflow tract, and incomplete fusion of right and left halves. SEM examination demonstrated that myocardial surfaces of diazepam-treated embryos exhibited areas of both bulging and flattened myocytes, while developing myocytes of untreated embryos bulged outward, forming a regular pebbled surface over the entire heart. Transmission electron microscopy of the myocardia of control embryos at post-looped stages of development evidenced an abundance of newly formed myofibrils consisting of thick and thin filaments inserting into amorphous Z substance. Nascent myofibrils terminated in developing intercalated disks at the cell periphery. In comparably staged diazepam-treated embryos, there was a noticeable paucity of myosin thick filaments and Z substance. We did not observe evidence of intercalated disk formation. Mitochondria, polyribosomes, desmosomes, and nuclei were apparently unaffected by diazepam treatment as judged by comparison with control embryos. This evidence suggests that expression of the myocardial myosin genome is necessary for normal cardiac development. (Support: HL13831, Chicago Heart Association, and PSU Research Initiation Grant)

T-PM-Po52 THE RELEASE OF A-BAND SEGMENTS FROM MYOFIBRILS WITH DNase I. F. Reinach, W. Ip and D. A. Fischman. Department of Anatomy and Cell Biology, SUNY-Downstate Medical Center, Brooklyn, New York 11203. (Introduced by Manfred Brust).

The property of DNase I to depolymerize F-actin has been utilized to prepare native A-segments from myofibrils of skeletal muscle. Glycerinated myofibrils from rabbit psoas and chicken breast muscles have been incubated with commercial (Sigma) or column purified DNase I (Liao, J. Biol. Chem. 249:2354,1974) in 100 mM KCl, 10 mM $MgCl_2$, 1 mM EGTA, 40 mM borate buffer pH-6.7 with 10^{-5} PMSF at a 2:1 molar ratio of DNase: G-actin at 25°C. When observed by phase contrast light microscopy, the I-bands exhibited a decline in phase density followed by a breakdown of myofibrils into segments of 3 to 5 sarcomeres by 2 hr. After 3 hr of incubation, mainly A-segments were seen. Washed 19,000 xg pellets and supernatants were compared by SDS-PAGE. Pellets contained thick filament proteins plus a variable actin contamination which may reflect the extent of filament overlap in the original myofibrils. The supernatants contained I-Z-I proteins plus DNase I. Thin sections revealed excellent retention of native A-band structure and the absence of well-defined thin filaments. Internal structure was difficult to study by negative staining because of high electron density; the A-segments measured 0.9-1.3 μm in diameter. If Mg-ATP was included in the DNase incubation buffer, A-segments disassembled completely into thick filaments of native length. Experiments are in progress to distinguish actin-myosin from M-bridge linkages in the maintenance of A-segment integrity. Supported by grants from CNP_q-200.096-80, Muscular Dystrophy and New York Heart Associations.

T-PM-Po53 STUDIES OF M-BAND PROTEINS BY FLUORESCENCE AND ELECTRON MICROSCOPY. John L. Woodhead and Susan Lowey, Rosenstiel Center, Brandeis University, Waltham, MA 02254.

Electron micrographs of rotary shadowed M-protein (mw 165,000) isolated from the M-band of chicken pectoralis muscle show that the protein is an extended molecule of 400 to 500 Å in length and approximately 50 Å in diameter. This is consistent with the 10:1 axial ratio calculated from hydrodynamic measurements, and is compatible with the suggestion that M-protein may be a component of the M-filaments. Chicken pectoralis myofibrils have been reacted with antibodies specific for M-protein and creatine kinase (the other known M-band component) by a fluorescein/rhodamine double labeling technique. Strong M-band fluorescence was observed for both antibodies in agreement with earlier observations (Trinick and Lowey, 1977; Walliman et al., 1977). These studies are being extended to monitor the appearance of M-band proteins during the various stages of embryonic muscle development. The *in vitro* interactions of M-protein and creatine kinase with the LMM fragment of myosin have been studied by electron microscopy. The banding pattern of the LMM paracrystals was not significantly altered in the presence of either of the M-band proteins. The banding pattern was enhanced, however, when paracrystals formed in the presence of M-protein were reacted with homologous antibody; this effect was not observed for creatine kinase. These results, together with the affinity chromatography and sedimentation equilibrium experiments of Woodhead (1980), suggest that *in vitro* interactions of the purified components are weak. Since the M-band proteins appear to be firmly bound to the myofibril under physiological conditions, this raises the possibility that additional components are needed in order to observe strong *in vitro* interactions. (Supported by grants from NIH, NSF and Muscular Dystrophy Association.)

T-PM-Po54 STRUCTURAL AND FUNCTIONAL RELATIONSHIPS OF THE CONTRACTILE APPARATUS OF *LIMULUS* STRIATED MUSCLE. M. M. Dewey, D. Colflesh*, P. Brink, R. J. C. Levine and B. Walcott. Anatomical Sciences, SUNY at Stony Brook and Anatomy, Medical College of Pa., Phila., Pa.

Limulus striated muscle developes maximum tension at a sarcomere length 7.0 μm(L_o). At sarcomere lengths between 3.5 and 10.0 μm, more than 50% maximal tension is produced (Walcott and Dewey, J. Cell Biol. 87:204, 1980). The A band increases in length, 3.0 μm to 6.5 μm from sarcomere lengths of 4.0 μm to 10.0 μm. Apparent increase in A band length in sarcomeres above 7.0 μm is due to skewing of thick filaments. Apparent shortening of the A band in sarcomeres from 7.0 μm to 4.0 μm is due to shortening of thick filaments. Thick filaments shorten (4.9 μm to 3.0 μm) and increase in diameter (23.0 nm to 37.0 nm) as sarcomeres shorten from 7.0 μm to 4.0 μm (Dewey, M. *et al.*, *Cross-Bridge Mechanism in Muscle Contraction*, Univ. Tokyo Press). Thin filaments extend approximately 2.8 μm on either side of the Z band. In sarcomeres from 7.0 μm to 10.0 μm the I band increases in width from 2.8 μm to 4.0 μm. In sarcomeres from 7.0 μm to 4.0 μm the I band remains constant in width. We interpret this to mean that during tension development in sarcomeres from 10.0 μm to 7.0 μm thin filaments slide past thick filaments and thick filaments realign in the A band. At L_o thin filaments overlap thick filaments by 60%. In sarcomeres from 7.0 μm to 4.0 μm thick-thin filament overlap remains constant and sarcomere shortening and tension development is contributed to by thick filament shortening. This shortening may involve protein phosphorylation and requires ATP (Brann *et al*, Nature 279:256, 1979).

This work was supported by NIH Grant GM26392.

T-PM-Po55 AN ECHINODERM SMOOTH MUSCLE CONTAINS PARAMYOSIN. Myra Elfvin, Kathryn McGlynn and Rhea J.C. Levine. The Medical College of Pennsylvania, Phila., PA. 19129

The longitudinal body wall muscle of the sea cucumber, *Parastichopus*, undergoes extreme lenght changes *in vivo*. Thus, a stressed cucumber shortens to 1/2 to 1/3 of its relaxed length. Such extreme length changes occur in both striated and smooth invertebrate muscles, but more commonly in the latter. Electron micrographs show that *Parastichopus* body wall muscle indeed is smooth, completely lacking sarcomeric organization. Instead of true Z-bands, it possesses small dense Z-bodies, many of which are at the sarcolemma. The thin muscle fibers (1-5μm in diameter) lack T-tubules, possess subsarcolemmal cisternae and very few mitochondria. Preliminary examination of thick filaments suggests that they are of smaller diameter than those of molluscan catch muscles. Non-uniformity of thick filament diameter in cross-section may reflect tapering of thick filament ends. Determination of thick filament length will require filament isolation. Electrophoresis on 6% polyacrylamide-SDS disc gels of homogenized glycerinated muscle shows a band which co-migrates with *Limulus* paramyosin and occurs only in gels of paramyosin containing invertebrate muscle. Integrating scans of 59 gels at 3 different protein loadings give a molecular ratio of paramyosin to myosin heavy chains of 0.7±0.14, a value considerably below our published value for *Mytilus* ABRM (2.88±0.72) but above that for *Limulus* telson levator (0.48±0.12).

(Supported by USPHS Grants GM21956 and HL15835 to the Pennsylvania Muscle Institute. Specimens were obtained at the Catalina Marine Science Center.)

T-PM-Po56 THE EFFECT OF SOLVENT HISTORY ON PARAMYOSIN SOLUBILITY. Nancy Letko and Sonja Krause, Dept. of Chemistry, Rensselaer Polytechnic Institute, Troy, New York 12181.

Acid-R-paramyosin from Mercenaria mercenaria adductor muscle was shown by Cooley, et al. [JBC 254, (1979)] to contain ∿3 removable phosphates/molecule. Continued investigation has shown that these are adsorbed phosphates; furthermore, differences in the manner in which the paramyosin is extracted from the muscle lead to variations in the number of adsorbed phosphates. Once extraction is completed, dialysis of stock paramyosin (A), i.e. acid-R-paramyosin in HISB (0.6M KCl, 0.01M $KHPO_4$, 0.01M K EDTA, 0.5 mM DDT, pH 7.5), against 0.01M KOH, 0.29M KCl, 0.5 mM DTT, pH 12, gives another sample B, in which all but ∿0.5 phosphates/molecule have been removed. Similarly, if A is dialyzed against 0.01M HEPES, 0.59 M KCl, 0.5 mM DTT, pH 7, for a week, a sample, C, is obtained which has lost all but 0.4 phosphates/molecule. It is interesting to note that B dialyzed against ∿9 volumes of HISB for 4 h, sample D, readsorbed all of the phosphates lost during KOH treatment. Solubility studies using equilibrium dialysis have been carried out on samples A to D using two different buffers, 0.01 M phosphate at pH 7 and 0.01M imidazole at pH 7. Ionic strengths were changed by addition of KCl. The solubility curves for all samples exhibited the expected high solubility at both ends of the ionic strength range, 0.01M and 0.40M (Cooley, et al. above). At intermediate ionic strengths, however, solubility was dependent on the history of the sample. Samples A, C, and D had approximately the same solubility profile in the phosphate buffer system while sample B was less soluble. In the imidazole system, sample A was again more soluble than B but C displayed an intermediate behavior. The solvent history of paramyosin thus causes a quantitative difference in its solubility behavior although the qualitative solubility curve for all samples remains the same.

T-PM-Po57 TWO-DIMENSIONAL GEL ELECTROPHORESIS OF SEVERAL INVERTEBRATE MUSCLES. Bruce Gaylinn and M. M. Dewey, Anatomical Sciences, SUNY at Stony Brook. N. Y. 11794

Telson muscle from the horseshoe crab, Limulus polyphemus, fast and slow abdominal flexor muscles from the lobster, Homarus americanus, red and white adductors from the chowder clam, Mercenaria mercenaria, and scutal adductor and depressor from the giant barnacle, Balanus nubulis, have been examined by the high resolution two-dimensional gel electrophoresis technique of O'Farrell (J. Biol. Chem. 250:4007-4021, 1975). Isoelectric focusing tube gels were scanned with a surface pH electrode and then fixed and stained by the method of Jackle (Anal. Biochem. 98:81-84, 1979) to allow visualization of separation patterns before they were electrophoresed on SDS slab gels in the second dimension.

The most striking result is the relatively large variation in the isolectric point of paramyosin. This may be interpreted to suggest phosphorylation of paramyosin. Current work is underway to determine how this correlates with such functions as thick filament shortening and catch. Tropomyosin also shows variability, being of one chain type in some muscles and two slightly different chain types in other muscles of the same animal. Difficulties were encountered in the isoelectric focusing of myosin. It tended to not enter the focusing gel or to enter as actomyosin. Aggregation problems during focusing were not eliminated by boiling samples in SDS prior to the addition of 9 Molar urea and 4% NP40, though little aggregation is seen in SDS gels.

This work was supported by NIH Grant 5 R01 GM26392.